They paved the way to understanding the Universe. Go on! Happy 2023!

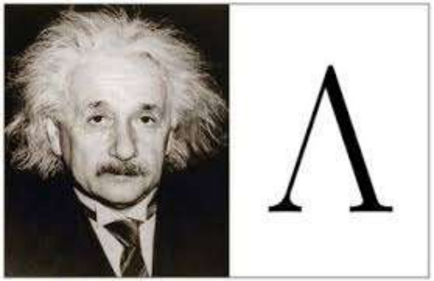


Victor Hess


Fritz Zwicky

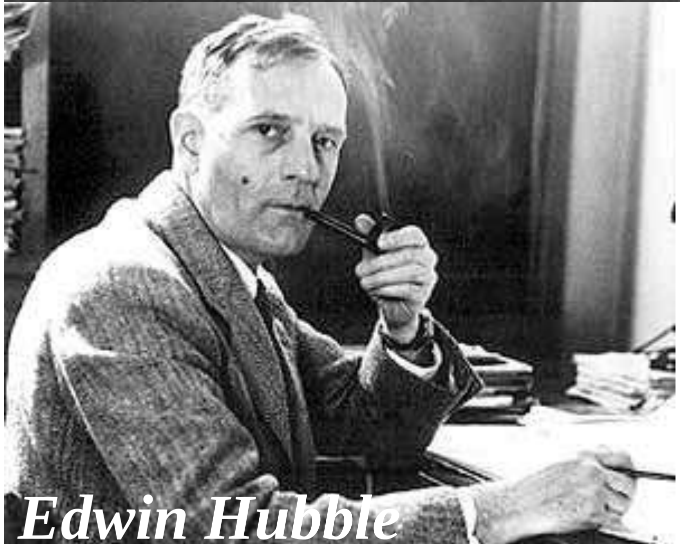
Edwin Hubble

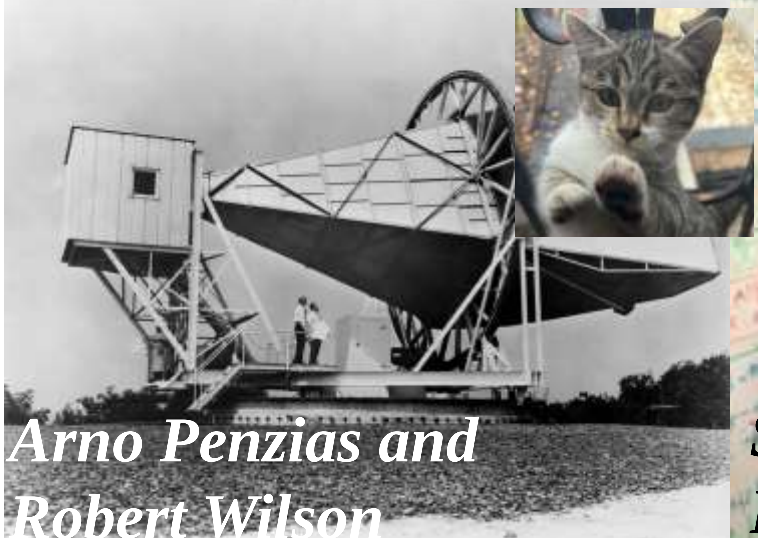
Arno Penzias and Robert Wilson


Saul Perlmutter

Новые тенденции в астрофизике высоких энергий

- Мультисенсорный сетевой подход (multi-wavelength observations, and multi-messenger studies).
- Концепция больших данных, моделирование физического процесса и отклика детектора на каждом этапе экспериментов, систематическое структурирование и исследование всего набора взаимосвязей, содержащихся в многомерных моделируемых и экспериментальных данных.
- Политика открытых данных: коды и базы данных становятся общедоступными, приглашая всех к участию в анализе, а внешние группы могут вносить новые идеи и методики.
- Понимание силы корреляционного анализа, дающего беспрецедентную точность в определении местоположения звездных объектов и в получении новых связей между различными явлениями.
- Синергия различных экспериментальных методов: от радио до ультра-релятивистских частиц.

Как Создавать Знание (Принципы и Процедуры)

- Понять и сформулировать проблему;
- Подготовить и провести эксперимент, собрать данные:
- Формулирование и тестирование гипотез;
- Сравнение с другими экспериментами;
- Выбор математических методов для анализа данных; оценка, выбор модели наилучшим образом объясняющую эксперимент, оценка параметров модели;
- Сформулировать результаты в виде допускающем проверку и сравнение с другими экспериментами;
- Подготовить и отправить статью в журнал;
- Ответить на комментарии рецензентов, проверить результаты и отправить для окончательного рецензирования.

Открытие космических лучей

- Измерен поток ионизирующего излучения падающего на землю излучения упали на земле;
- Из чего он состоит (состав, энергии)?
- Возможные источники (солнце, Галактика, SNR, AGN, черные дыры, нейтронные звезды?
- Детекторы (Космические, наземные);
- Как решить обратную задачу?
- Моделирование; модели распространения и взаимодействия космических лучей, данные с коллайдеров; проверка модели: верификация и валидация;
- Модель измерения: от электронных сигналов с детекторов к интенсивностям; классификация частиц.

Experiments

- Cosmic rays: Imaging Cherenkov Telescopes and high-latitude surface arrays: MAGIC, LHAASO
- Gravitational Waves, Black holes, Neutron stars mergers, LIGO-VIRGO
- Dark matter searches, LHAASO
- Gamma observatories in space: FERMI LAT
- High-energy atmospheric physics, Aragats Cosmic ray Observatory

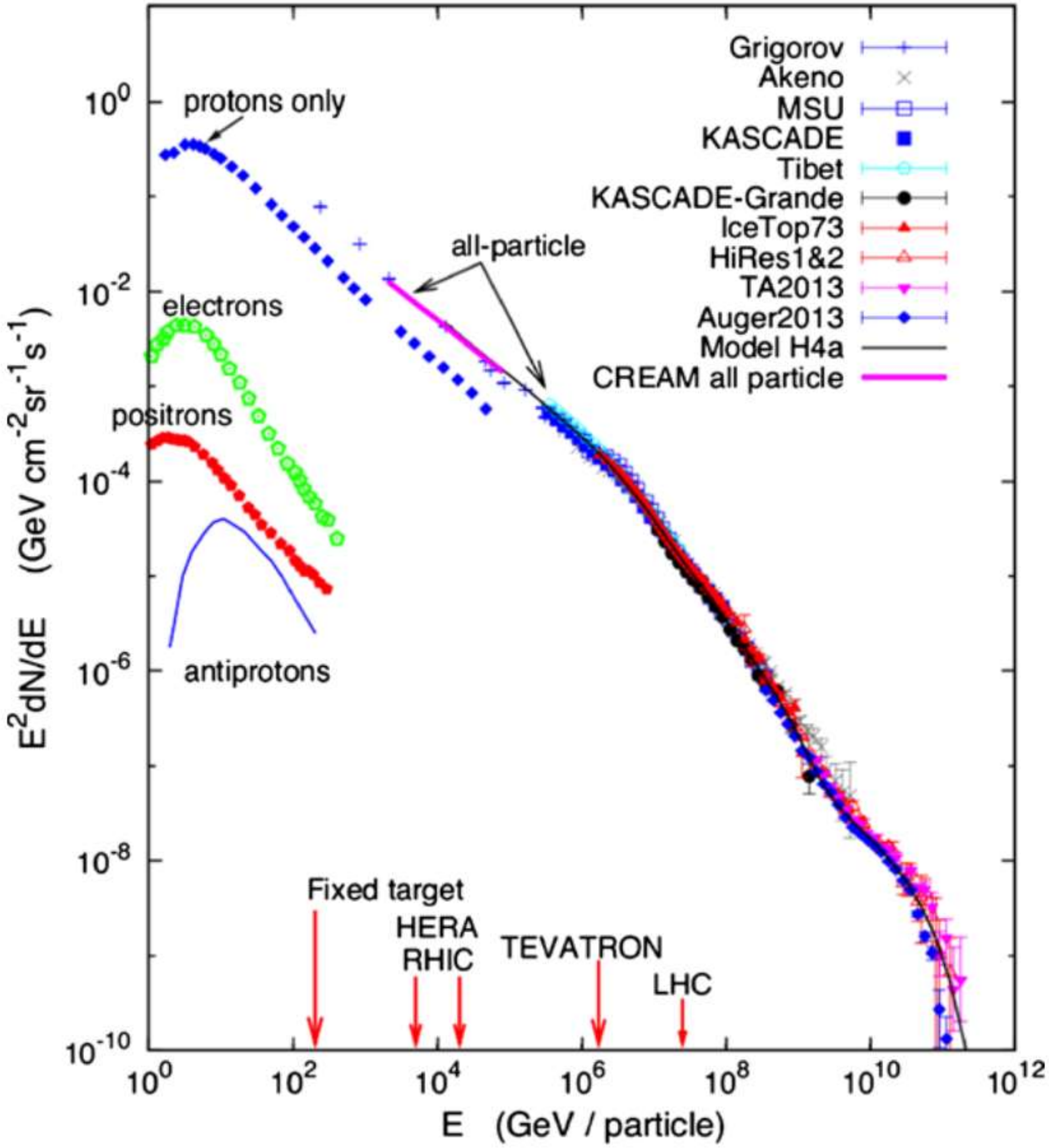

In the case of p-p collision at LHC, with 7 TeV per proton 14 TeV is available for new particle production.

For a **Fixed target**, considering a proton moving with energy **E_1** colliding with a fixed target formed for a proton at rest ($m_2 \cdot c^2 \sim 10^{-3}$ TeV) to get **14 TeV** we need **E_1** to be:

$\sqrt{s} \sim \sqrt{(2E_1 . m_2 . c^2)}$

$14 = \sqrt{(2E_1 . 10^{-3})}$

$E_1 \sim 10^5$ TeV

It is very clear the advantage by using collider vs fixed target.

Universe is full of Particle Accelerators

Galaxies that point their jets at us are called "blazars"

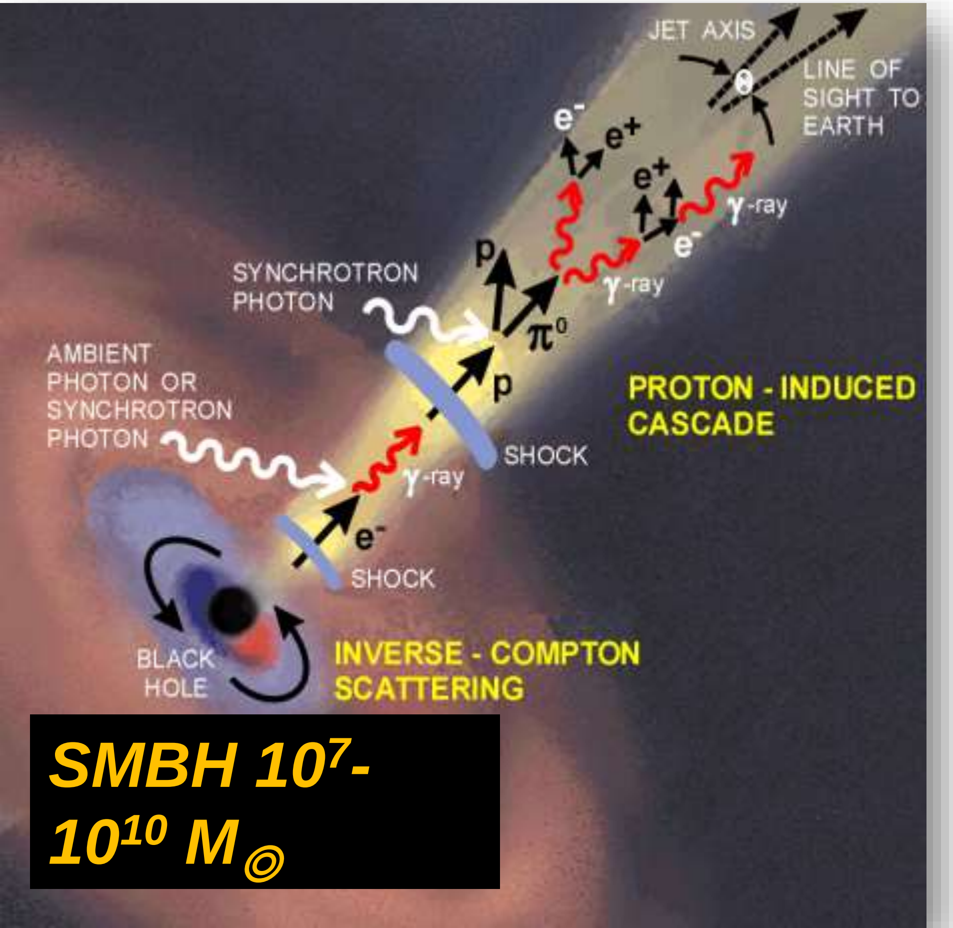

SMBH 10^{7}-10^{10} $M_{\odot}$

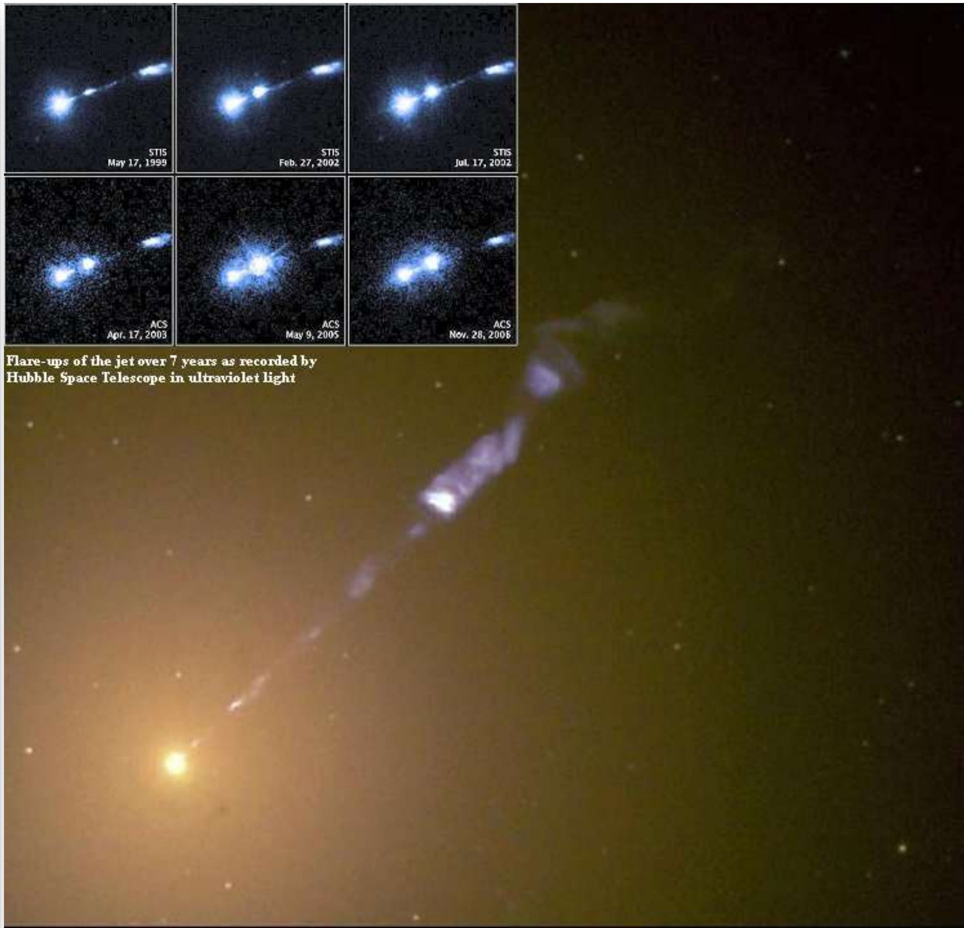

Flare-ups of the jet over 7 years as recorded by Hubble Space Telescope in ultraviolet light

Supernovae remnants – major candidates to accelerate CR up to 10^{17} eV.

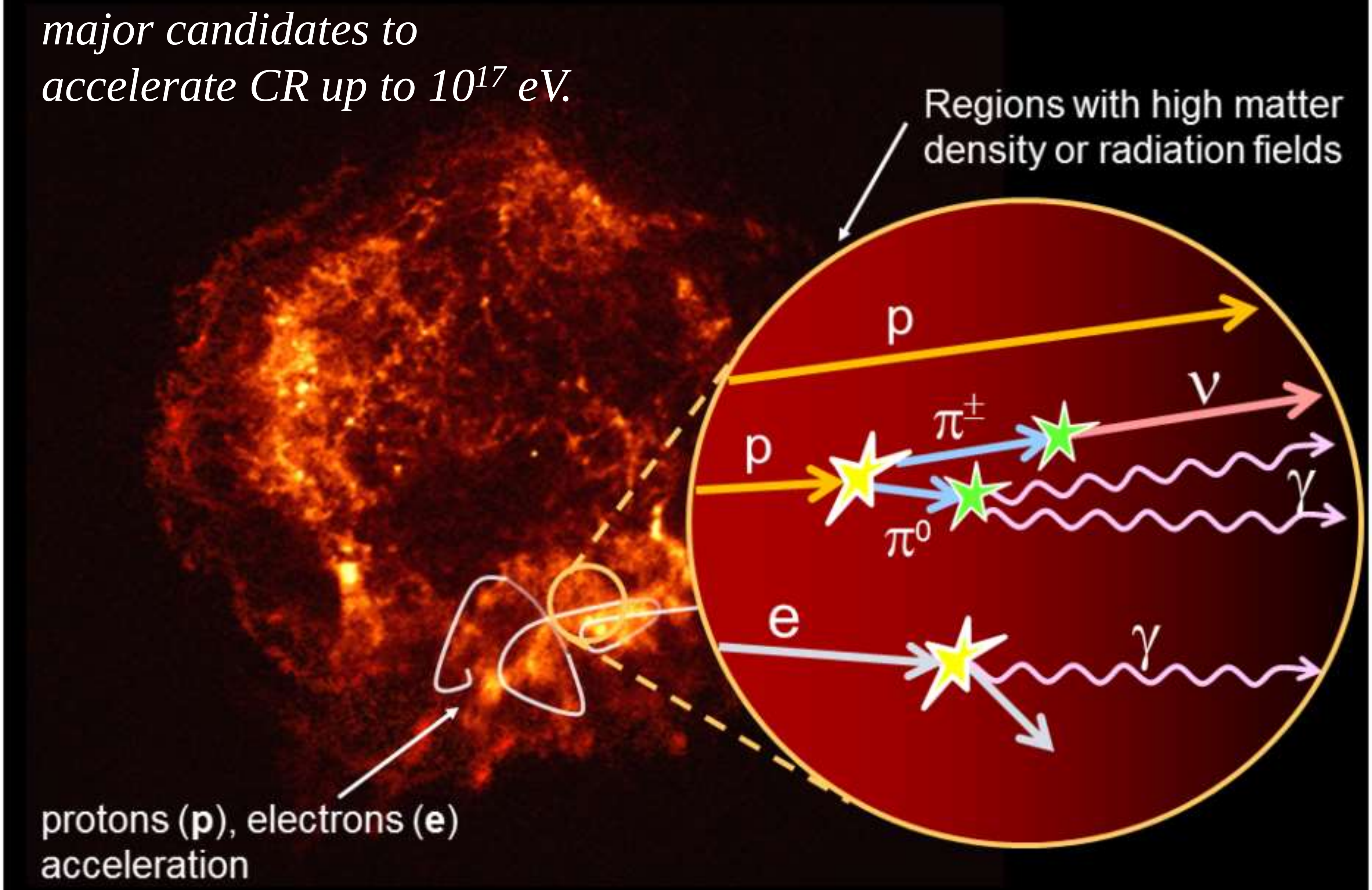

Gamma ray and neutrino astronomy,
CR astrophysics

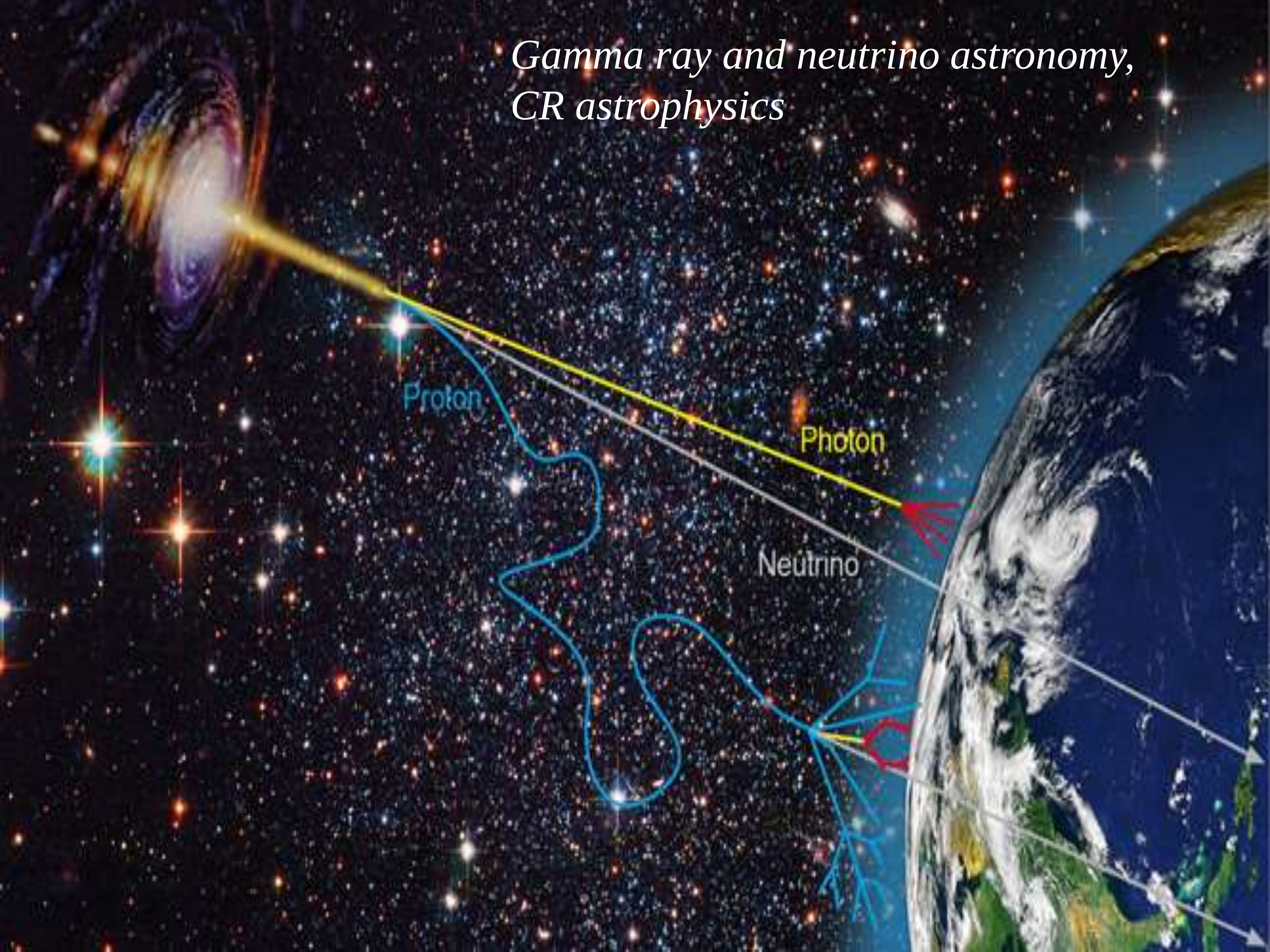

Particle detectors: our interface to particle physics

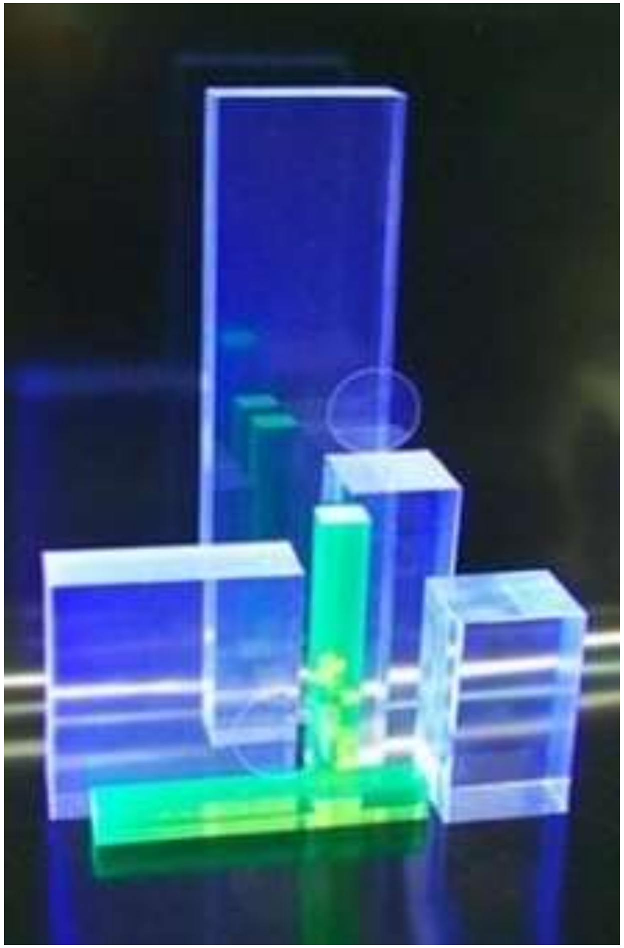

What are scintillators good for?

- Count particles
- Measure energy release
- measure the time of particle passing
- measure location

How do they work?

- passing charge excite molecules in the plastic
- as molecules de-excite, a small fraction release optical quanta
- this light propagates inside the plastic to the registering surface sensitive to the light

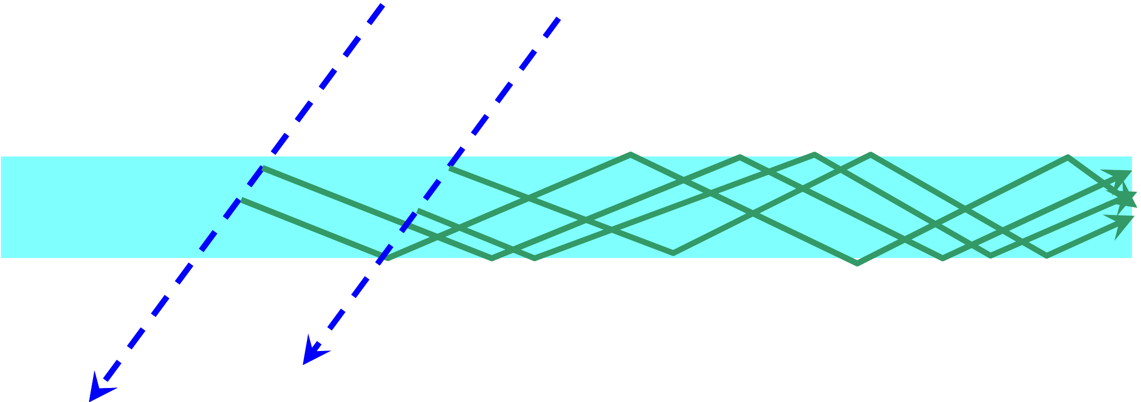

Phototubes: Electronic Retinas

- See light pulse from scintillator
- Very sensitive
  - huge amplification
  - they can detect a single photon !
- Produce a signal quickly
  - important for **triggering**
  - precise timing

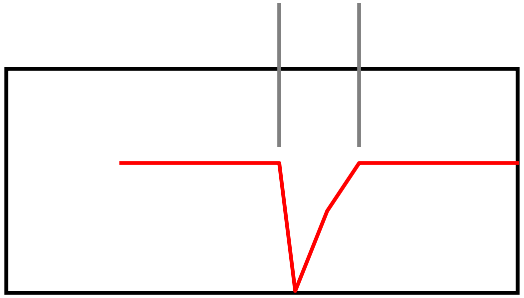

output pulse 20 ns

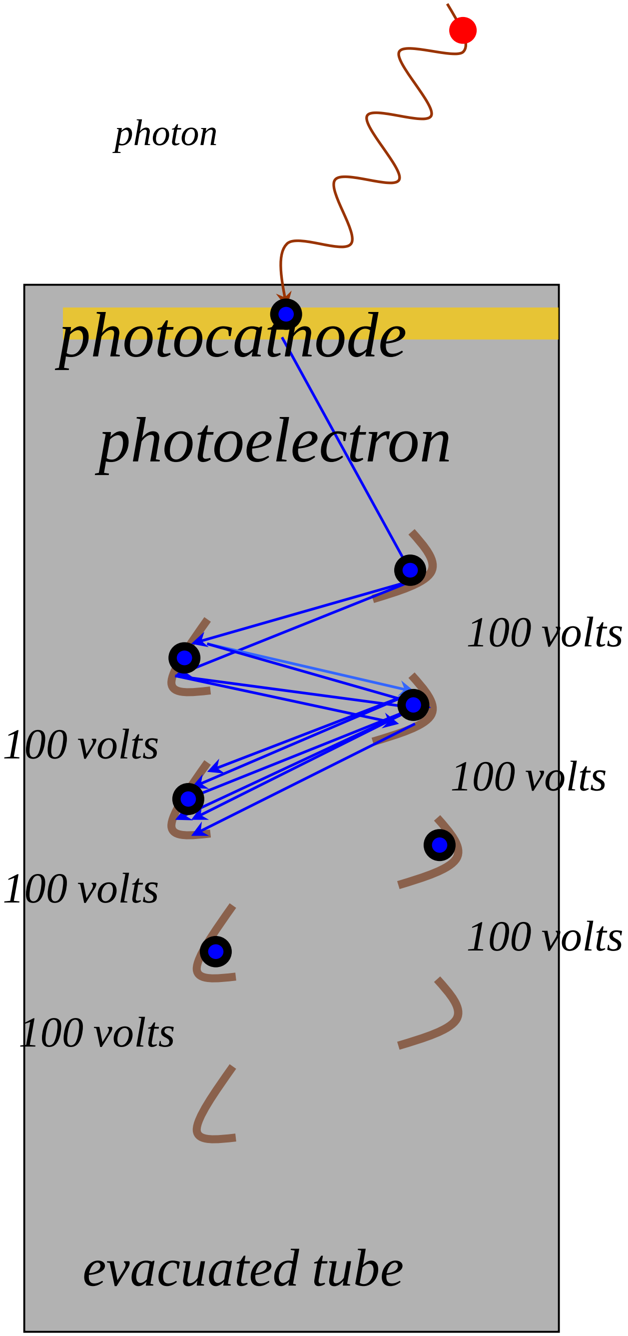

Electromagnetic “Sampling” Calorimeter:
A layer cake of scintillator & lead

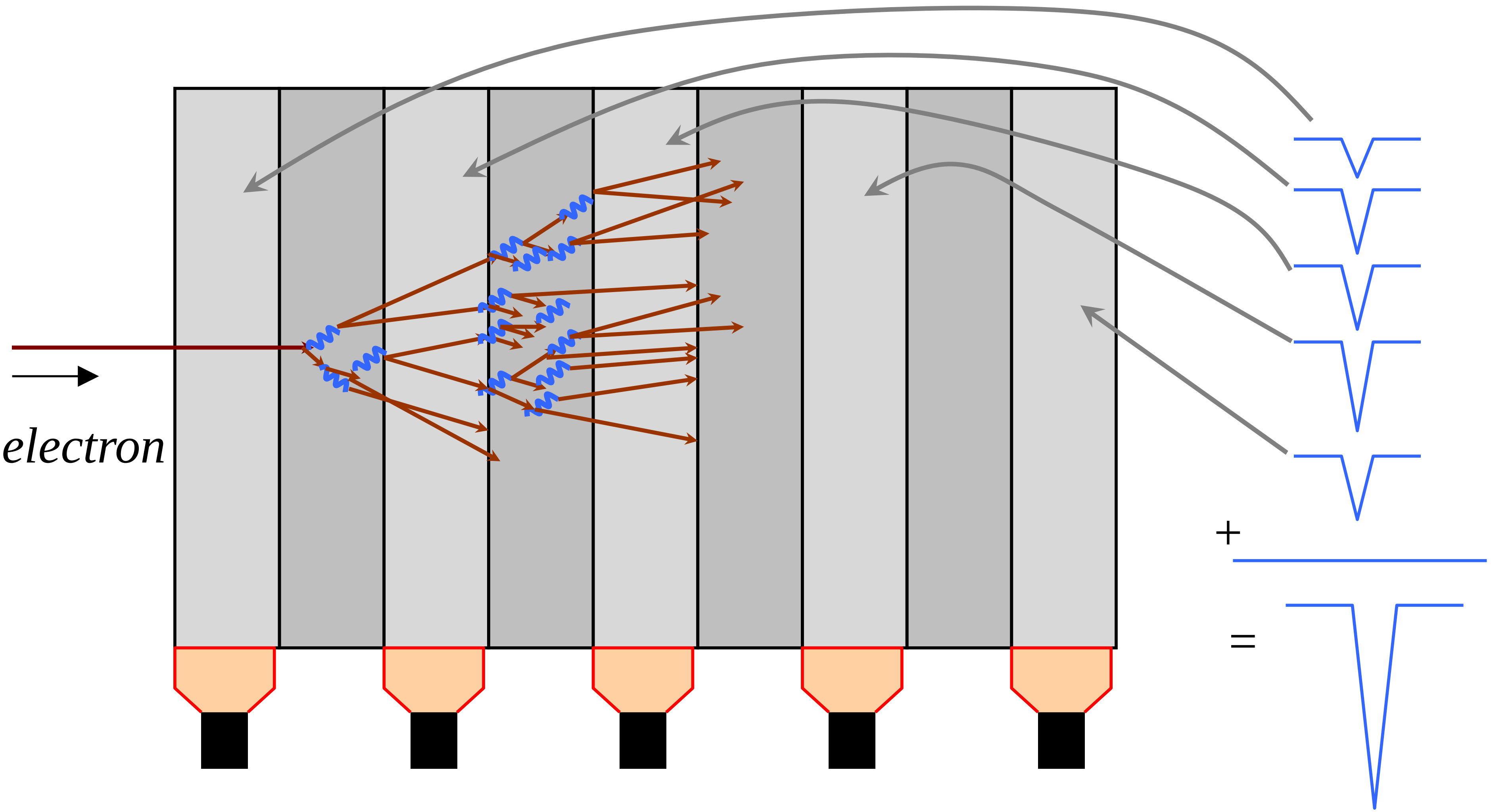

Sum the phototube signals to measure energy of the entering particle !

Separating signal from noise

Discriminators

- not all pulses are made by a passing particle.
- there are also “noise” sources
- we use a discriminator to clean up the noise

- If the pulse is larger than the discriminator threshold
  ➔ output is TRUE, otherwise FALSE

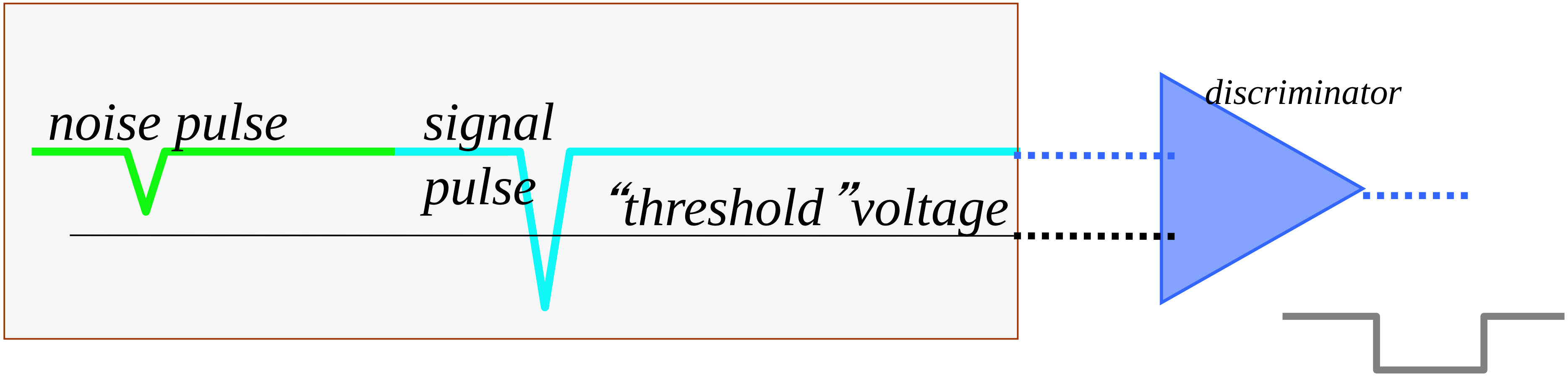

A digital output pulse is generated when the signal crosses the threshold

Coincidences techniques

Phototube + discriminator

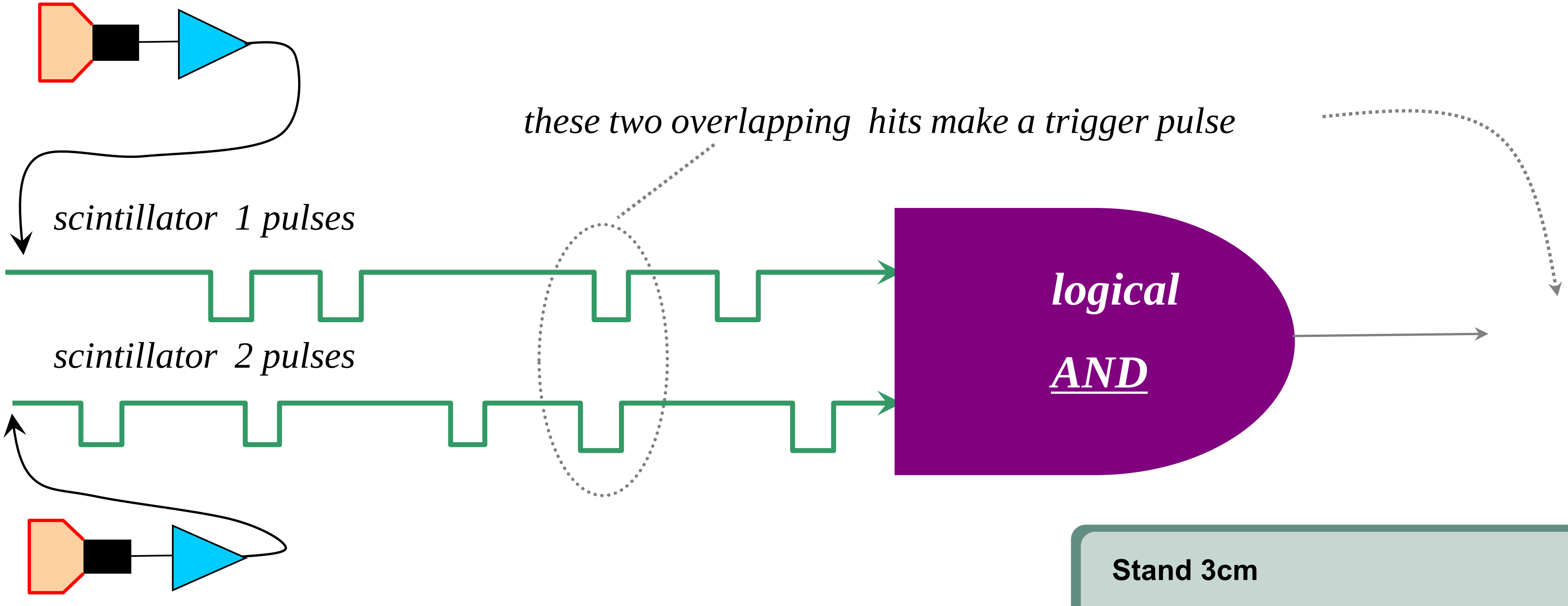

these two overlapping hits make a trigger pulse

scintillator 1 pulses

scintillator 2 pulses

logical

AND

Time axis

1 μsec

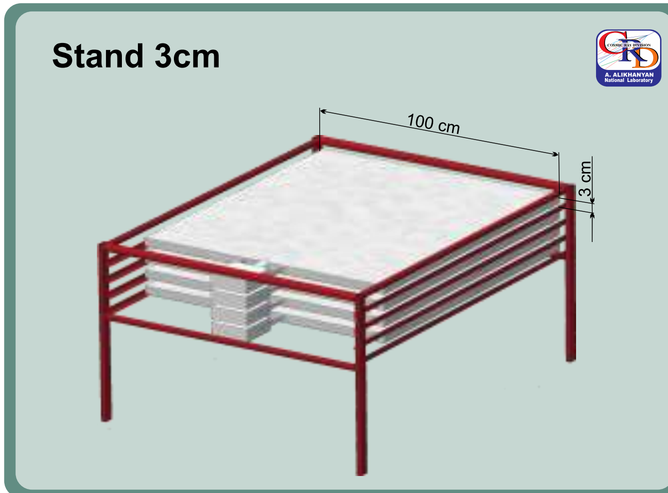

Stand 3cm

Aragats Solar Neutron Telescope ASNT

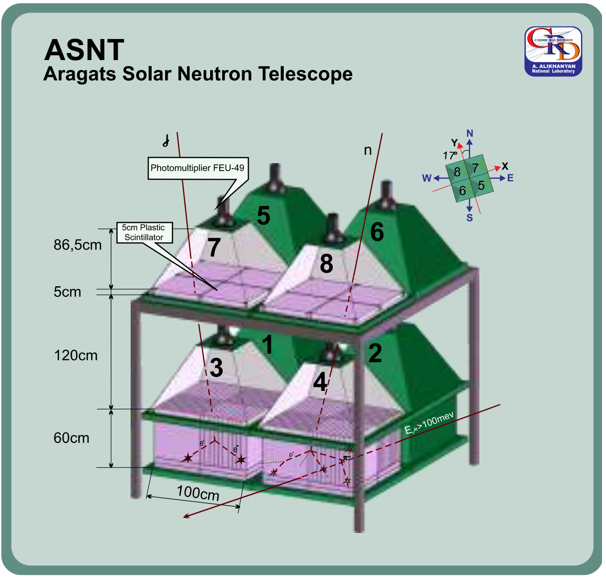

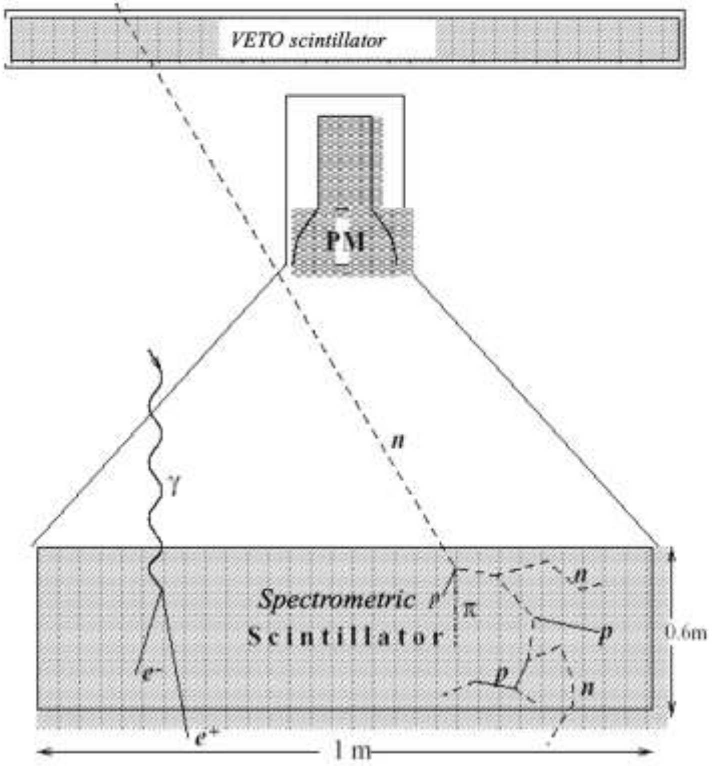

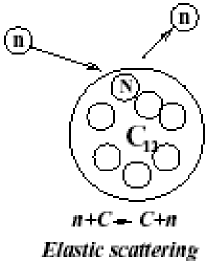

$n+C \rightarrow C+n$

Elastic scattering

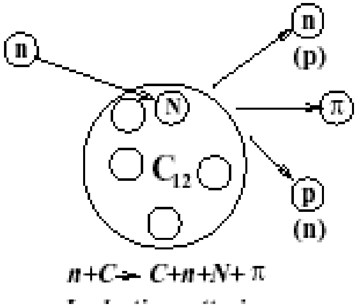

$n+C \rightarrow C+n+N+\pi$

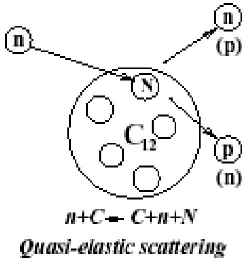

$n+C \rightarrow C+n+N$

Quasi-elastic scattering

ASNT registered coincidences (01; 11), between all 8 scintillators, and energy release histograms in 5 and 60-cm thick scintillators

Logic of experiment: electronics boards

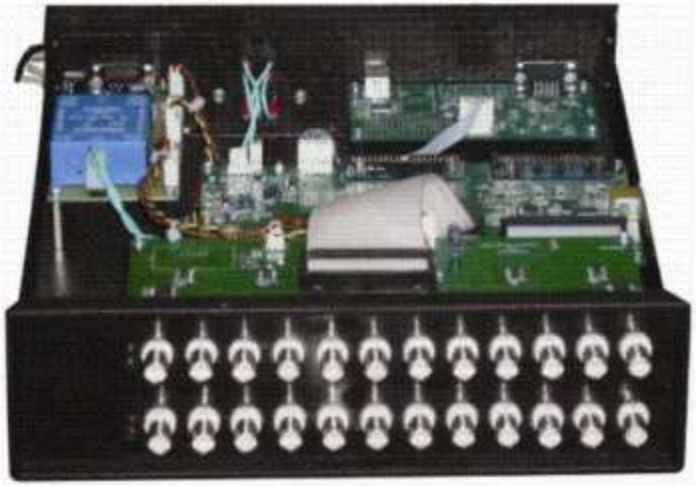

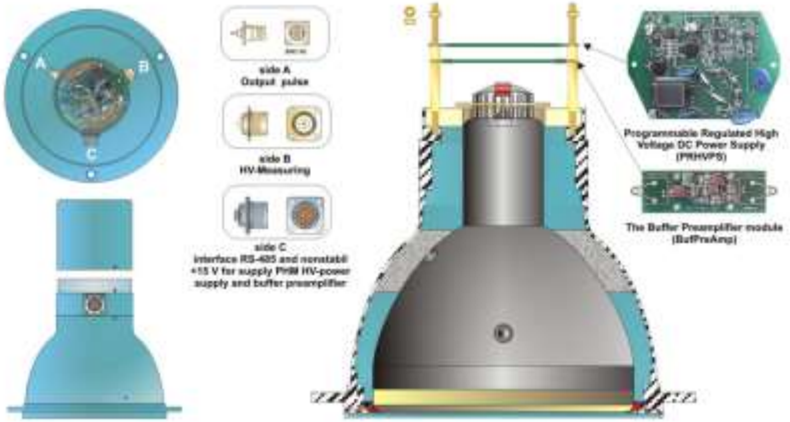

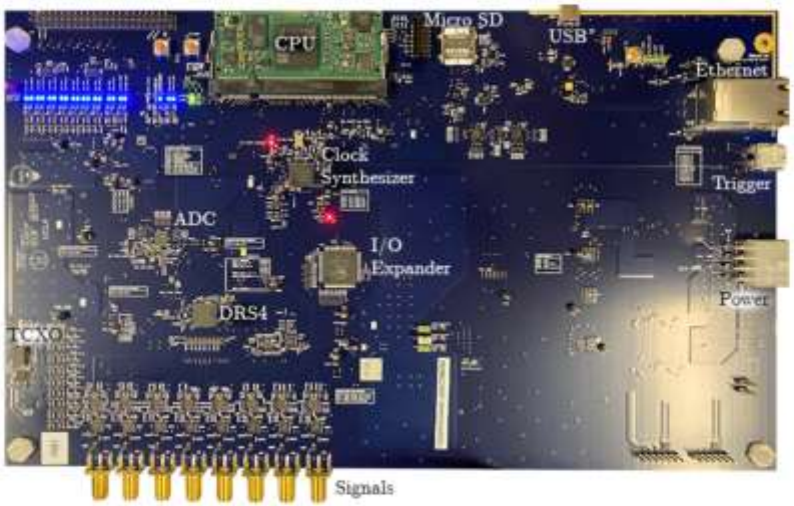

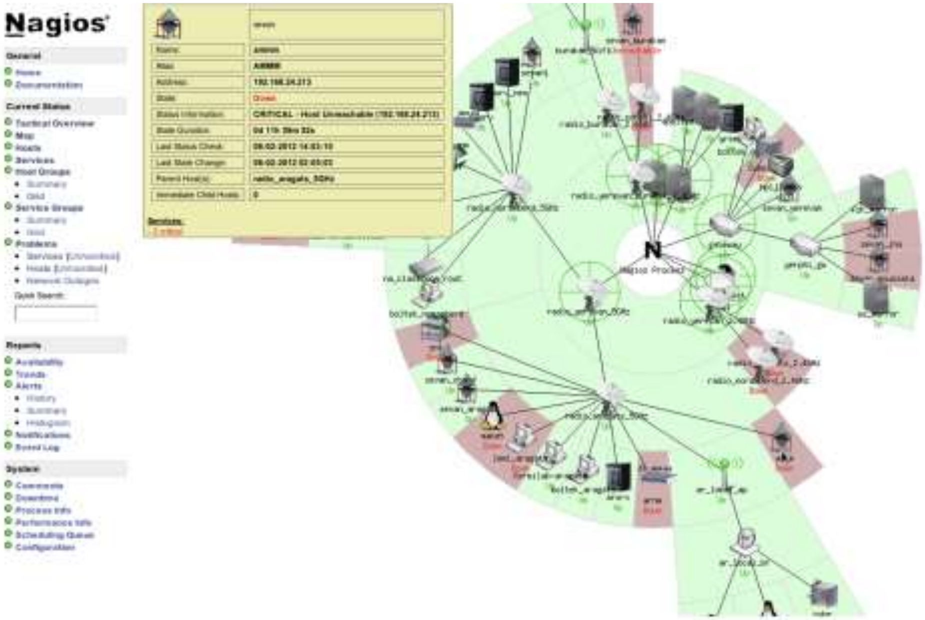

Name:	[illegible]
Alias:	[illegible]
Address:	192.168.24.213
State:	Down
Status Information:	CRITICAL - Host Unreachable (192.168.24.213)
State Duration:	0d 11h 39m 32s
Last Status Check:	08-02-2012 14:03:10
Last State Change:	08-02-2012 02:05:03
Parent Host(s):	radio_aragats_5GHz
Immediate Child Hosts:	0

Services:

LHAASO (Large High Altitude Air Shower Observatory, 4,400 meters above sea level) consists of a KM2A (1 km^2 array, electrons, muons), a WCDA (Water Cherenkov Detector Array), a WFCTA (Wide FOV Cherenkov Telescope Array)

LHAASO measures PeV gamma rays' point sources and the cosmic ray species’ spectra at high precision from 5 x 10^{13} eV to 10^{18} eV

The one square kilometer array(KM2A) consists of 5216 electromagnetic particle detectors (EDs) and 1188 muon detectors (MDs). The ED is a scintillation detector covered by a 5-mm-thick lead plate to absorb low-energy charged particles and to convert high-energy γ rays into electron-positron pairs. The MD is a water Cherenkov detector, a tank of 36 m^2 with pure water filled in. Each MD is covered by overburdened soil 2.5 m thick, which absorbs most of the secondary electron/positrons and γ rays in showers

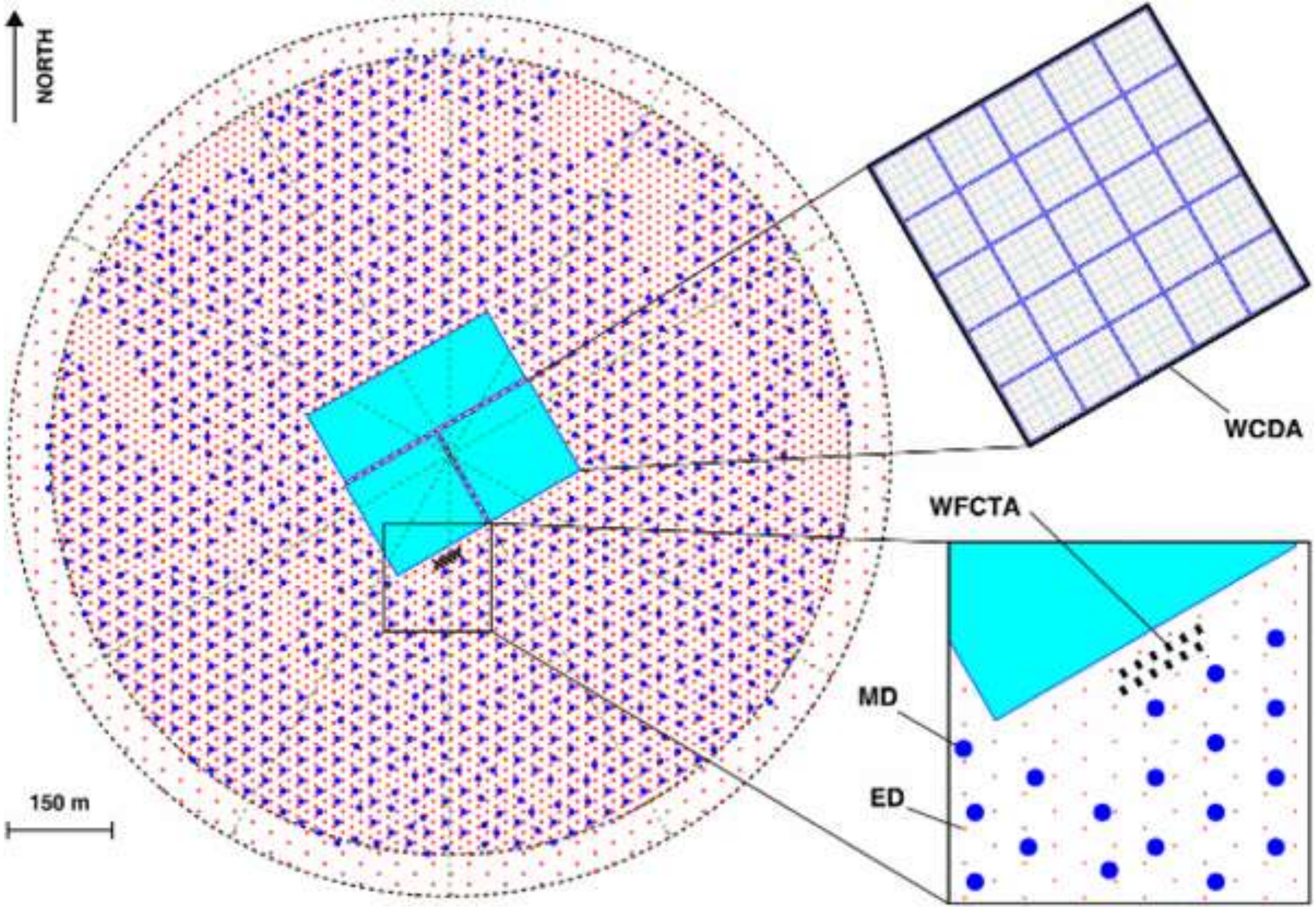

WFCTA has 18 Cherenkov telescopes. Each Cherenkov telescope consists of an array of 32 × 32 SiPMs and a $\sim 5\text{m}^2$ spherical aluminized mirror. It has a field of view (FOV) of $16^{\circ} \times 16^{\circ}$ with a pixel size of approximately $0.5^{\circ} \times 0.5^{\circ}$.

WFCTA, WCDA, and muon detectors in KM2A are combined together as a calorimeter-like complex detector to measure air shower energy and composition.

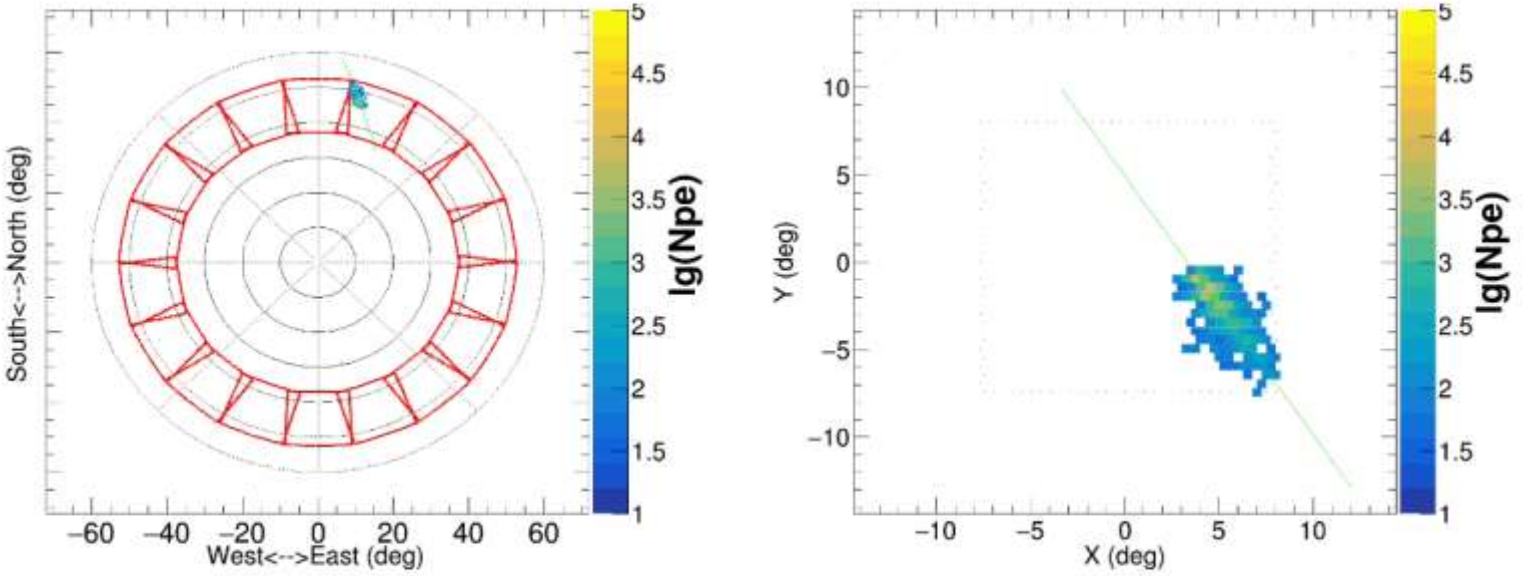

WCDA, divided into 3 separate arrays, will make survey observations on the gamma-ray sky of 100 GeV - 30TeV. The Crab Nebula has been detected with a significance of **77 σ.**

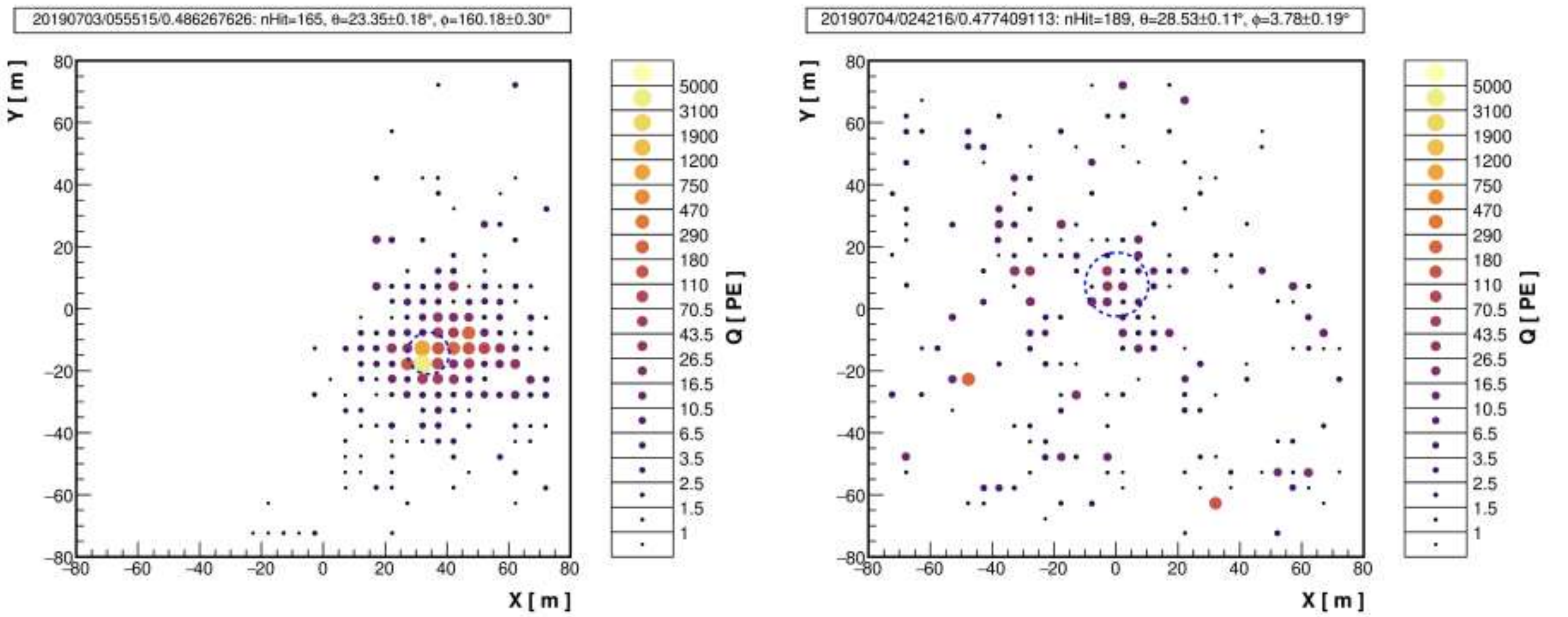

WCDA-1 is composed of 900 detector units optically separated by non-reflecting black plastic curtains. Each unit is a 5 m × 5 m cell equipped with two upward-facing PMTs on the bottom at the center of the unit. *The Cherenkov photons in each detector unit are sampled by the PMTs, thus forming a footprint of the shower.*

A gamma-ray candidate event from the direction of the Crab Nebula (left panel) and a similar background cosmic-ray event with (right panel).

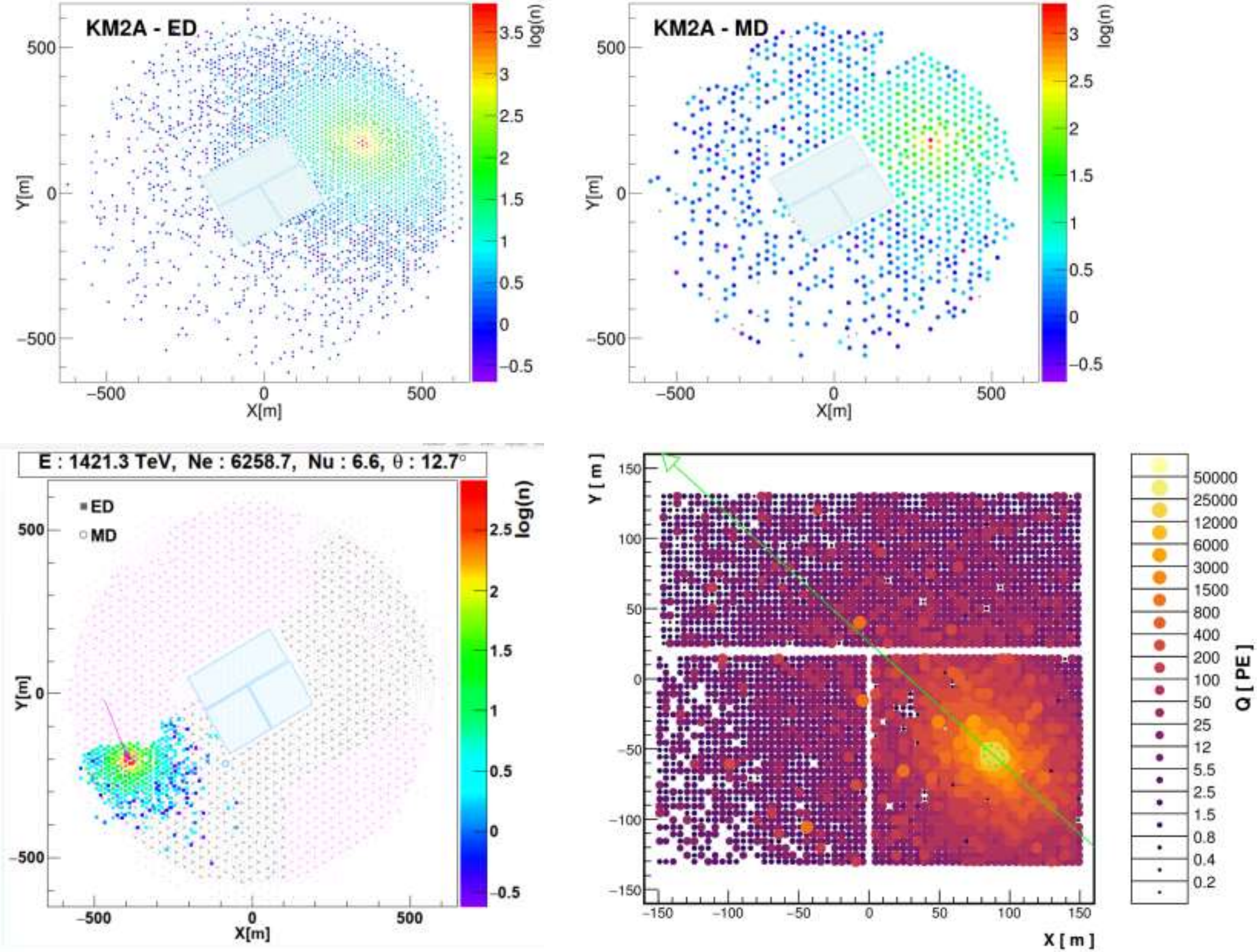

WCDA or ED array can measure the shower arrival direction with a resolution of 0.2°and shower location with a resolution of 2 m. WCDA can measure the energy flux in a range of 5 m ×5 m around shower cores. Muon detector array can measure μ content with a dynamic range of $1 - 10^4$ muons.

LHASSO can select gamma showers by muon-poor EASs

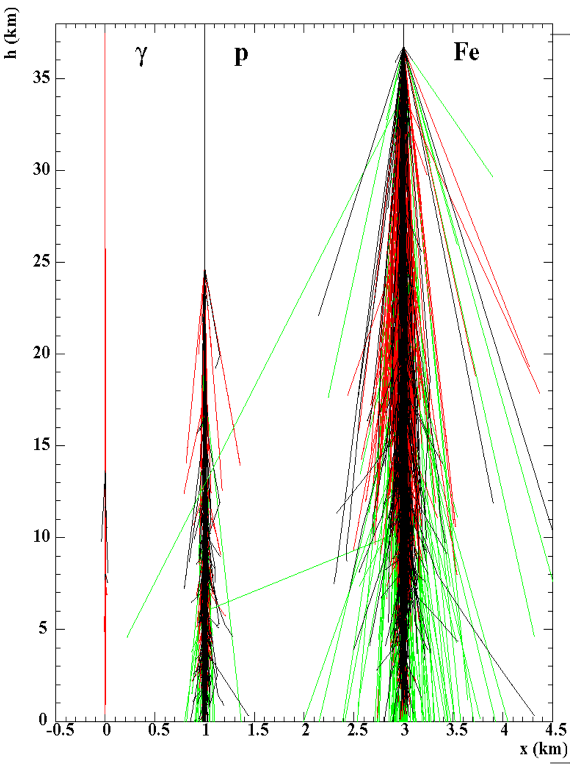

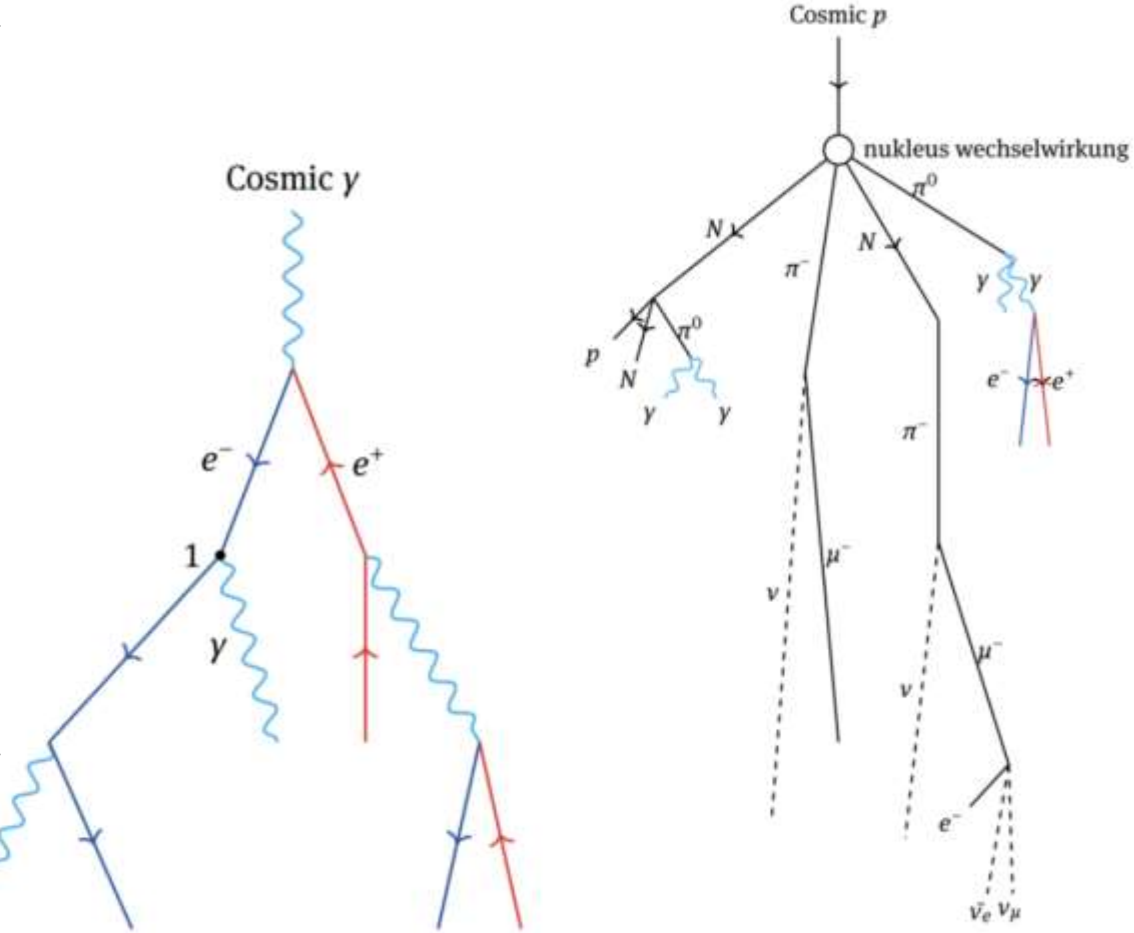

(a) Electromagnetic

(b) Hadronic

Monte Carlo Statistical Inference

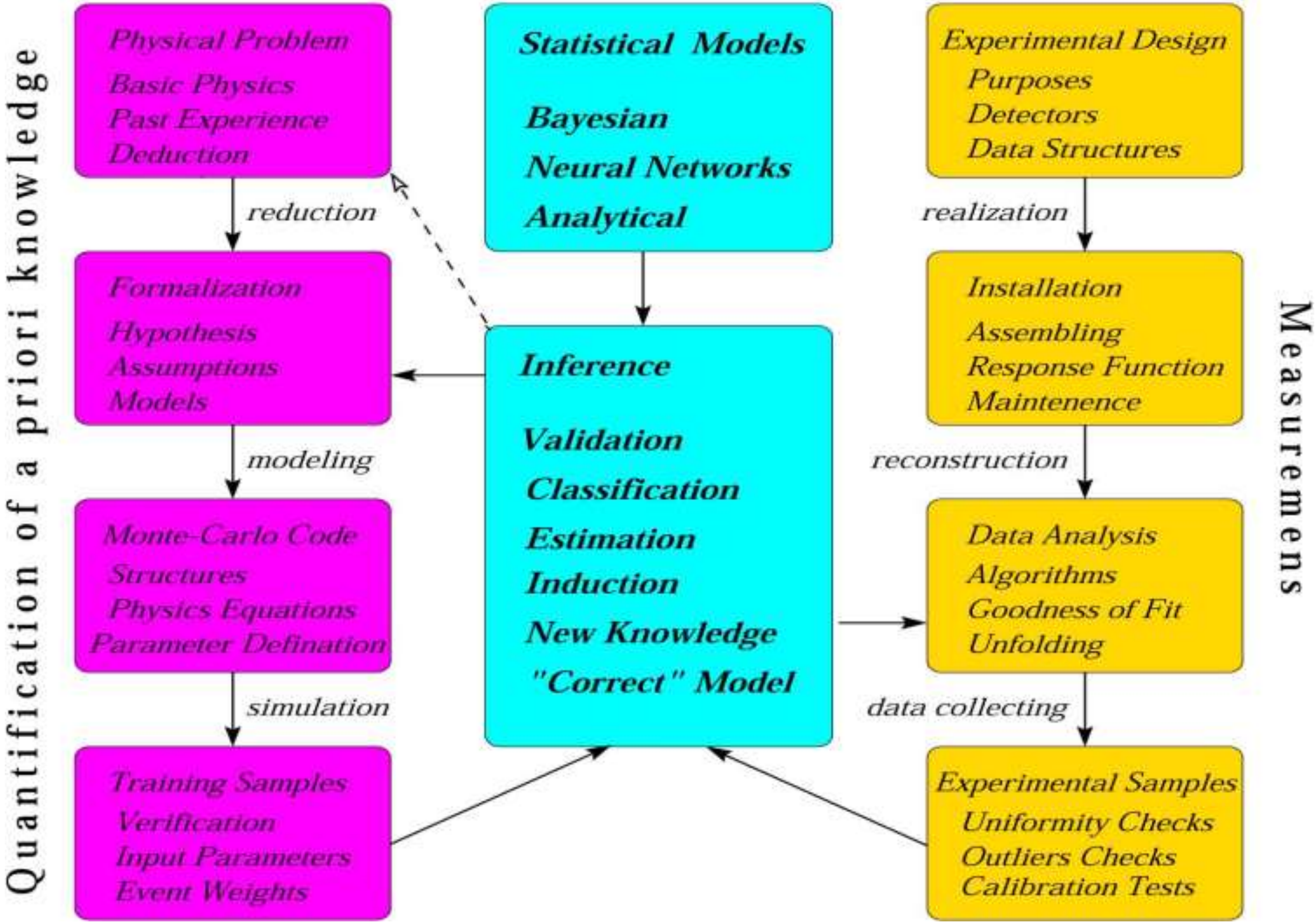

Quantification of a priori knowledge

Physical Problem
Basic Physics
Past Experience
Deduction

reduction

Formalization
Hypothesis
Assumptions
Models

modeling

Monte-Carlo Code
Structures
Physics Equations
Parameter Defination

simulation

Training Samples
Verification
Input Parameters
Event Weights

Statistical Models

Bayesian
Neural Networks
Analytical

Inference

Validation
Classification
Estimation
Induction
New Knowledge
"Correct" Model

Experimental Design
Purposes
Detectors
Data Structures

realization

Installation
Assembling
Response Function
Maintenence

reconstruction

Data Analysis
Algorithms
Goodness of Fit
Unfolding

data collecting

Experimental Samples
Uniformity Checks
Outliers Checks
Calibration Tests

Measuremens

Classification of primary hadron to light and heavy nuclei

Suppose data sample with two types of events: Protons and Iron nuclei obtained from the simulation – solving direct problem of CR!

- *We have found discriminating input parameters Ne and Nmu*
- *What decision boundary should we use to select Iron nuclei ?*

Rectangular cuts? ***A linear boundary?*** ***A nonlinear one?***

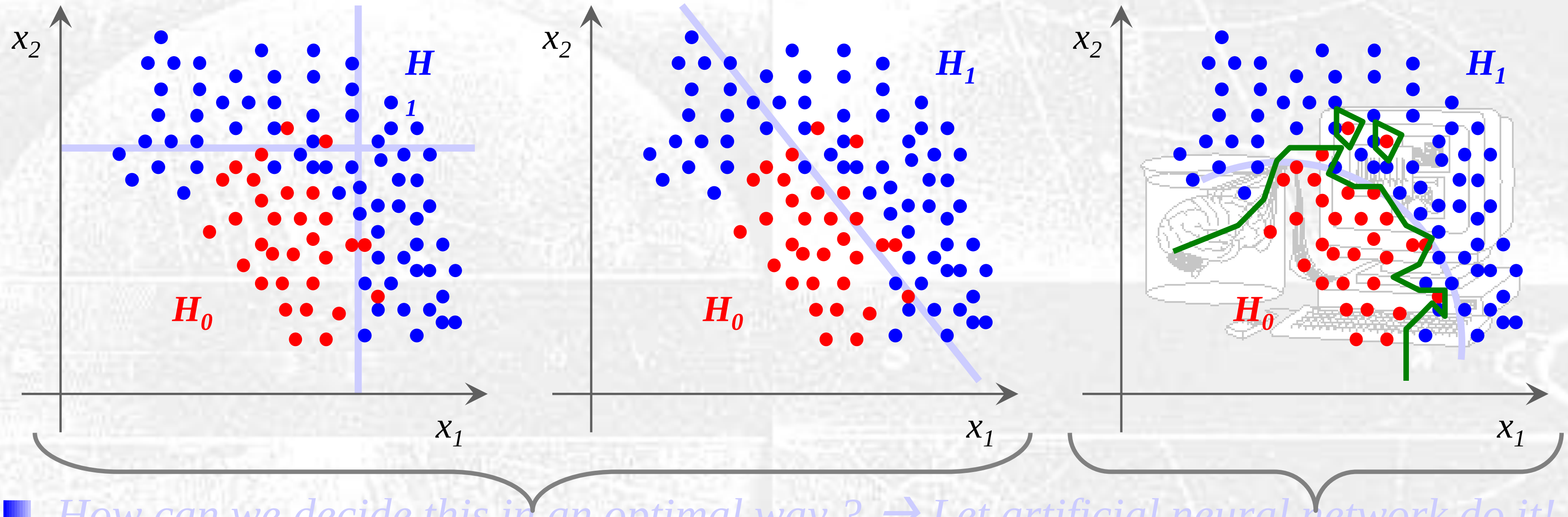

- *How can we decide this in an optimal way ? → Let artificial neural network do it!*
- *We need training samples – training with teacher – simulations, direct CR problem*

Neural Network (NN) 2-way Classification of EAS data (purity-efficiency plots)

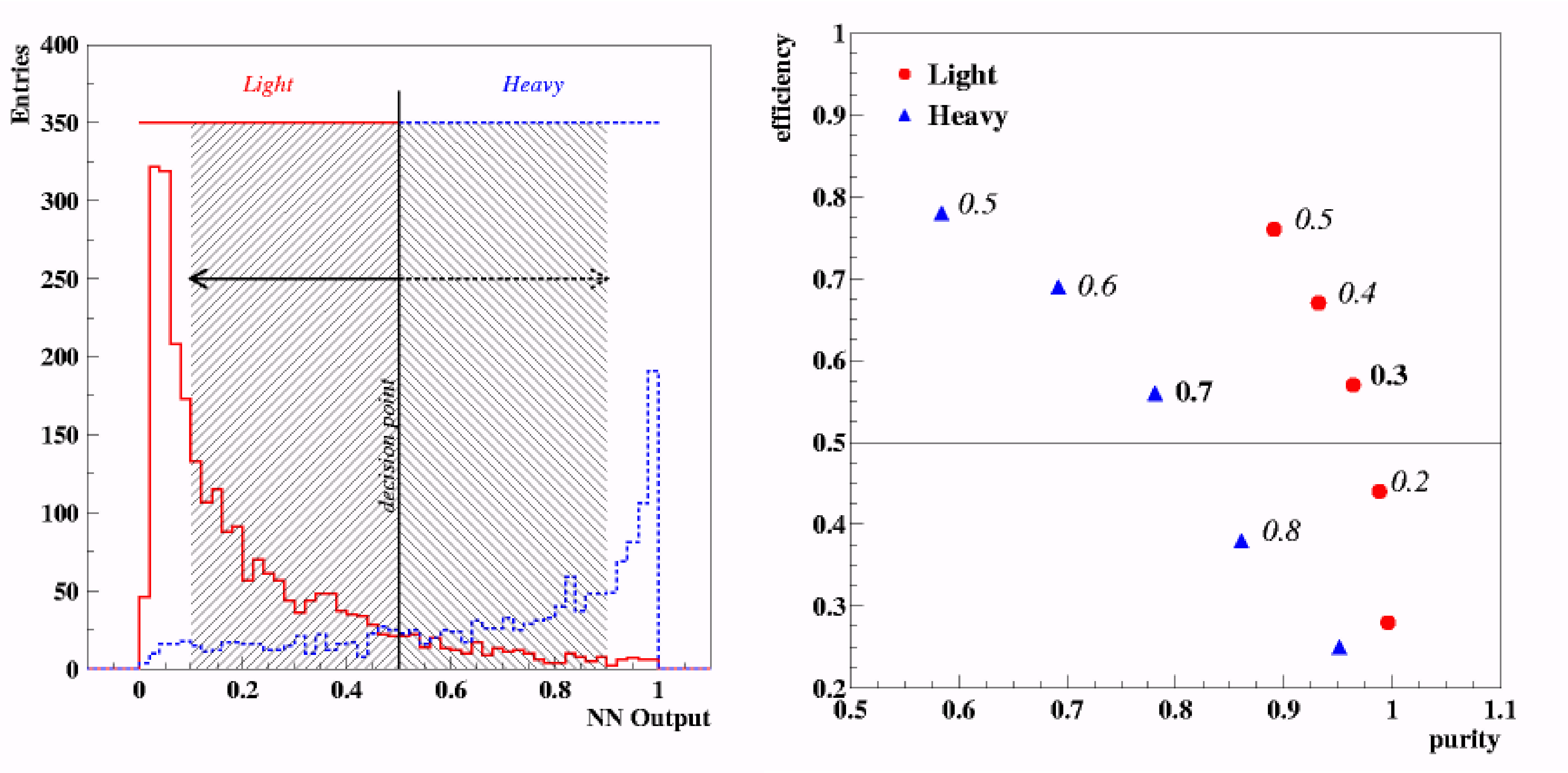

Neural classification of the all particle energy spectra to Light and Heavy Nuclei

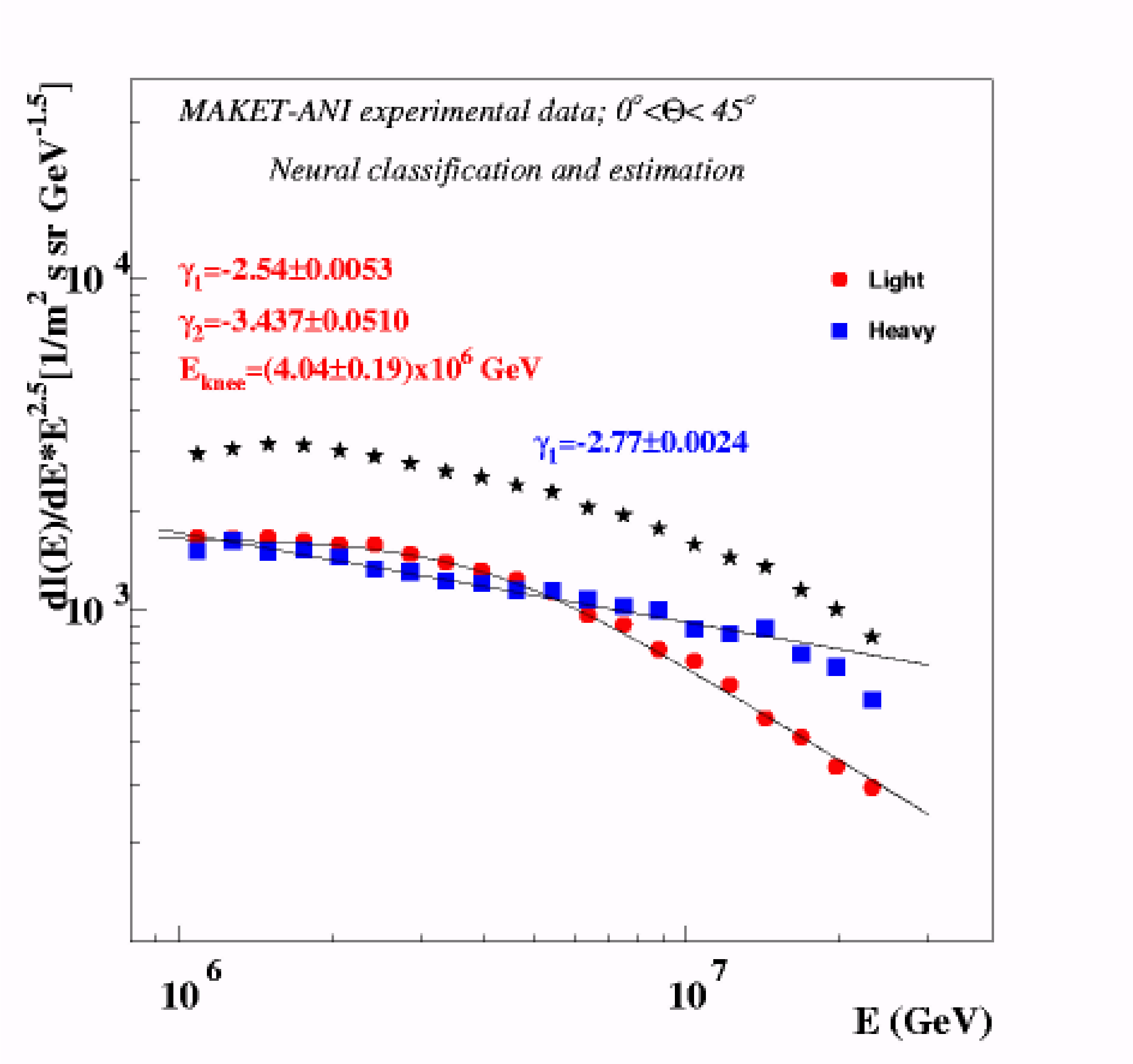

Credit, Chilingarian A., Hovsepyan G. et.al., (2004), ApJ, 603, L29

3-way KASCADE Data Classification

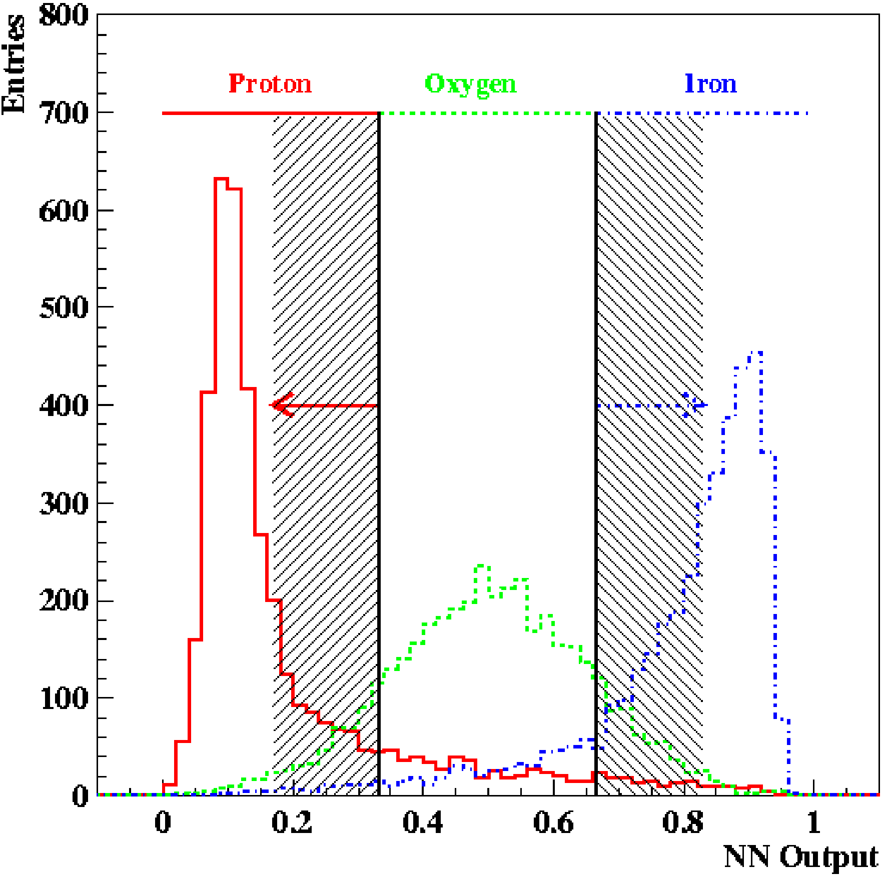

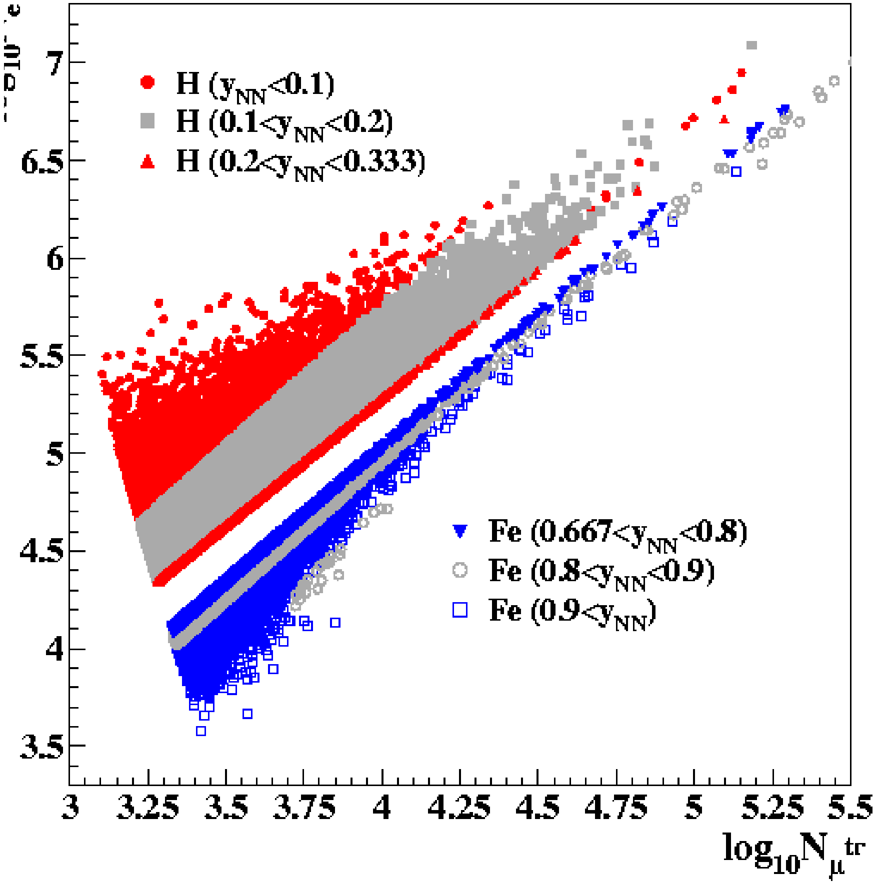

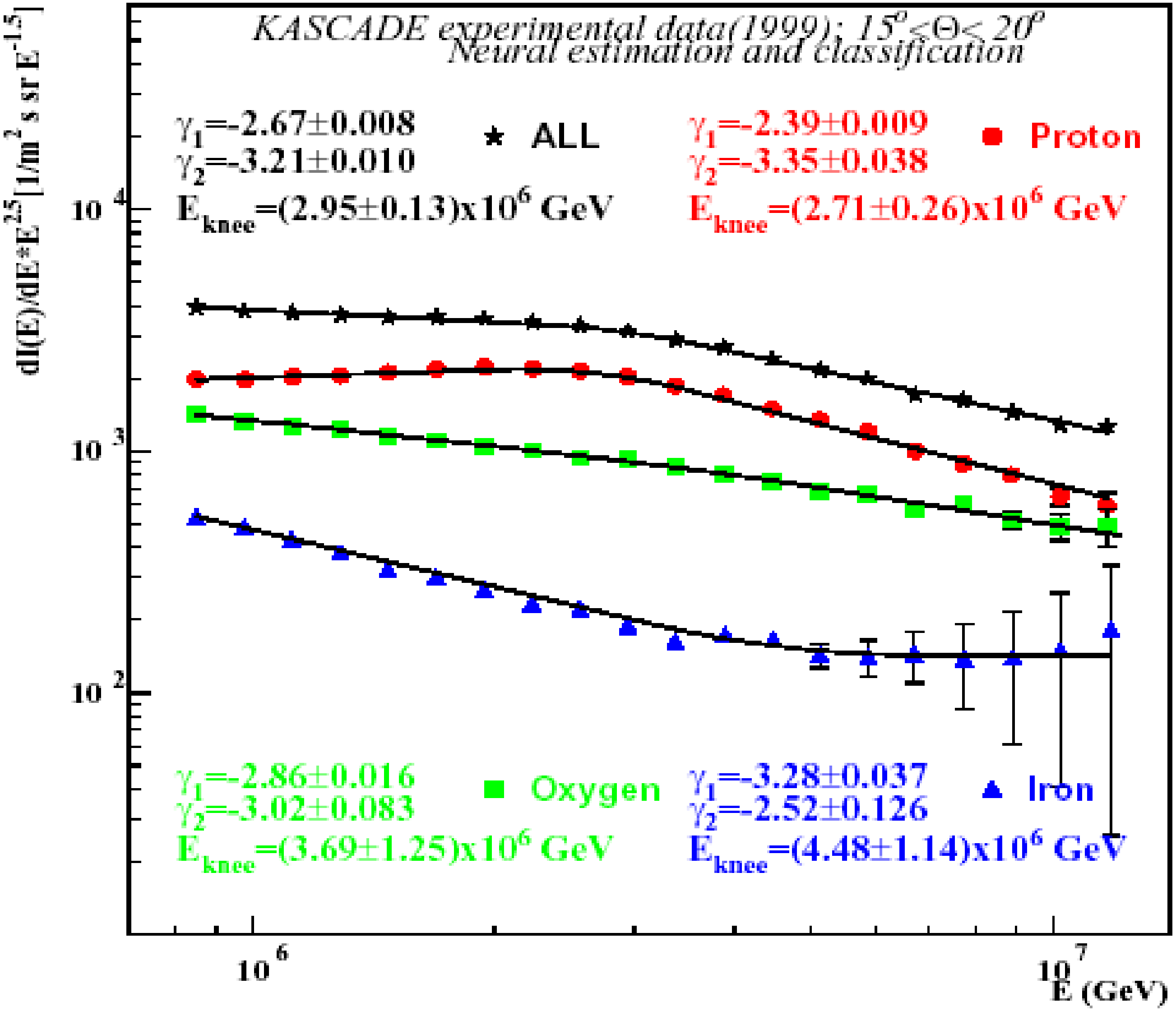

Credit, Vardanyan A., A.Chilingarian , M.Roth for the KASCADE collaboration, (1999), in Proceedings of the workshop ANI 99, Nor-Amberd, 1999, Preprint FZK 672, p.23.

Significant emission > 100 TeV

Cao+ (2021) Nature 594 33

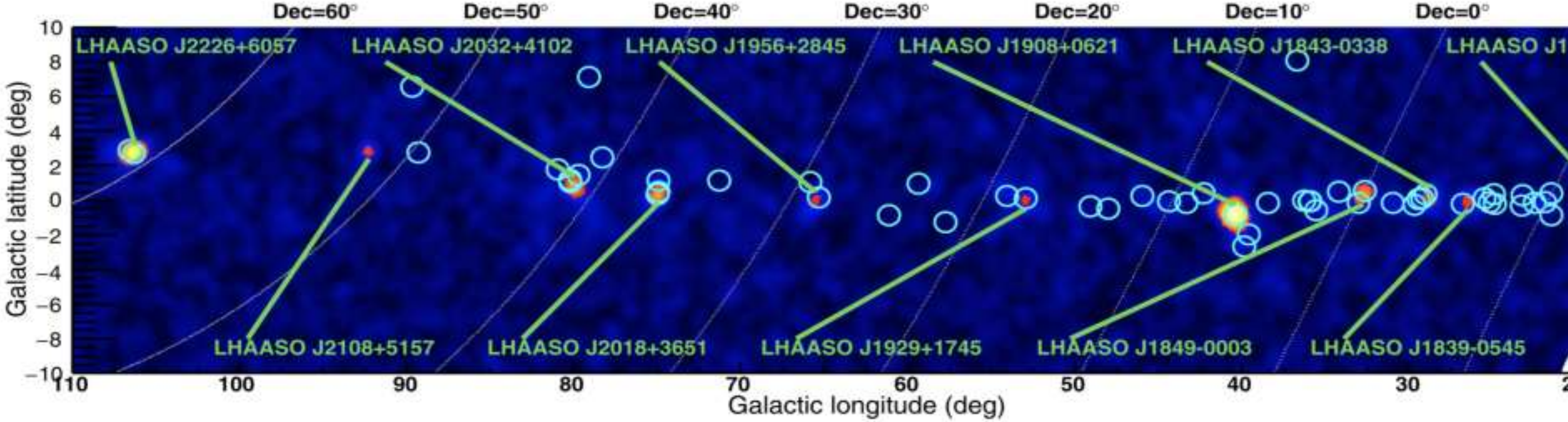

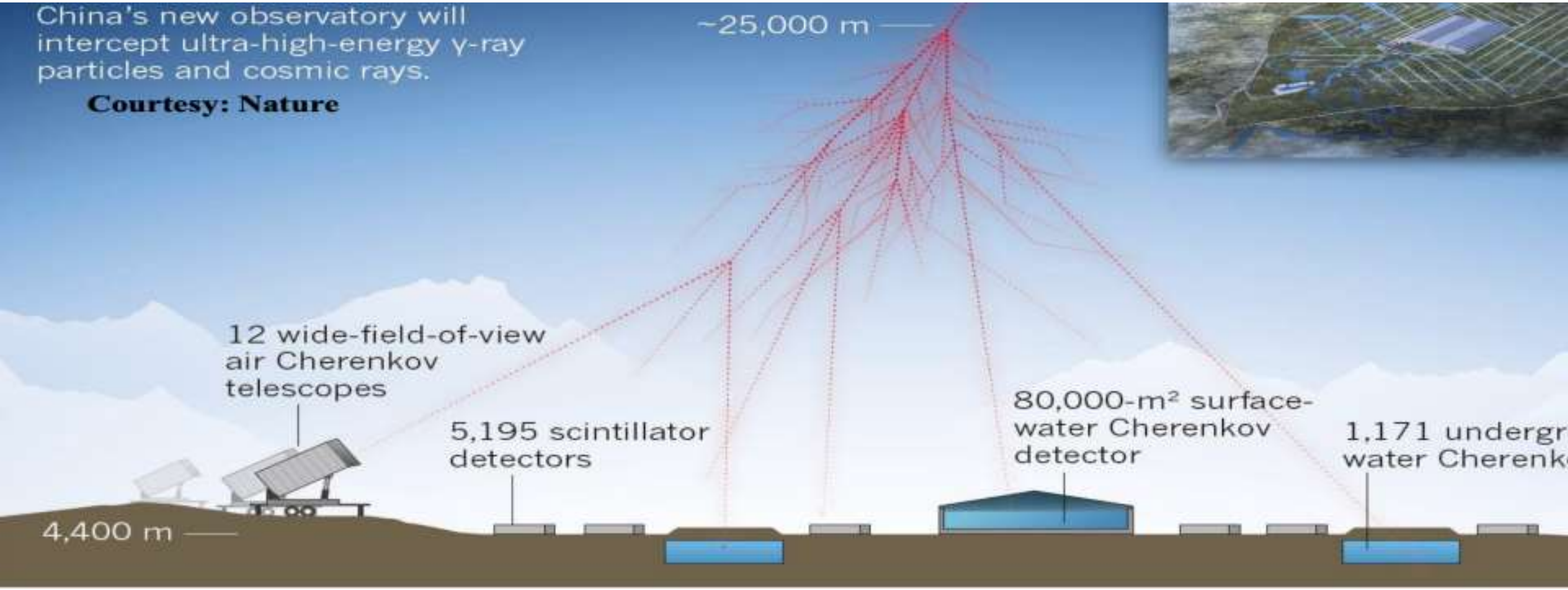
China's new observatory will intercept ultra-high-energy γ-ray particles and cosmic rays.

Courtesy: Nature

CR origin: Hadronic and leptonic models of ultra-high energy gamma rays

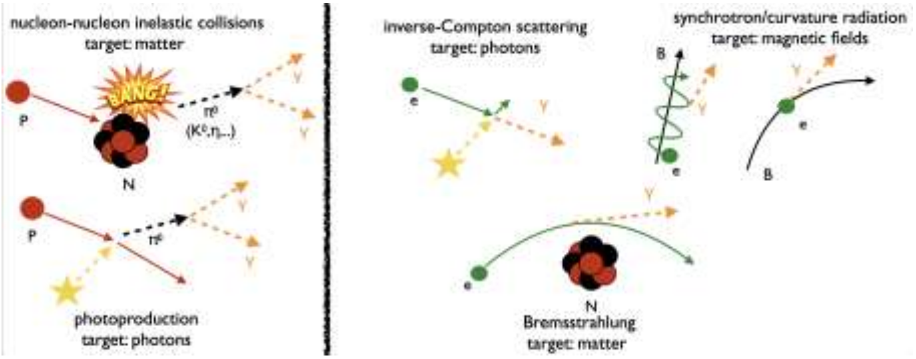

Multiwavelength (MWL) spectral energy distribution (SED).

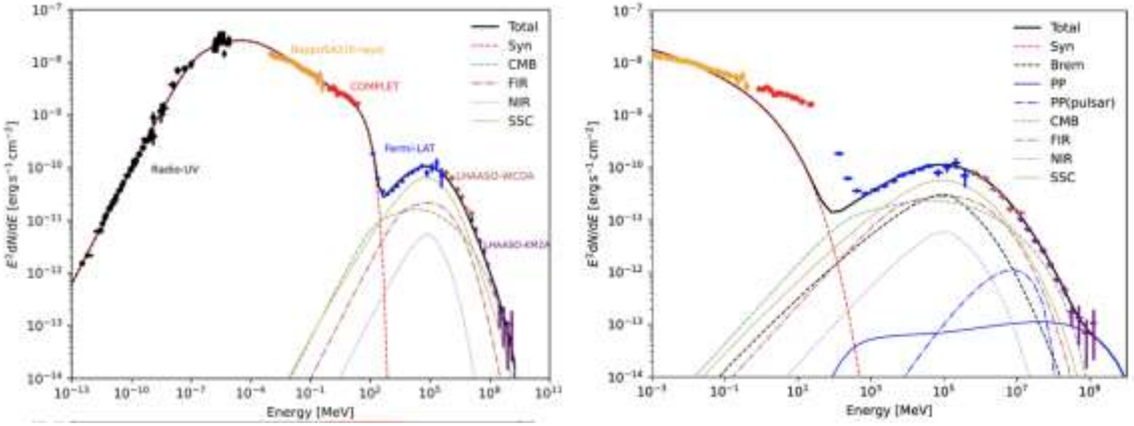

Multi-wavelength Spectral Energy Density of the Crab nebula, from radio to PeV. A fit for pure leptonic model on the left. On the right, a fit to the non-thermal data, only, with a leptonic+hadronic production model.

The observations of the Crab Nebula, (the standard candle for γ-ray astronomy) led for the first time to an extension of the Crab spectral energy distribution up to the PeV, showing inconsistency with the pure leptonic model of the Crab emission. The contribution of hadronic interaction is hardly constrained at the highest energy, where they seem to contribute especially in the energy range exceeding the PeV. More statistics will clearly clarify the picture and LHAASO expect about 1-2 PeV γ-ray per year.

Nie L, Liu Y, Jiang Z and Geng X 2022 The Astrophysical Journal 924 42 URL https://doi.org/10.3847/1538-4357/ac348d

The MAGIC Telescopes: 2 x 17m Ø IACTs

@ the Frontier of VHE γ-Ray Astro-Physics

ORM @ ENO,
2200 m a.s.l.

F/D=1; inter-telescope distance = 85m

La Palma,
Canary Islands,
Spain

Imaging Cherenkov Telescope

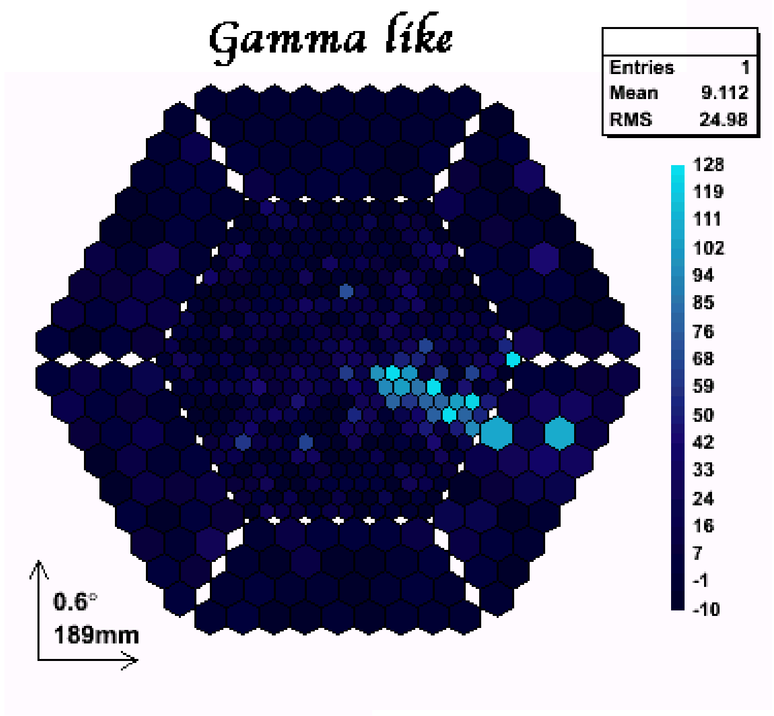

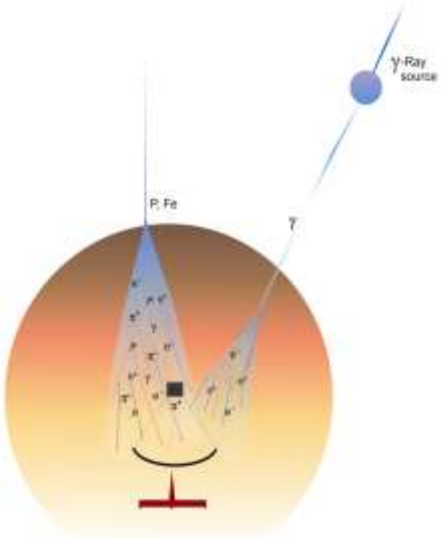

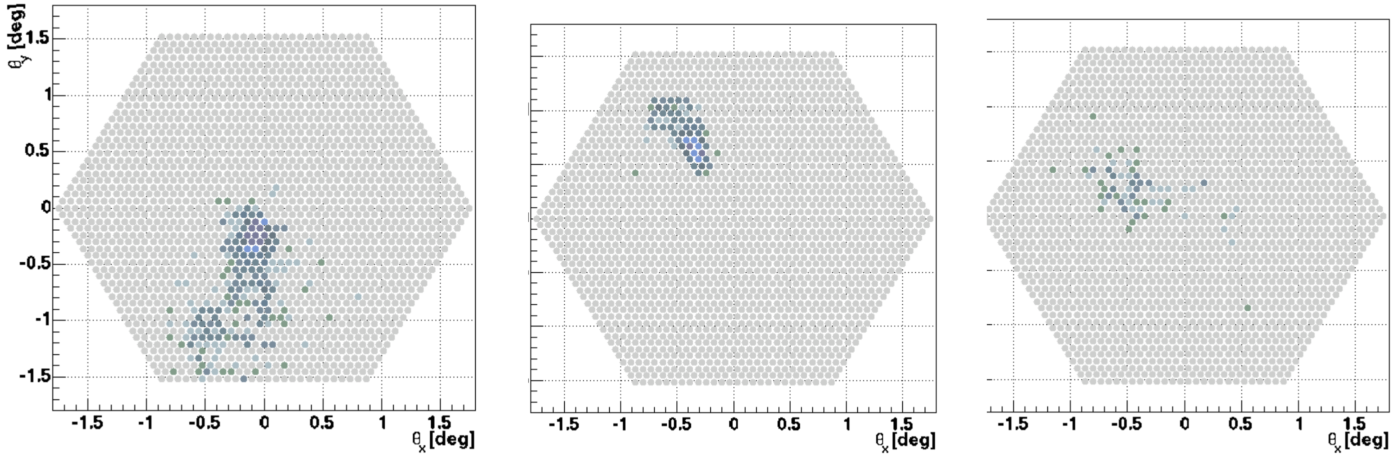

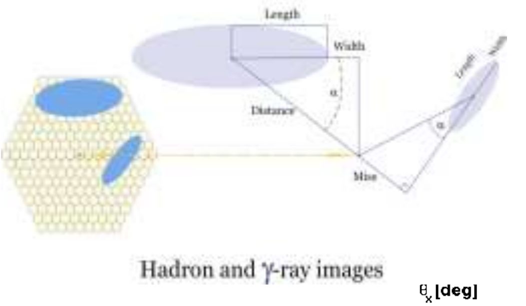

Hadron and γ-ray images

New Type of NN – Mapping Networks - Maximizing Signal Significance – by optimizing the shape of Gamma Domain

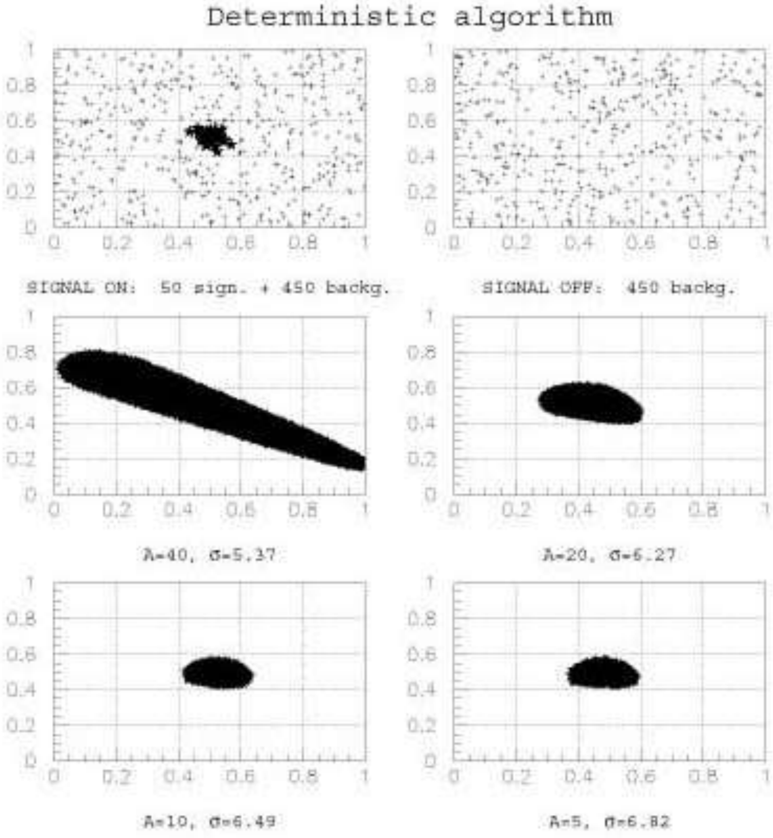
Deterministic algorithm

SIGNAL ON: 50 sign. + 450 backg.

SIGNAL OFF: 450 backg.

A=40, σ=5.37

A=20, σ=6.27

A=10, σ=6.49

A=5, σ=6.82

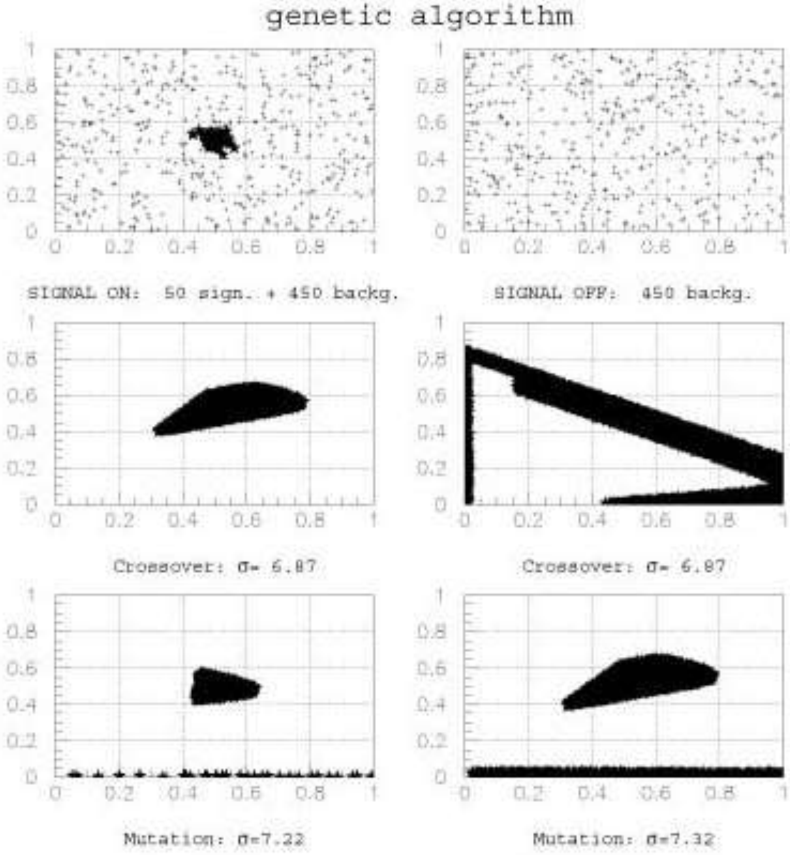
genetic algorithm

SIGNAL ON: 50 sign. + 450 backg.

SIGNAL OFF: 450 backg.

Crossover: σ= 6.87

Crossover: σ= 6.87

Mutation: σ=7.22

Mutation: σ=7.32

The Cherenkov Telescope Array (CTA) is the next-generation ground-based observatory for gamma-ray astronomy at very-high energies. With more than 100 telescopes located in the northern and southern hemispheres, CTA will be the world's largest and most sensitive high-energy gamma-ray observatory

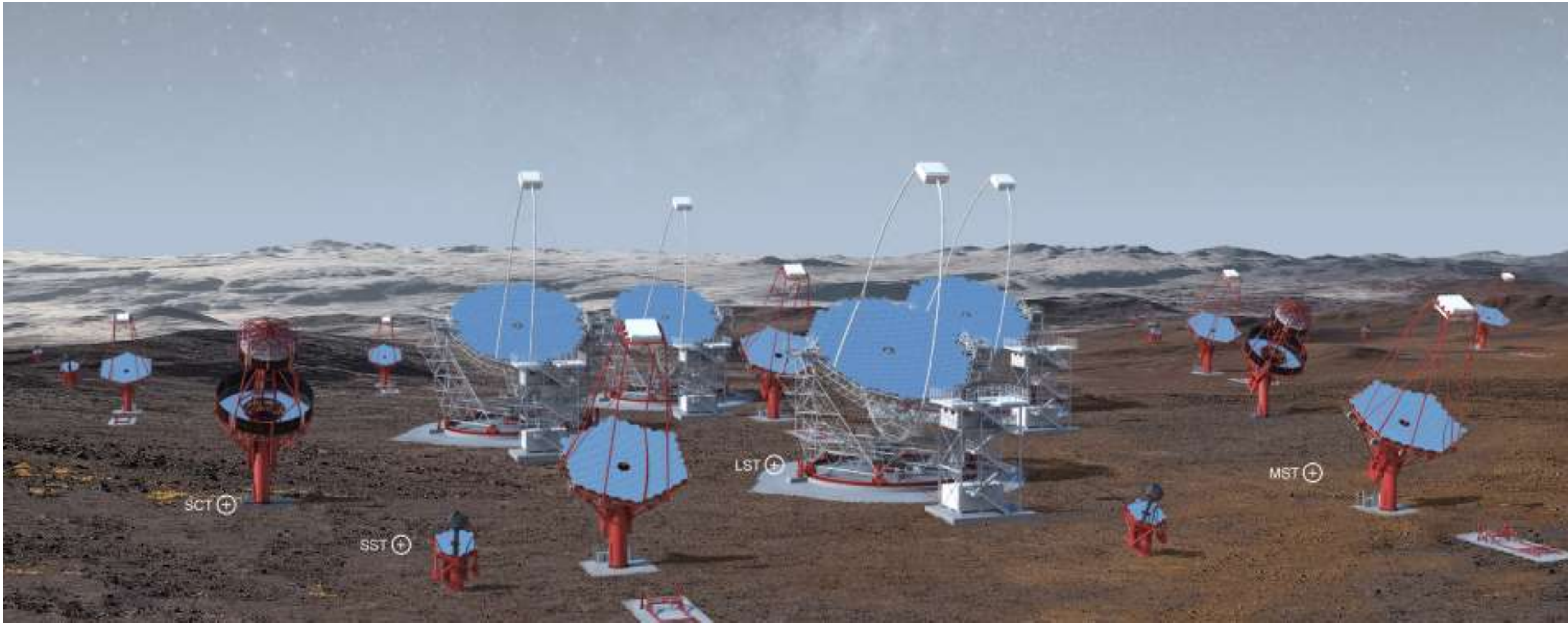

Four Large-Sized Telescopes (LST, 23m, 400 m^2) will be arranged at the centre of the northern hemisphere array at Canarias to cover the unique low energy sensitivity of Cherenkov Telescope Array (CTA) between 20 and 150 GeV.

The structure of the Universe: how the shape changed from uniform (flattened by radiation) to a connected network?

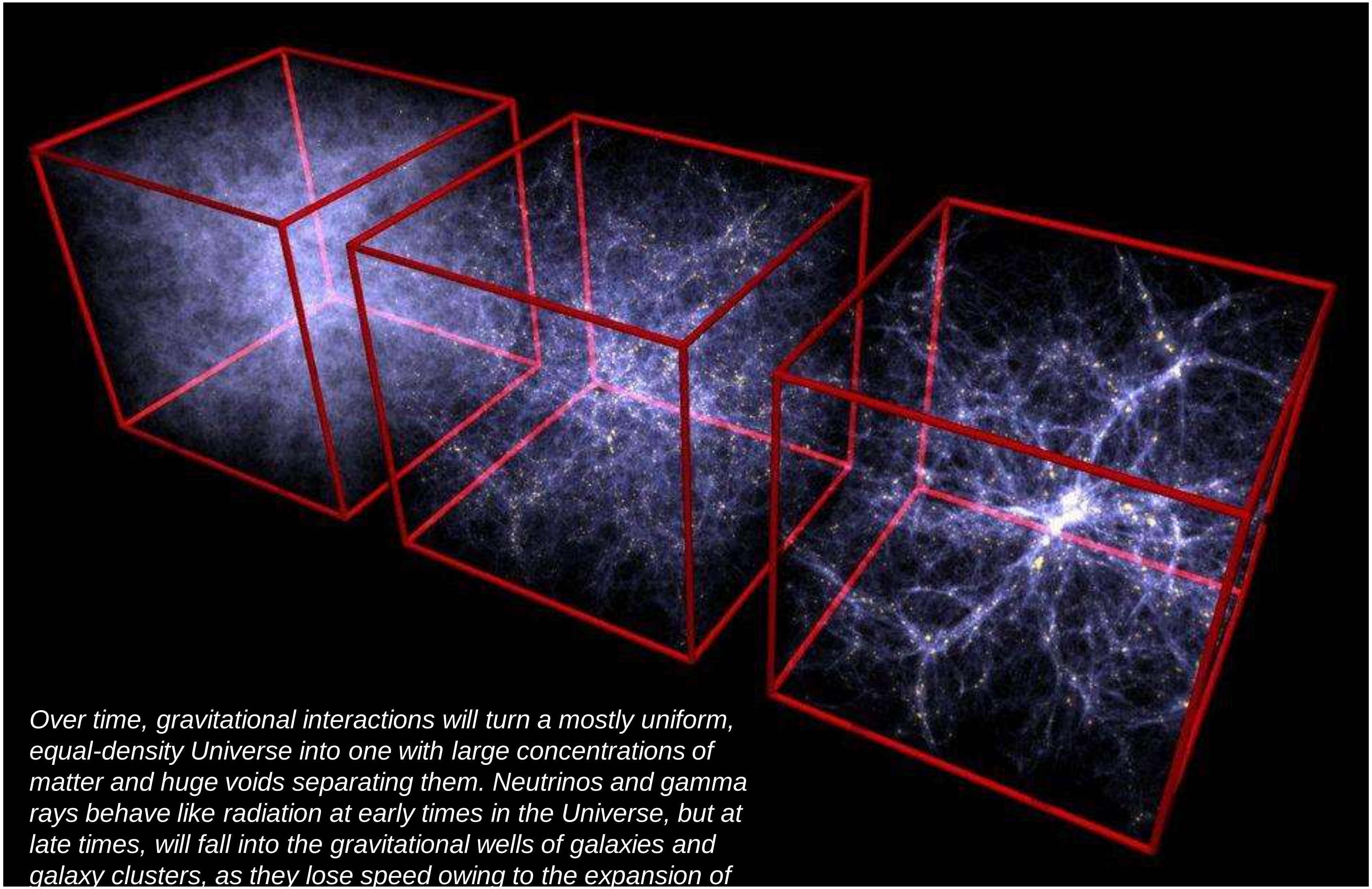

Over time, gravitational interactions will turn a mostly uniform, equal-density Universe into one with large concentrations of matter and huge voids separating them. Neutrinos and gamma rays behave like radiation at early times in the Universe, but at late times, will fall into the gravitational wells of galaxies and galaxy clusters, as they lose speed owing to the expansion of

The cosmic web that we see, the largest-scale structure in the entire Universe, is dominated by dark matter. On smaller scales, however, baryons can interact with one another and with photons, leading to the stellar structure but also leading to the emission of energy that can be absorbed by other objects. Neither dark matter nor dark energy can accomplish that task; our Universe must possess a mix of dark matter, dark energy, and normal matter

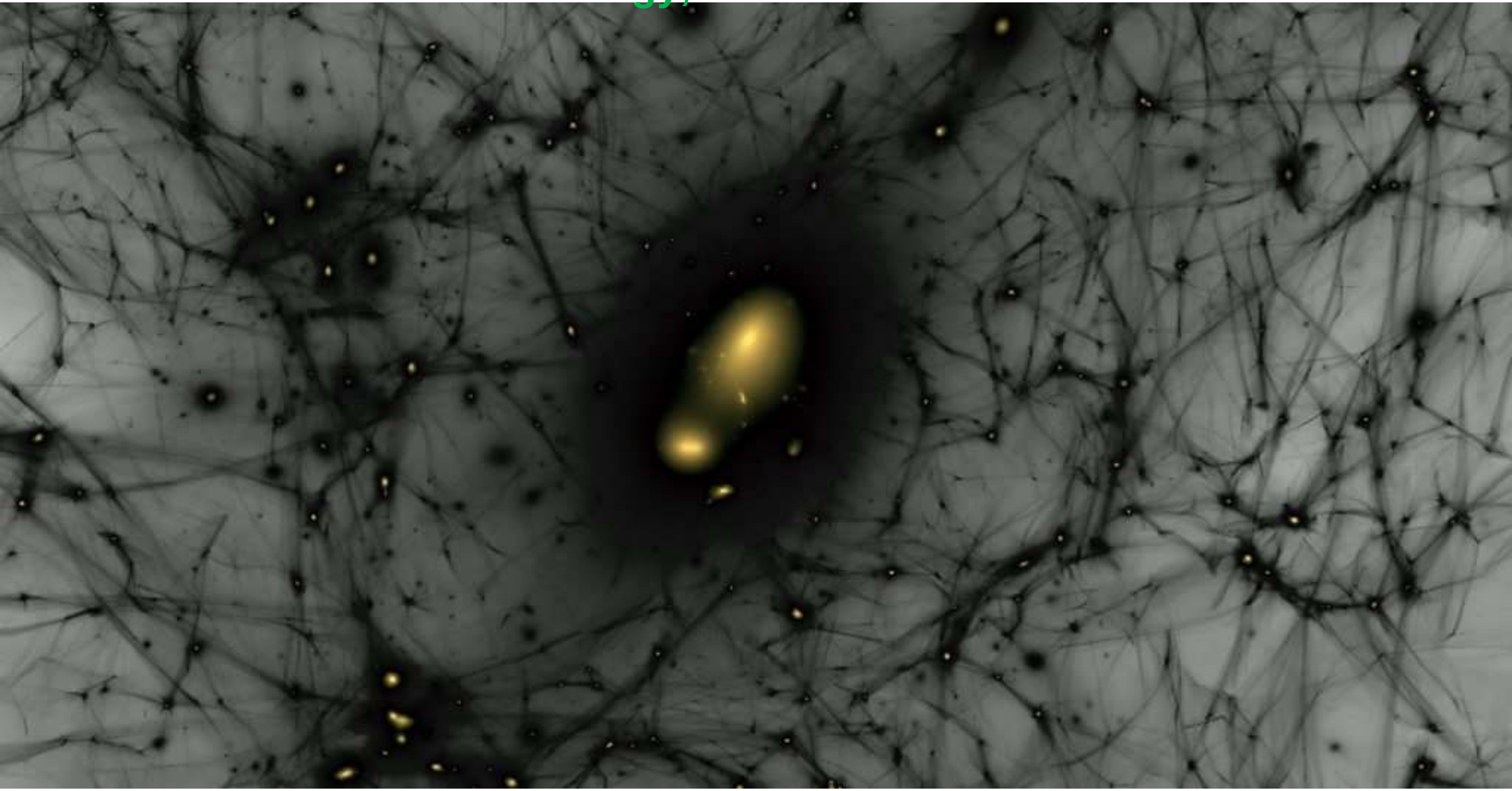

In a talk given in 1884, [Lord Kelvin](#) estimated the number of dark bodies in the [Milky Way](#) from the observed velocity dispersion of the stars. A publication from 1930 points to Swedish [Knut Lundmark](#) being the first to realize that the universe must contain much more mass than we can observe. Dutchman and radio astronomy pioneer [Jan Oort](#) also hypothesized the existence of dark matter in 1932. In 1933, Swiss astrophysicist [Fritz Zwicky](#), applied the [virial theorem](#) to the [Coma Cluster](#) and obtained evidence of unseen mass he called dunkle Materie ('dark matter'). Further indications of [mass-to-light ratio](#) anomalies came from measurements of galaxy rotation curves, 1939, [Horace W. Babcock](#).

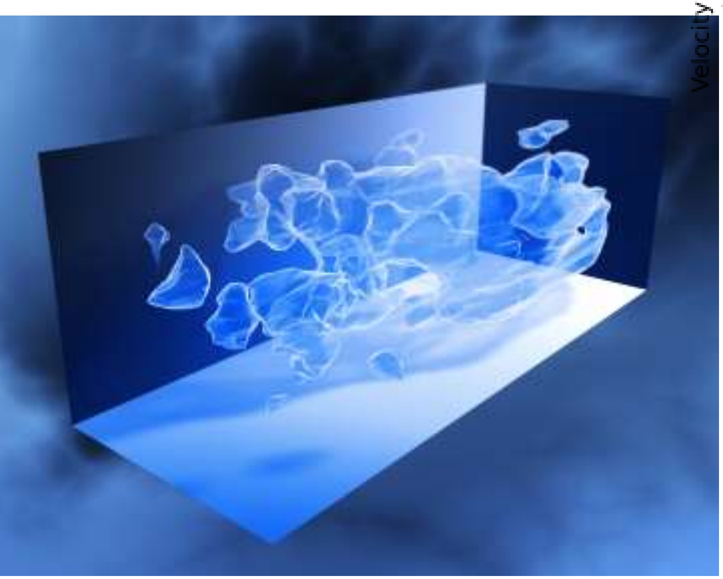

Large-scale distribution of dark matter from [weak gravitational lensing](#) by the [Hubble Space Telescope](#).

CMB temperature fluctuations: $\delta T/T \sim 10^{-5}$, $\delta T/T \sim 10^{-3} - 10^{-4}$ are required. Planck's results affirm that about 27% of the energy-matter density is in the form of dark matter, while only 5% is in the form of ordinary matter.

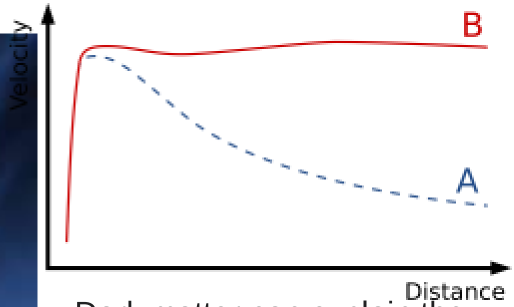

Dark matter can explain the 'flat' appearance of the velocity curve out to a large radius.

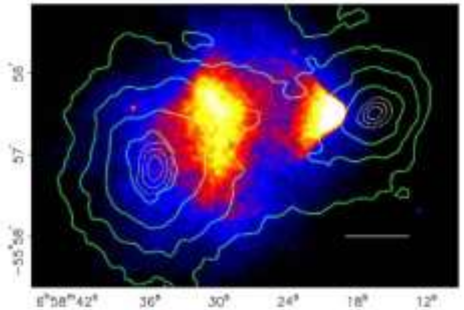

Images of the Bullet cluster merging with the mass distribution reconstructed using weak gravitational lensing (green contours) . X-ray image of the bullet cluster (colored regions: blue least dense to white most dense), taken by the Chandra

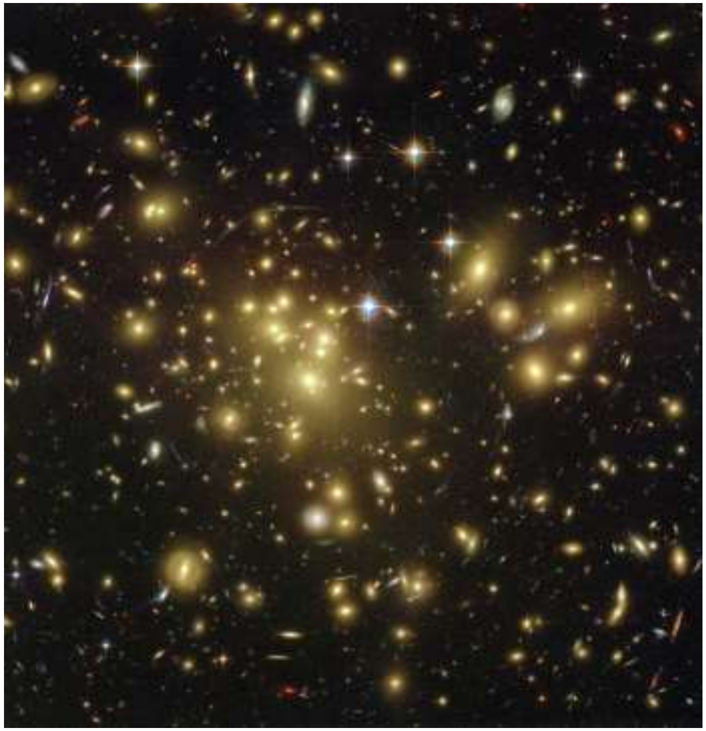

Strong gravitational lensing as observed by the [Hubble Space Telescope](#) in [Abell 1689](#) indicates the presence of dark matter

Searches of the Dark Matter (DM)

- Exploring and confirming the DM would require it to interact with the ordinary matter in an alternative way other than gravitationally.
- The direct detection method looks for scattering events of DM particles with underground ordinary matter targets.
- DM searches at colliders to look for hints of the production of DM particles in ordinary matter collisions (possibly PeV colliders, not TeV will be needed).
- Astrophysics approach: looking for DM decay from different regions of the Galaxy (assuming that the flux will be larger from the denser regions)
- Obtaining no signals of DM from all experiments physicists establish tight upper limits reaching now a lifetime of 10^{29} s
- Estimates of DM mass vary within 50 orders of magnitude

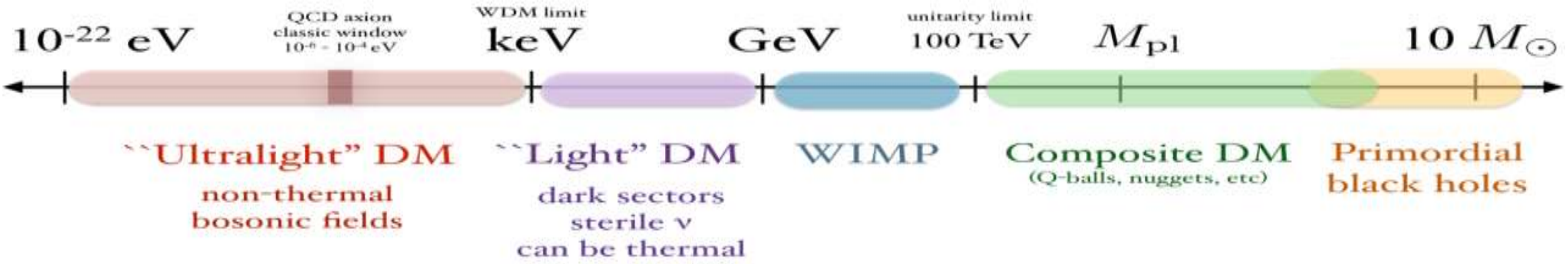

Attempts to Detect Dark Matter Decay with Tibet ASγ

Finding no such signs, the search puts an upper limit on the decay rate of dark matter particles with masses in the PeV range.

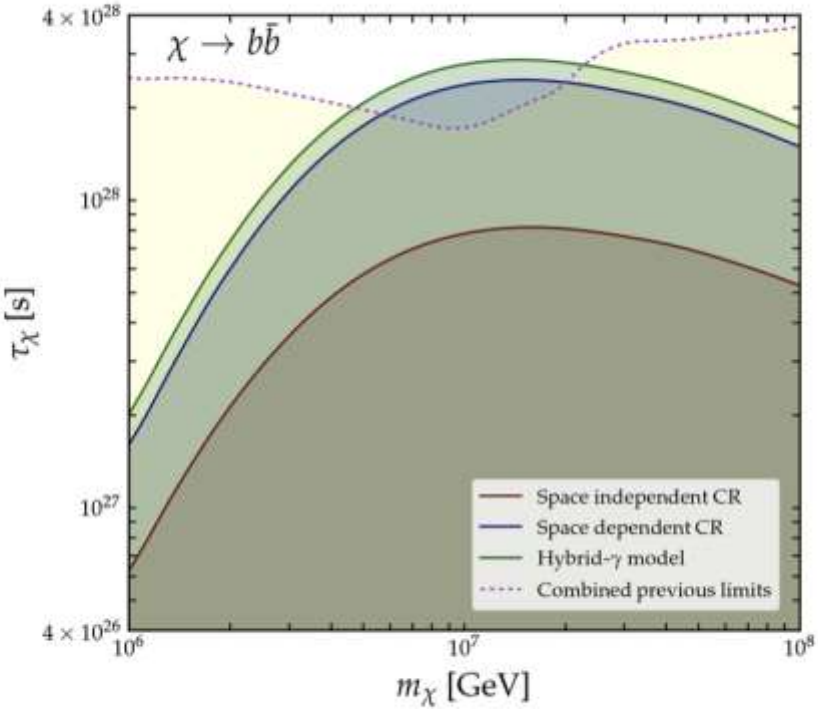

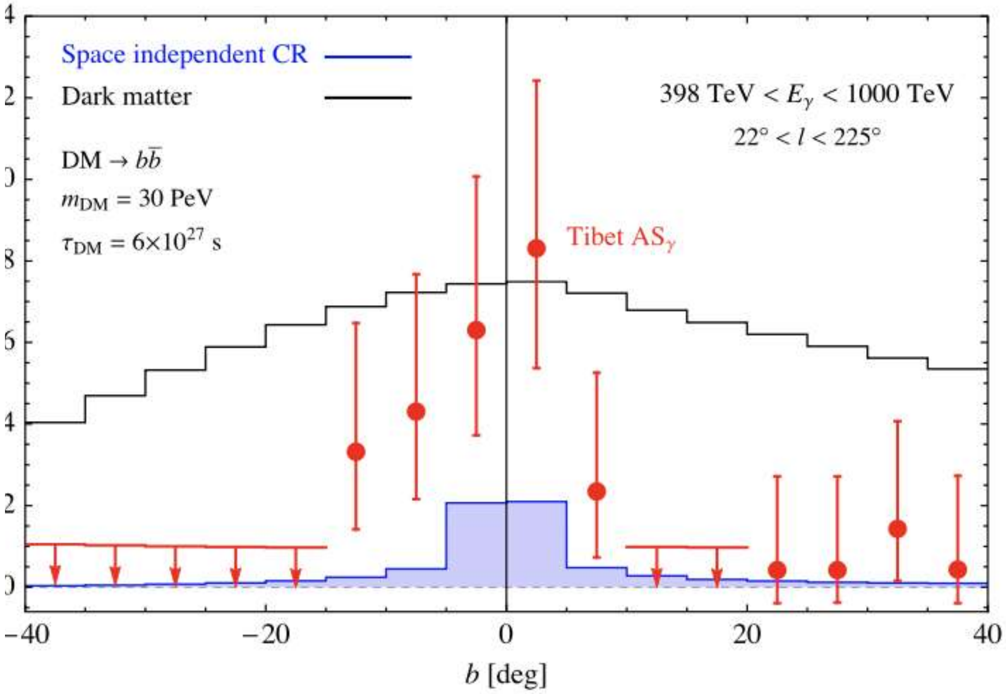

The upper limit on DM lifetime as a function of its mass

According to mass models of the Milky Way, dark matter density should be greatest near the Galactic Center. Thus, if decaying dark matter produces high-energy gamma rays, the measured flux should vary between survey areas. As no such difference was detected, the researchers conclude that PeV-mass dark matter has a lifetime of at least $6*10^{27}$ s.

Tibet ASγ experiment consists of some 700 *scintillators* spread over an area of 65,700 square meters at an altitude of 4,300 meters (14,000 feet) near Yangbajing in Tibet. To distinguish gamma-ray-induced air showers from similar events produced by cosmic rays, the observatory also contains an underground array of 64 muon detectors.

[74] Tarak Nath Maity, Akash Kumar Saha ,Abhishek Dubey et al., PHYSICAL REVIEW D 105, L

Constraints on Heavy Dark Matter from 570 Days of LHAASO Observations: we find no excess of dark matter signals, and thus place some of the strongest γ-ray constraints on the lifetime of heavy dark matter particles with a mass between 10^5 and 10^9 GeV.

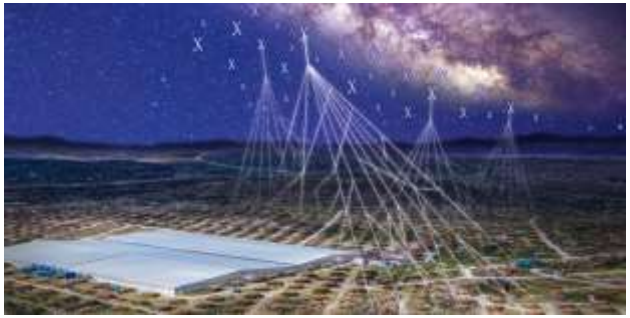

Recently, new DM constraints [74] were obtained by considering the Tibet-ASγ data along the Galactic plane; our constraints are generally stronger by about one order of magnitude than their model-independent limit. Our limits are subject to overall systematic uncertainties, estimated to be 21%, which is a quadrature sum of uncertainties from the detector response (~7%) and γ/hadron separation procedure (~20%), and model error. These uncertainties would not affect physical

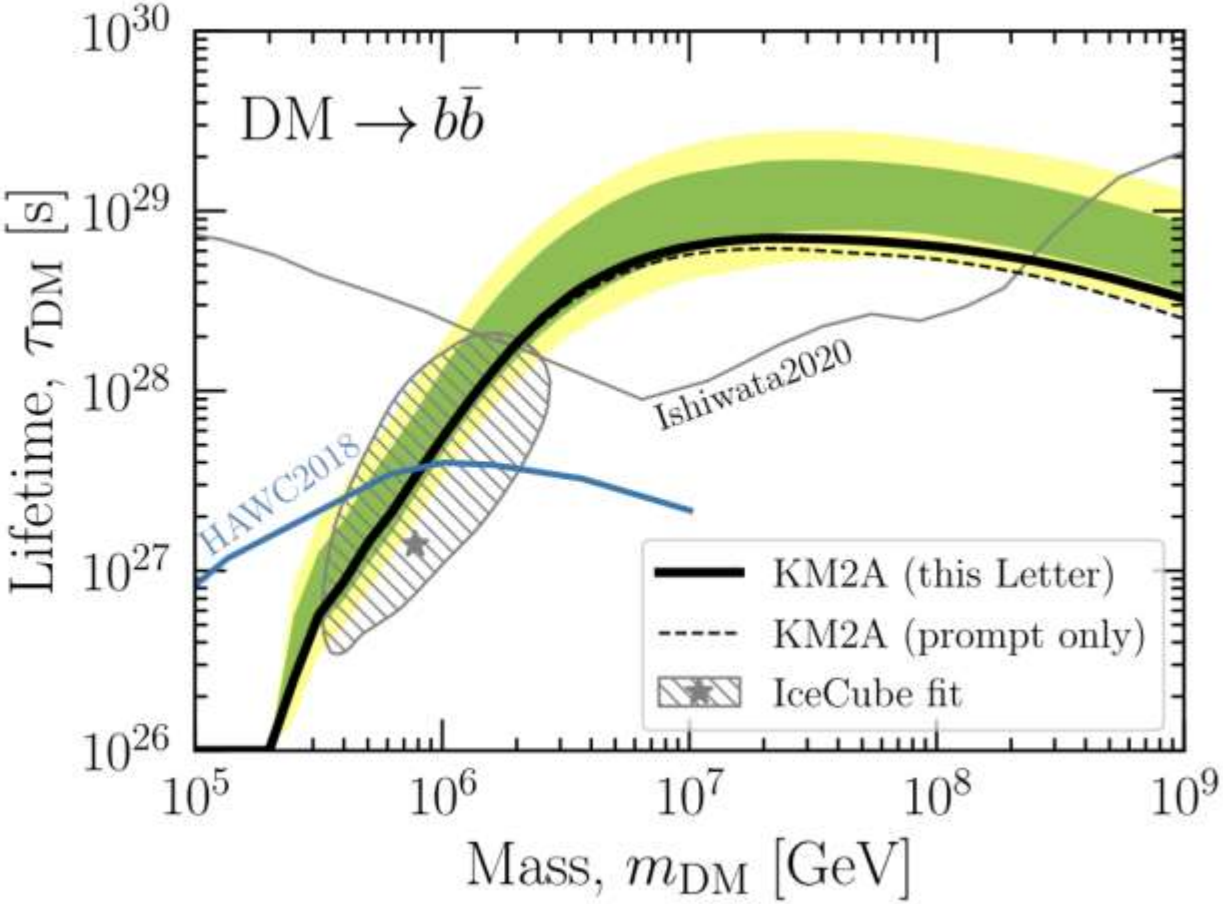

Fig. 1. 95% one-sided lower limits on DM lifetime for DM decaying into b quarks. Previous limits and those from HAWC are shown with gray and blue lines. The hatched regions show the 1σ DM parameter space favored by IceCube high-energy neutrino flux.

Zhen Cao,F. Aharonian,Q. An, et al., PHYSICAL REVIEW LETTERS 129, 261103 (2022)

Particle Desert: Future Circular Collider (100 km ring, 100TeV, red) and LHC (blue, 14 TeV)

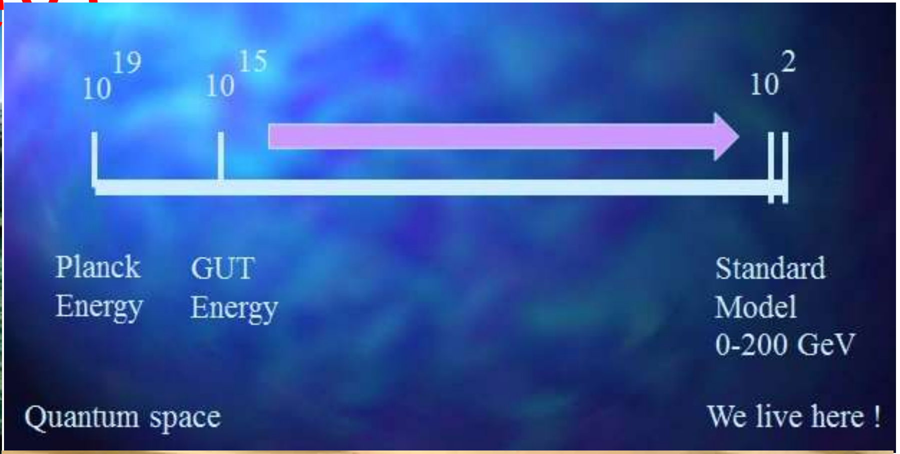

At the Large Hadron Collider at CERN, among the trillions of interactions studied up to energies of 14,000 GeV, no new physics has been seen in the furthest decimal points of the Standard Model predictions since 2012; not so much as a hint that something else has to be added to bring it back in line with actual data. It is a theory that appears not to be broken at energies over 1000 times higher than it was designed for!

Neutrino astronomy with IceCube

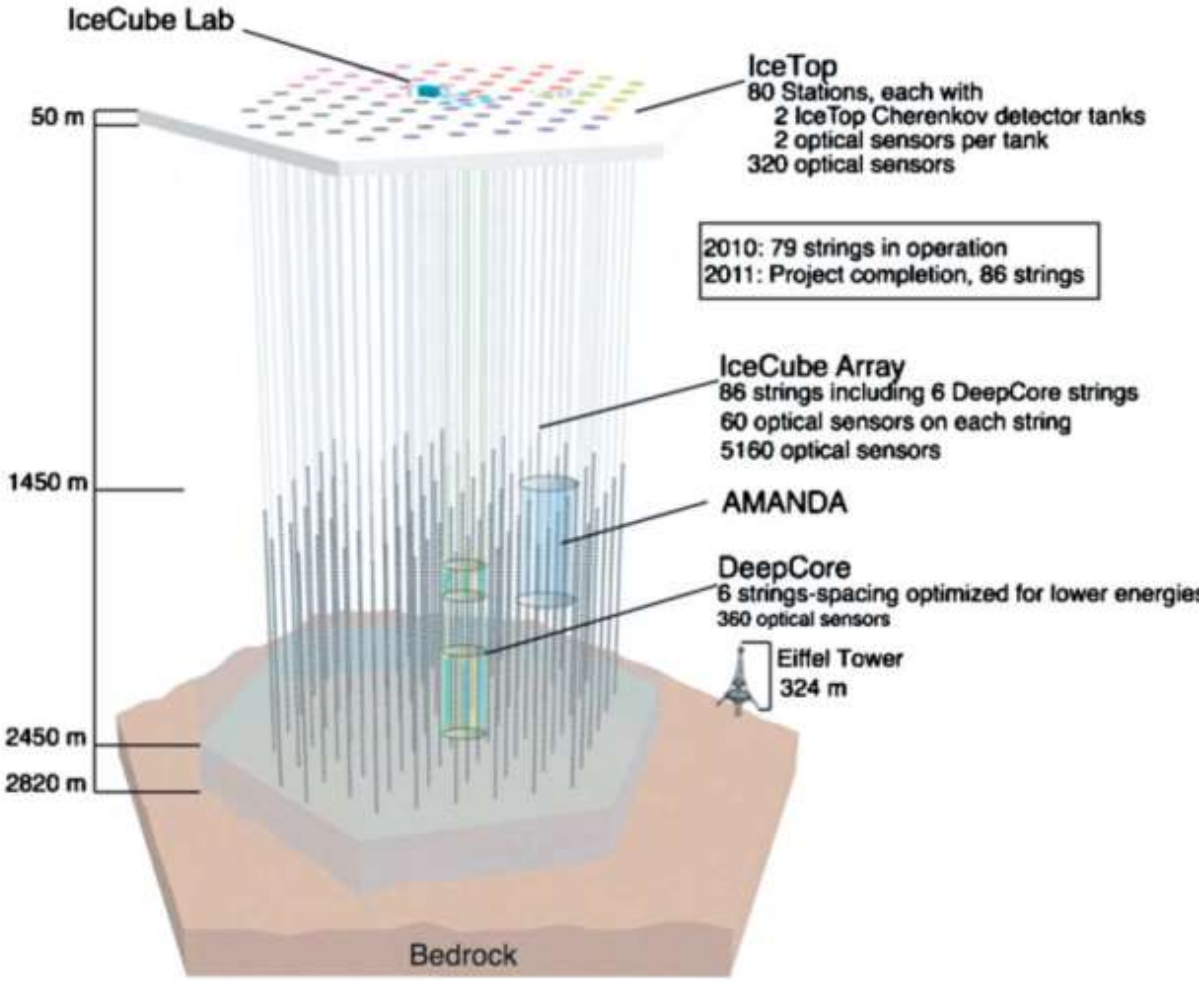

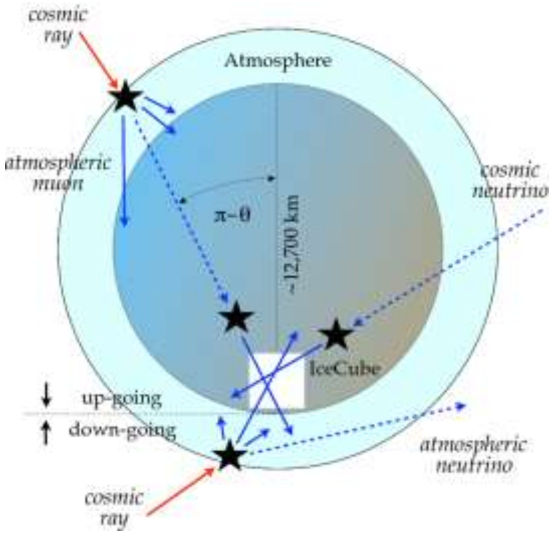

A neutrino is absorbed by the nucleus and produces a lepton corresponding to the neutrino's flavor (electron, muon, etc.). If the charged resultants are moving fast enough, they can create Cherenkov light captured by PM. For high-energy interactions, the neutrino and muon directions are the same, so it's possible to tell where the neutrino came from. IceCube detects more than 50,000 neutrino candidates every year, but only about 10 of them are at the very high energies that indicate that they come from outside the Milky Way galaxy

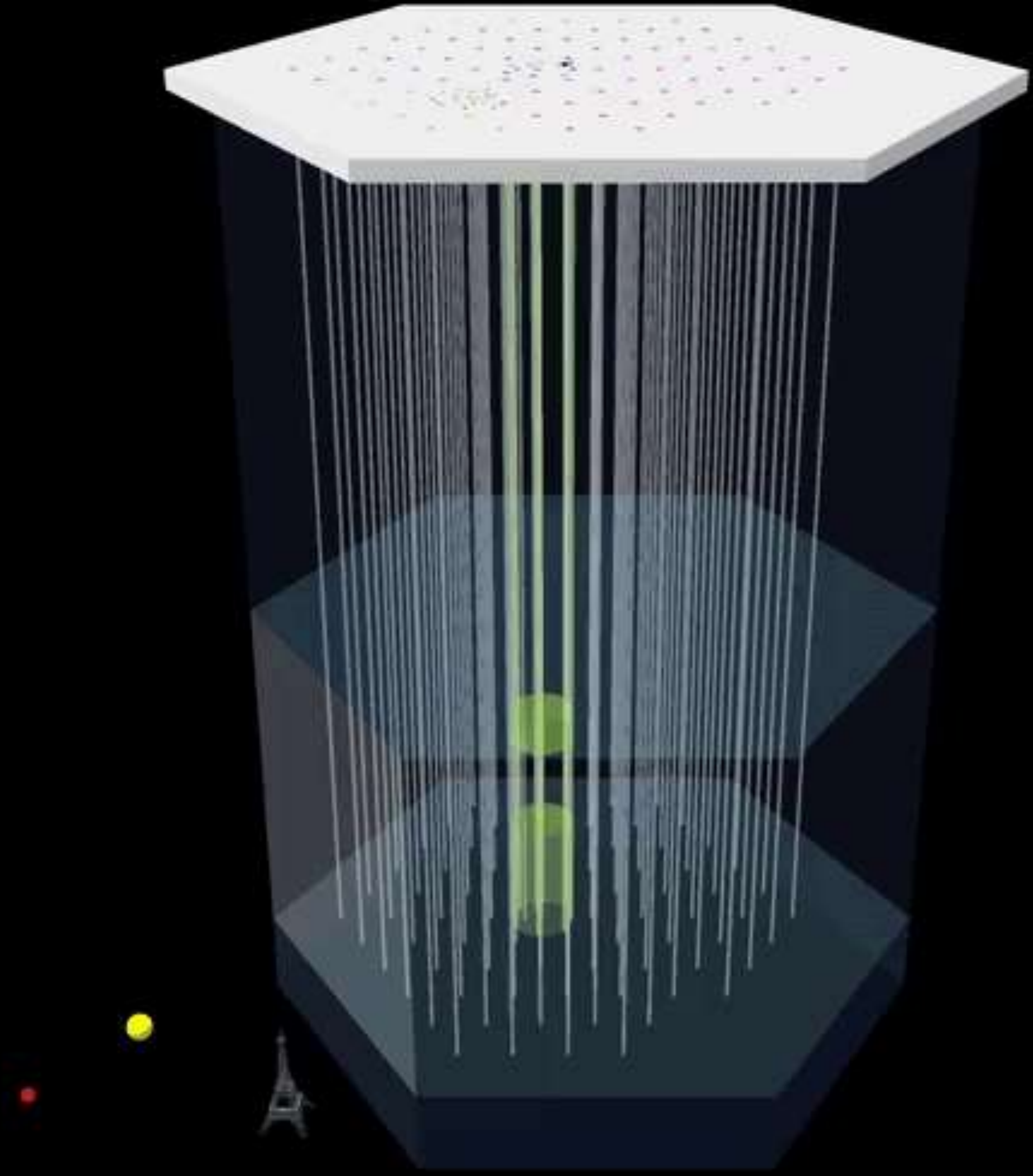

Air shower detected in coincidence by IceTop and IceCube. Left: Sketch of the shower development and the different shower components measured at the surface and in the ice. 10 PeV proton-induced shower

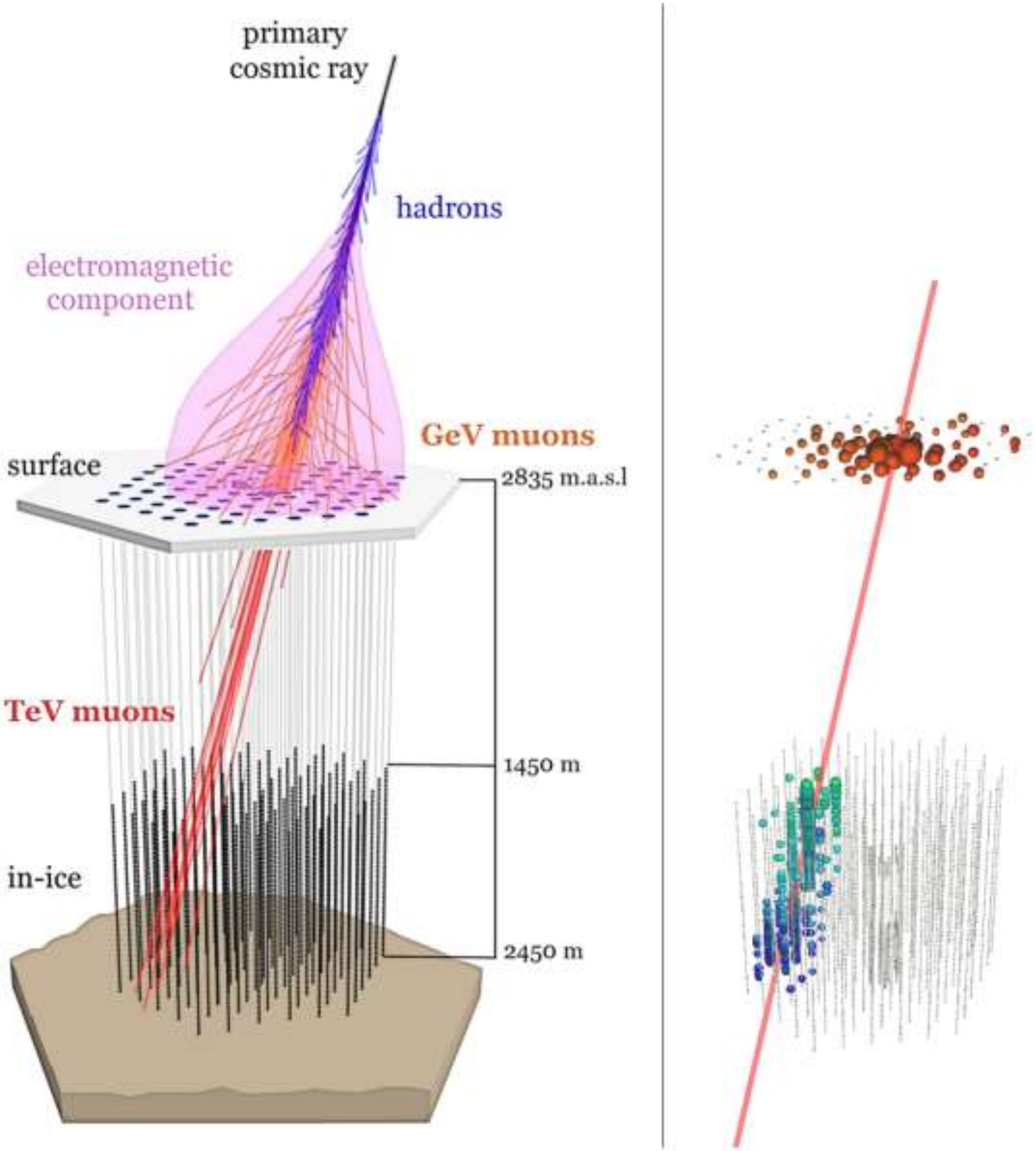

The PeV neutrinos observed in IceCube, have a thousand times the energy of the highest energy neutrinos produced with earthbound accelerators and a billion times the energy of the neutrinos detected from supernova SN1987 in the Large Magellanic Cloud

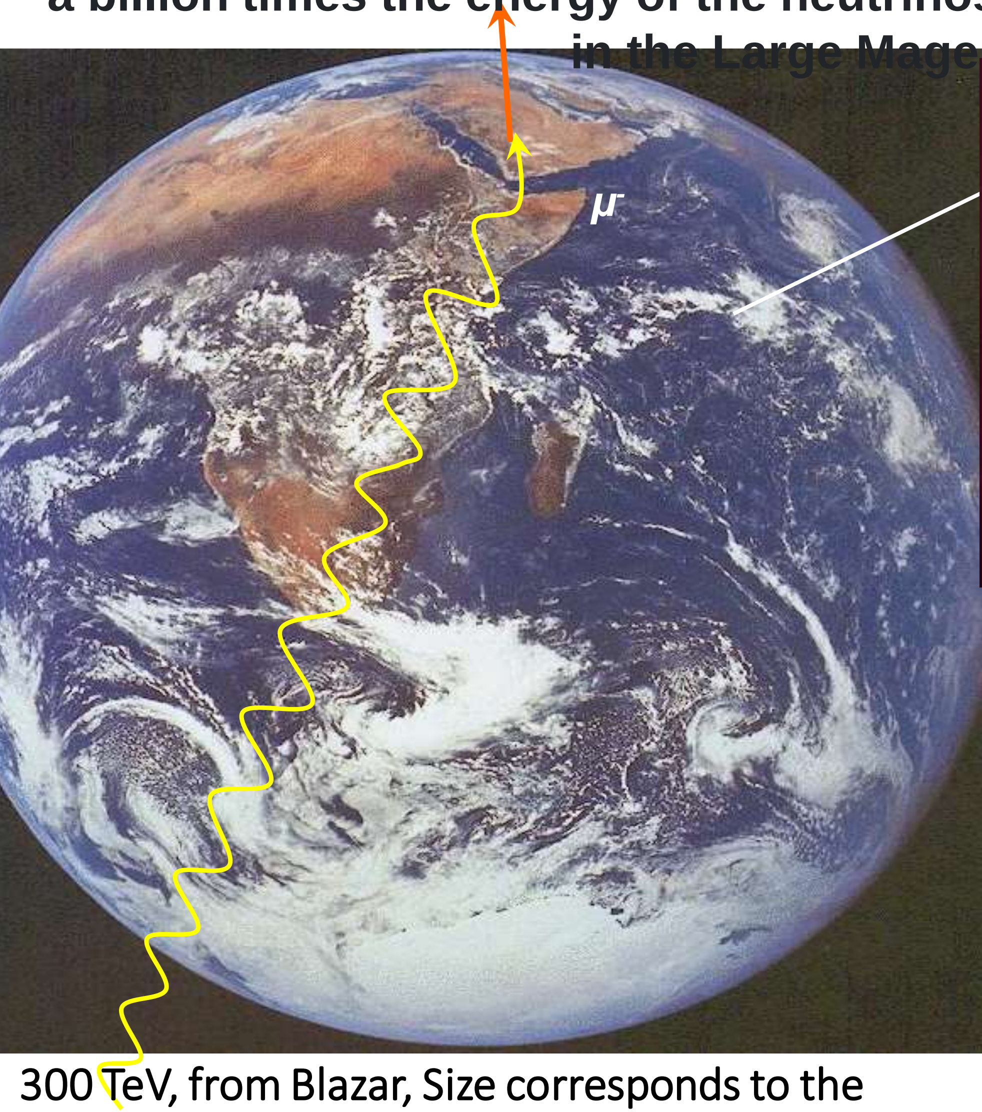

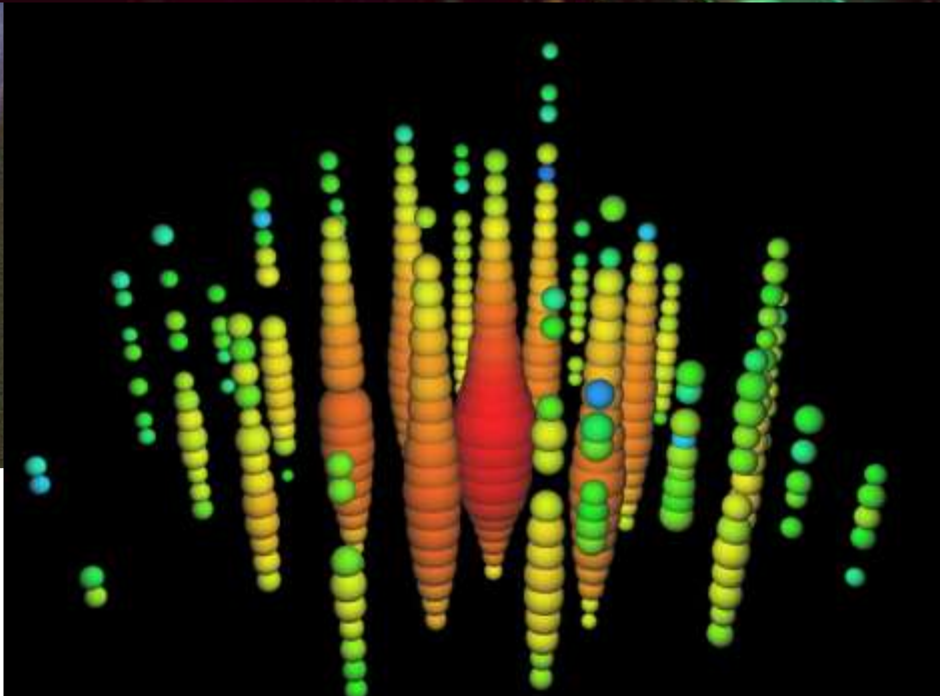

300 TeV, from Blazar, Size corresponds to the number of photons observed; color indicates time (red is earliest; blue, latest).

A supermassive black hole, obscured by cosmic dust, powers the nearby active galaxy NGC 1068. From the NGC 1068, an excess of 79 neutrinos at TeV energies was observed over a period of 3186 days, with a significance of 4.2σ

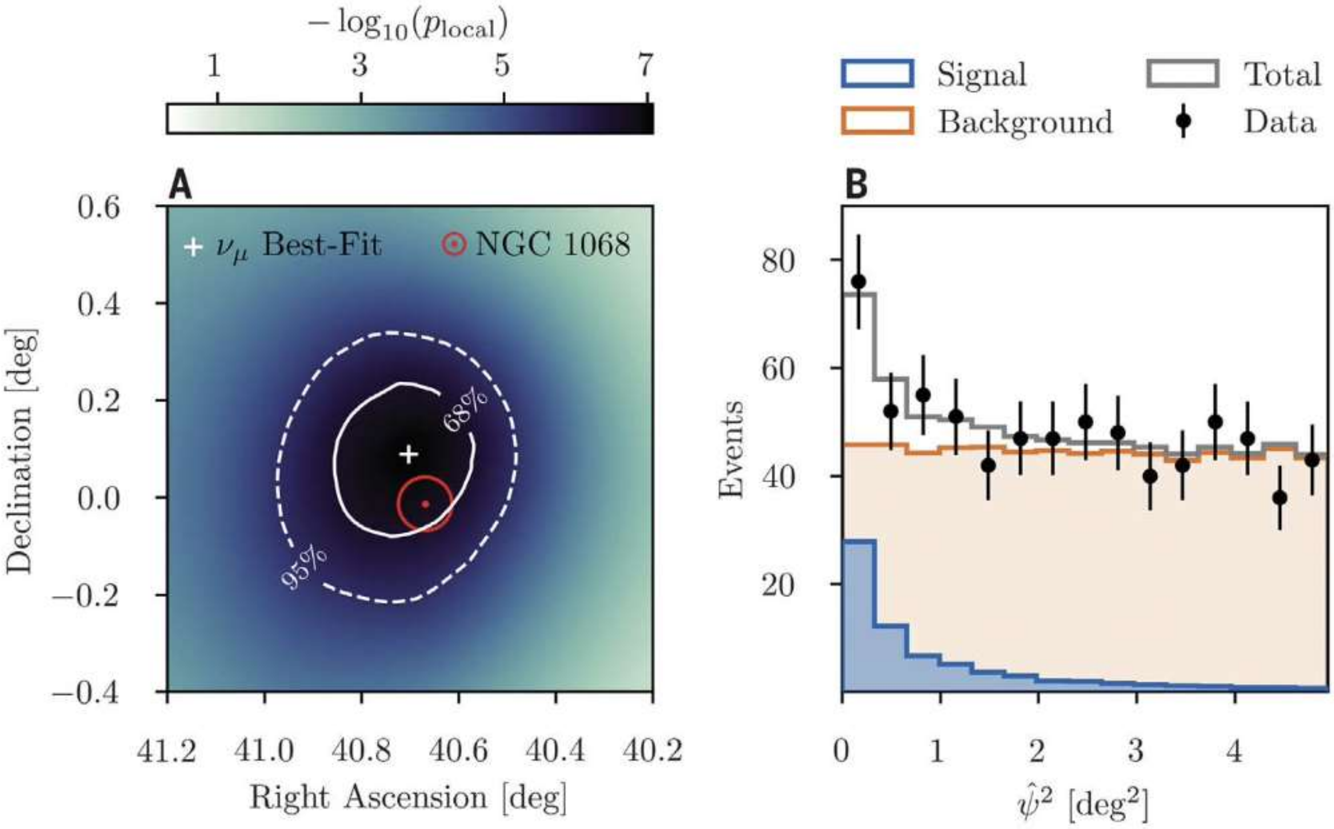

(A) High-resolution scan around the most significant location marked by a white cross. The red dot shows the position of NGC 1068, and the red circle is its angular size in the optical wavelength. (B) The distribution of the squared angular distance, between NGC 1068 and the reconstructed event

Observations of high-energy cosmic rays (protons and atomic nuclei from space), up to 10^{19} eV, have demonstrated that powerful cosmic particle accelerators must exist, but their nature and location remain unknown. High-energy neutrinos are generated near astronomical sources as decay products of charged mesons, which are themselves produced in proton-proton interactions. Neutrinos are not affected by intergalactic absorption, so they could potentially be used to probe these accelerators. AGNs can launch a strong, narrow jet of accelerated plasma. If such a jet is oriented close to the line of sight, the AGN is observed as a blazar. AGNs are potential neutrino emitters.

R. Abbasi et al. [IceCube], Science 378 (2022
n6619, 538-543 doi:10.1126/science.abg33

First association of a ~300 TeV neutrino to a γ-ray source

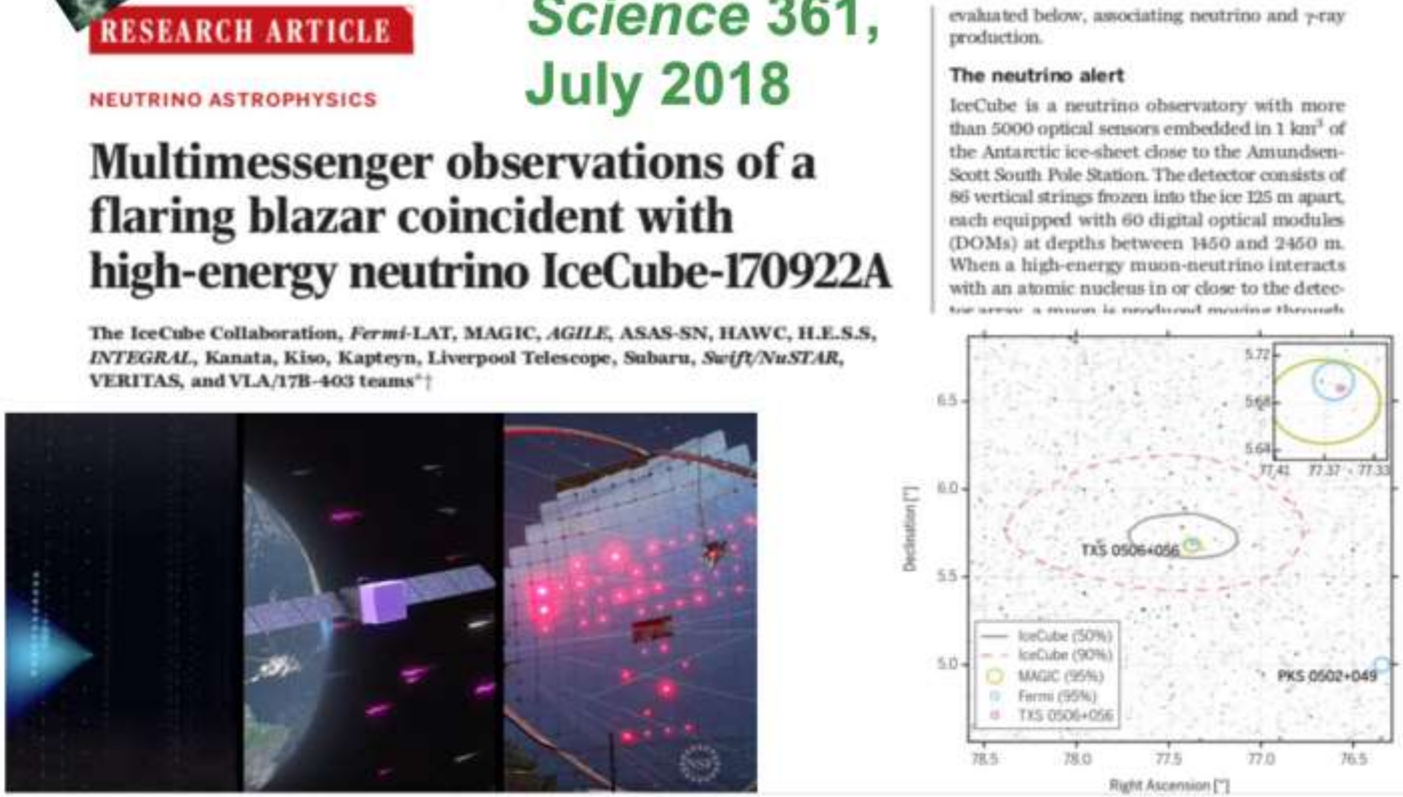

Science 361, July 2018

RESEARCH ARTICLE

NEUTRINO ASTROPHYSICS

Multimessenger observations of a flaring blazar coincident with high-energy neutrino IceCube-170922A

The IceCube Collaboration, *Fermi*-LAT, MAGIC, *AGILE*, ASAS-SN, HAWC, H.E.S.S., *INTEGRAL*, Kanata, Kiso, Kapteyn, Liverpool Telescope, Subaru, *Swift/NuSTAR*, VERITAS, and VLA/17B-403 teams*†

evaluated below, associating neutrino and γ-ray production.

The neutrino alert

IceCube is a neutrino observatory with more than 5000 optical sensors embedded in 1 km³ of the Antarctic ice-sheet close to the Amundsen-Scott South Pole Station. The detector consists of 86 vertical strings frozen into the ice 125 m apart, each equipped with 60 digital optical modules (DOMs) at depths between 1450 and 2450 m. When a high-energy muon-neutrino interacts with an atomic nucleus in or close to the detector array, a muon is produced moving through

How to prove a “new physics”Higgs boson discovery at CERN LHC (ATLAS and CMS experiments)

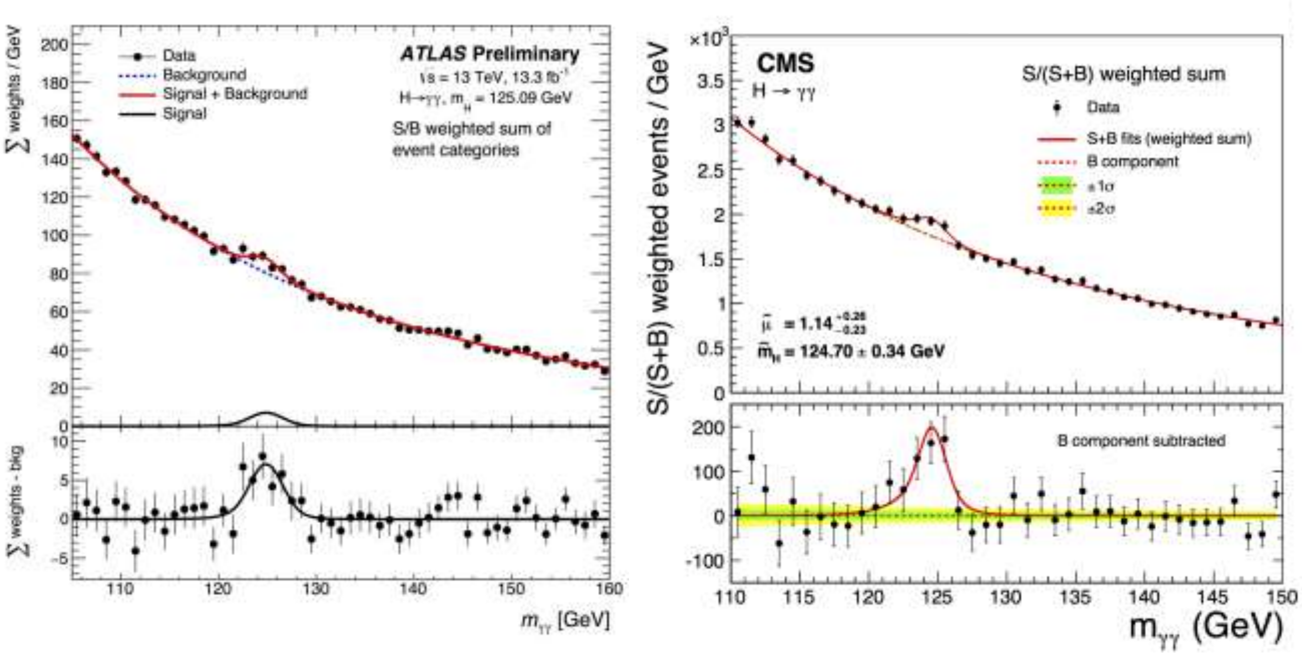

The distribution of the invariant mass of the two photons in the ATLAS and SMS experiments at LHC. Measurement of H→γγ using the full 2015+2016 data set. An excess is observed for a mass of ~125 GeV (5 stigmas!)

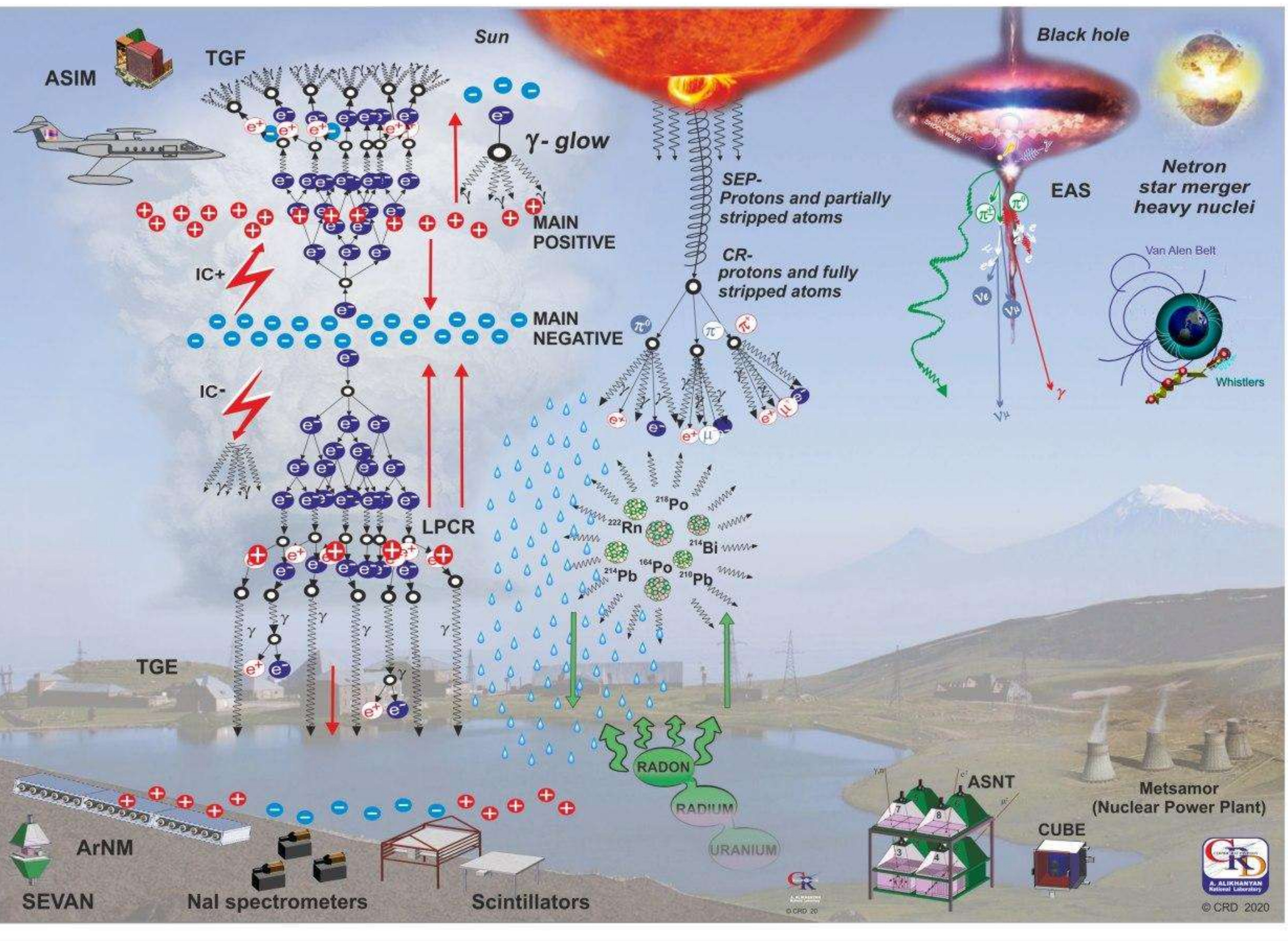

A.Chilingarian, High Energy Physics in the Earth's Atmosphere, Природа 3, 11, 2021.

New physics and new sources depend on N$\boldsymbol{\sigma}$, what it is: Proof in exp. physics

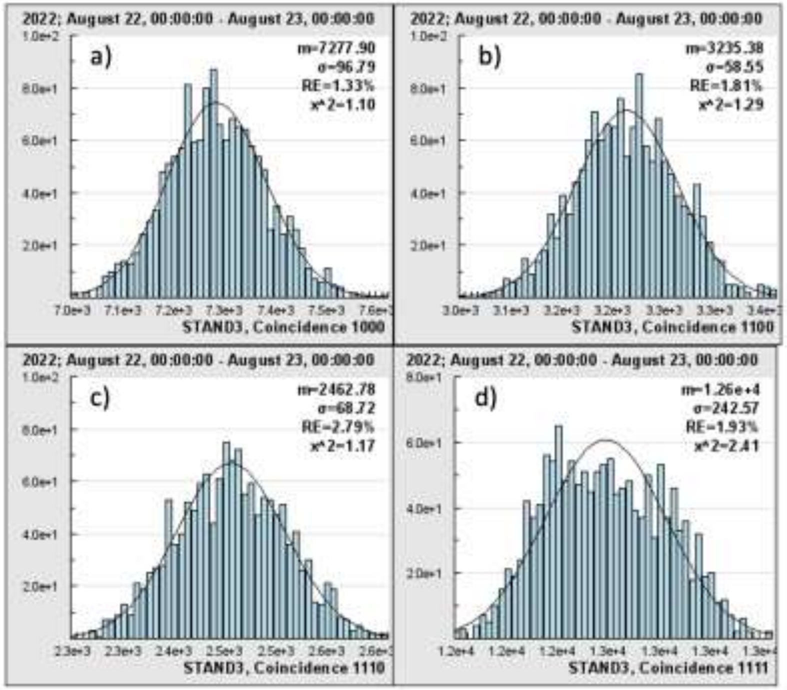

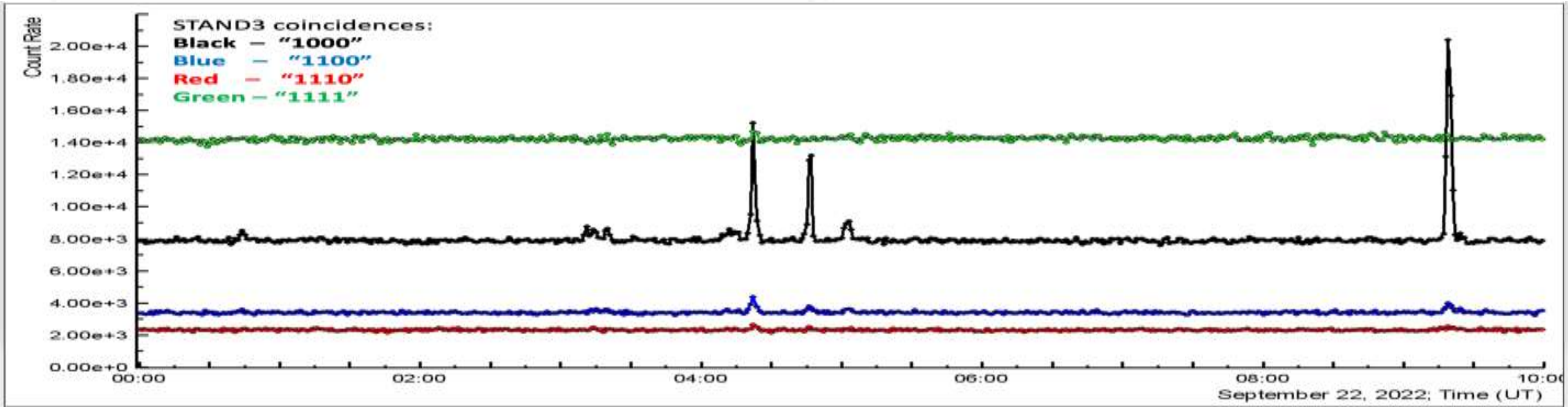

Johann Carl Friedrich Gauss

German mathematician, physicist, and astronomer

1777-1855

$$f(x)=\frac{1}{\sqrt{2\pi\sigma^2}}e^{\frac{-1}{2}\left(\frac{x-\mu}{\sigma}\right)^2}$$

Henri Pointcaré on the uniquity of the normal distribution:

« Everyone believes in it: experimentalist believing that it is a mathematical theorem, mathematicians believing it is an empirical fact »

Claims of new physics and new sources depend on N**σ**, what it is? Proof in physics

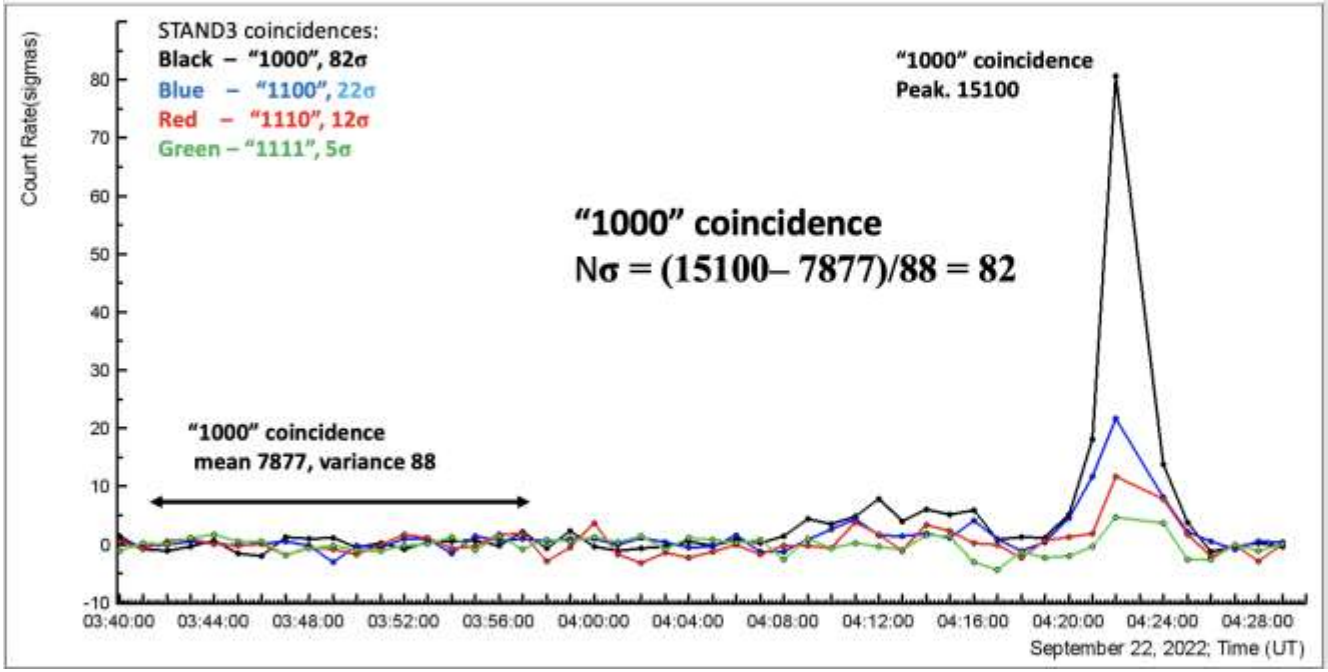

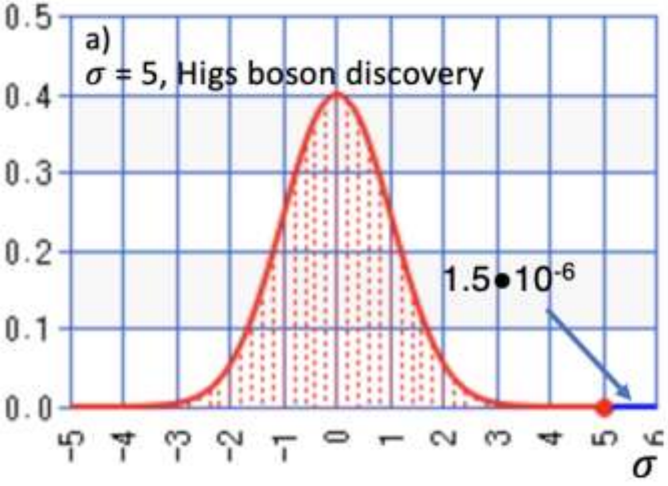

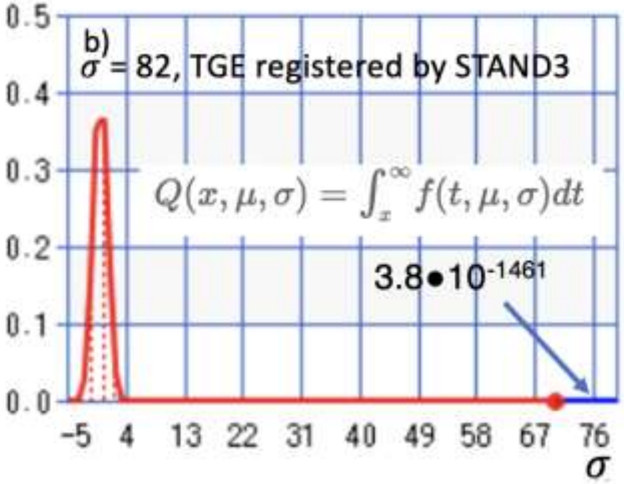

$$Q(x,\mu,\sigma) = \int_x^\infty f(t,\mu,\sigma)dt$$

Space-time tells matter how to move and matter tells space-time how to curve

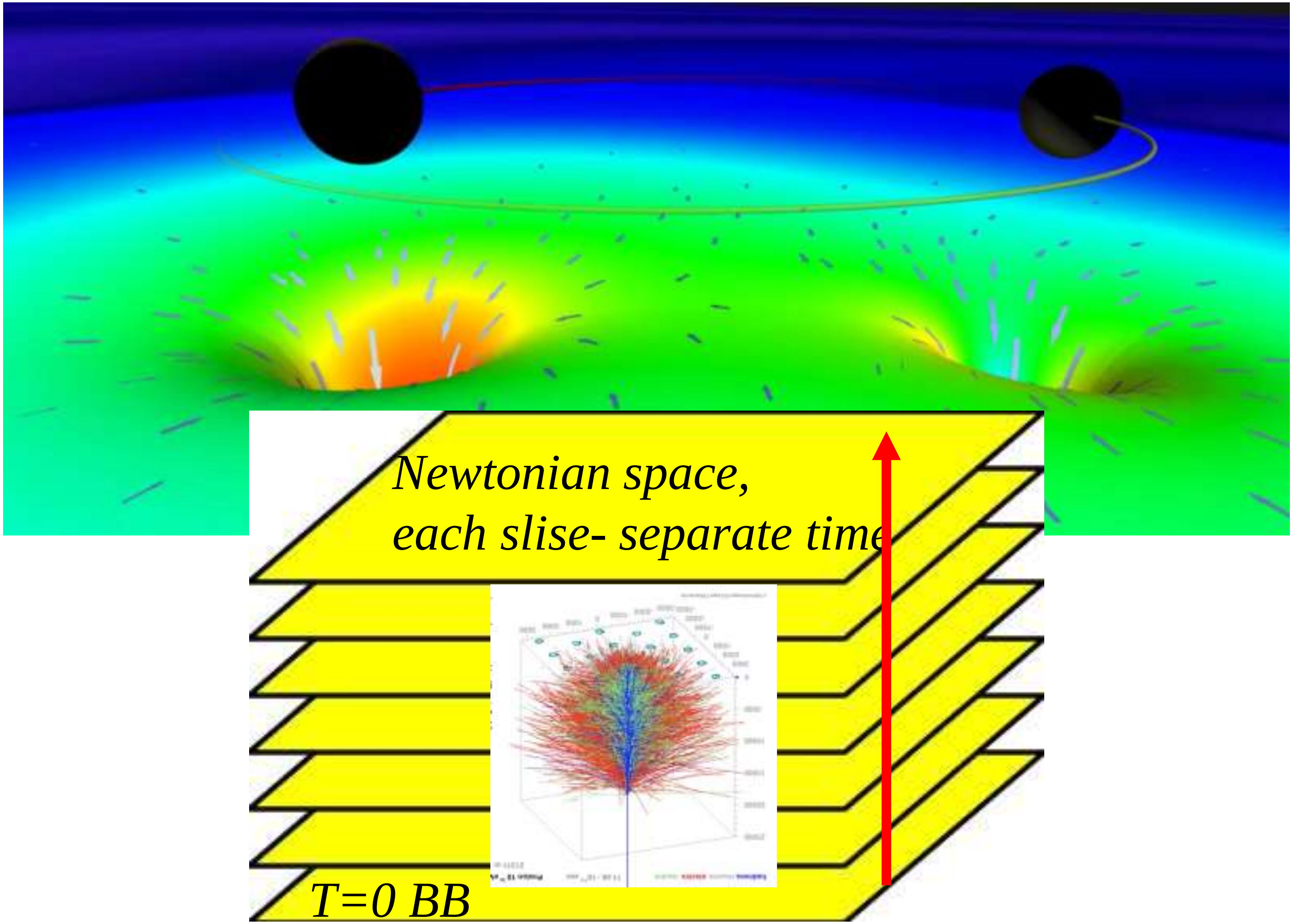

Newtonian space,
each slise- separate time

T=0 BB

Do gravity and light propagate at identical speeds?

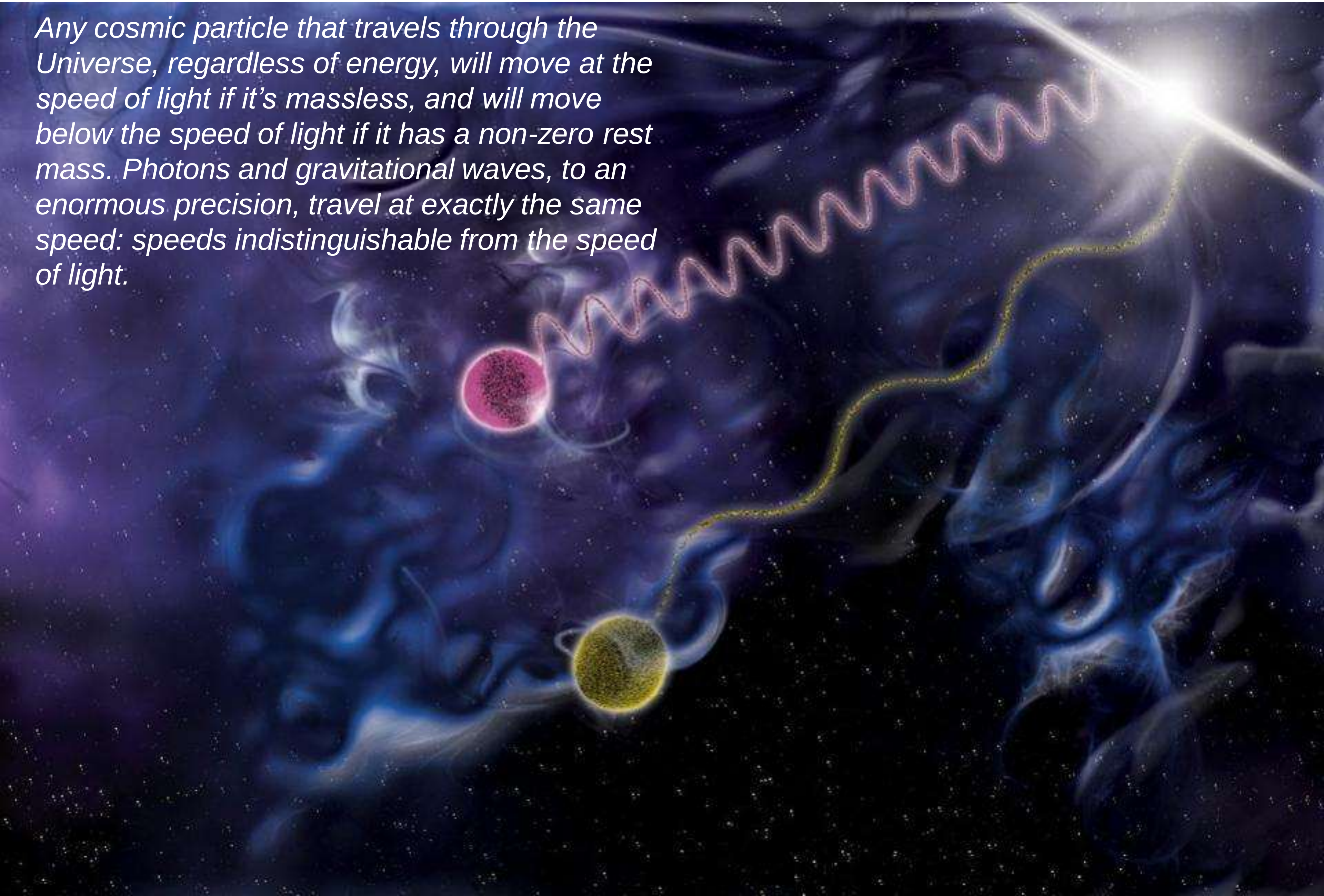

Any cosmic particle that travels through the Universe, regardless of energy, will move at the speed of light if it’s massless, and will move below the speed of light if it has a non-zero rest mass. Photons and gravitational waves, to an enormous precision, travel at exactly the same speed: speeds indistinguishable from the speed of light.

14 September 2015
at 9:50:45 UTC

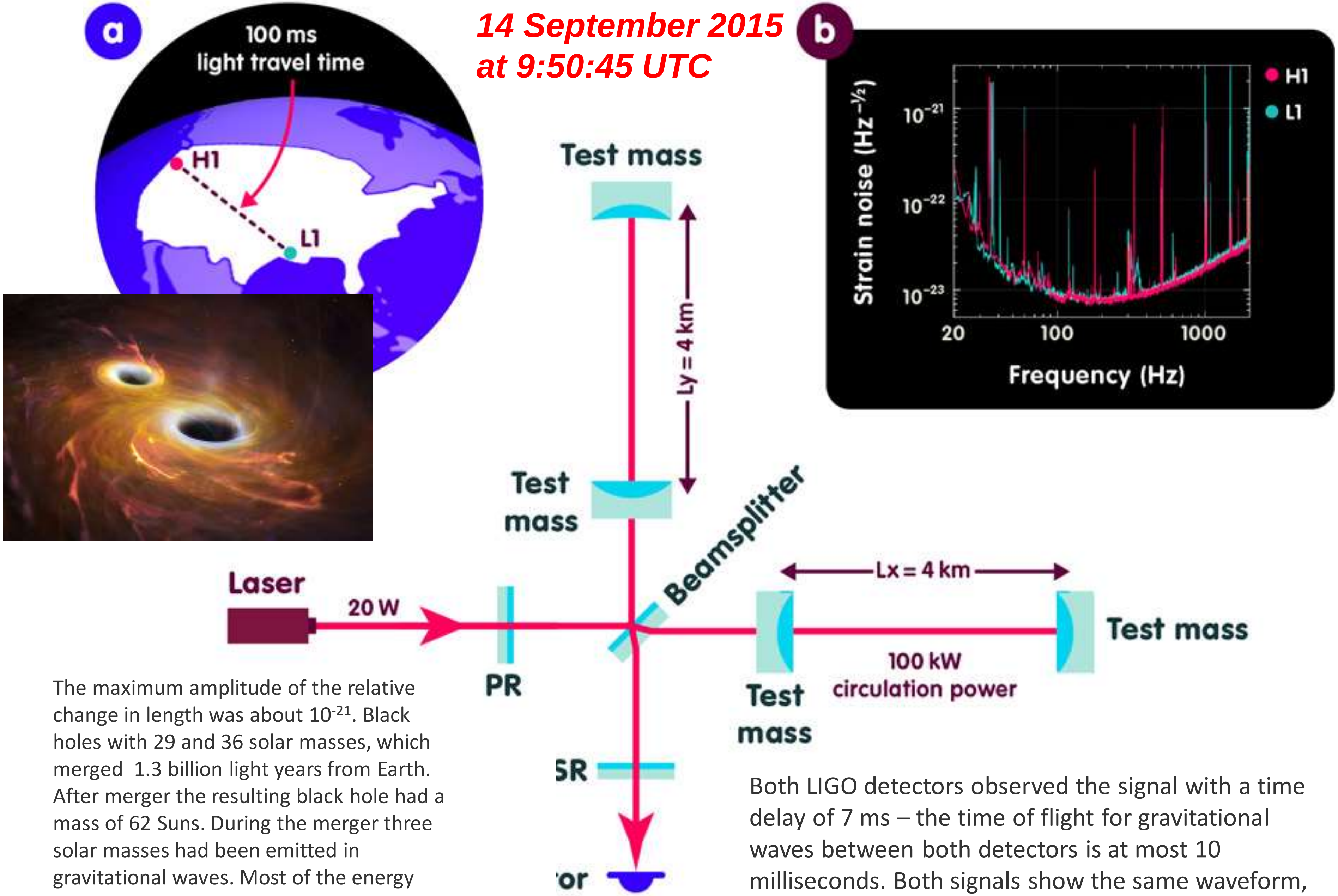

The maximum amplitude of the relative change in length was about 10^{-21}. Black holes with 29 and 36 solar masses, which merged 1.3 billion light years from Earth. After merger the resulting black hole had a mass of 62 Suns. During the merger three solar masses had been emitted in gravitational waves. Most of the energy had been released in the last 0.2 seconds – gravitational waves were emitted with a power ten times larger than the luminosity of all stars in the observable universe.

Both LIGO detectors observed the signal with a time delay of 7 ms – the time of flight for gravitational waves between both detectors is at most 10 milliseconds. Both signals show the same waveform, which is to be expected for an astrophysical source in view of nearly the same alignment of the detectors.

The window of 200 ms of the signals measured on 14 September 2015 at 9:50:45 UTC in the two LIGO detectors at Hanford (red, top left) and at Livingston (blue, top right). Below, is the model of a binary black hole merger (note the frequency increasing from 30 Hz to about 200 Hz)

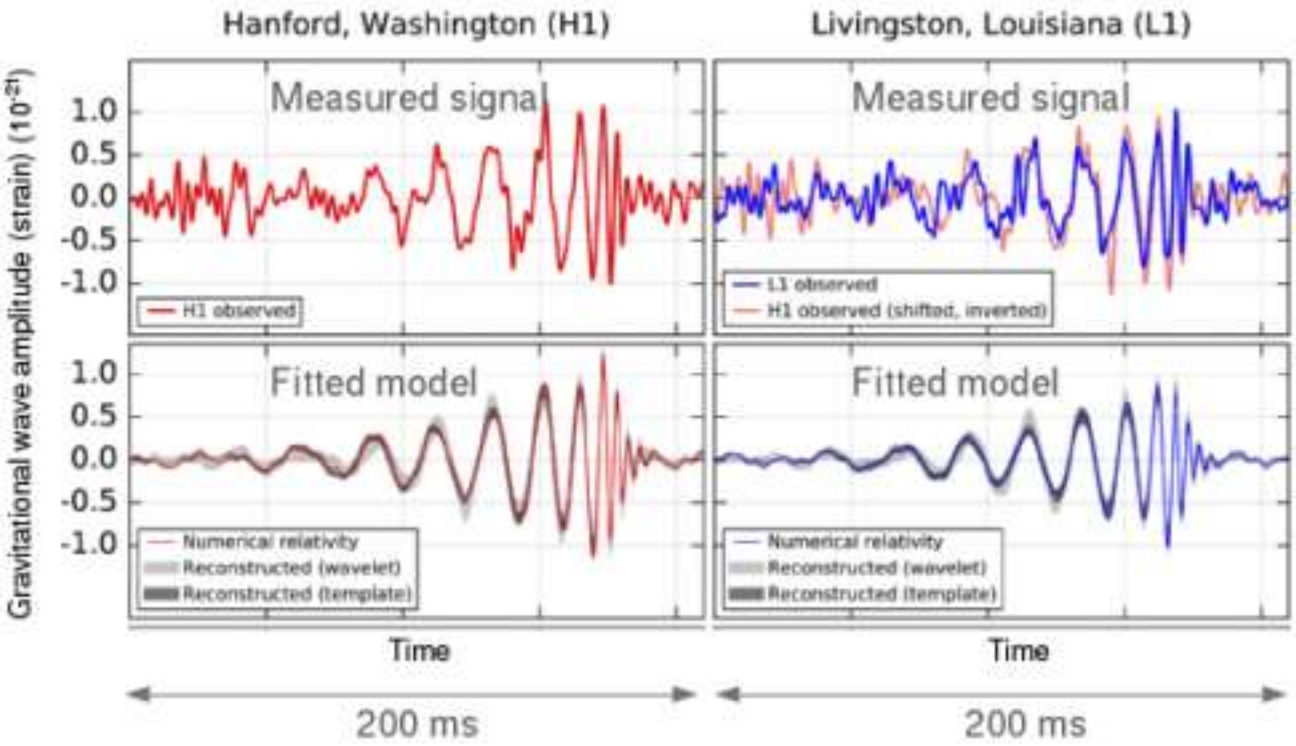

The maximum gravitational wave amplitude reached 10^{-21}: it means that the distance between the LIGO mirrors, separated by 4 km varied, by only 2 billionth of billionth of a meter!

The strain equivalent spectral amplitudes as a function of the frequency. Most relevant contributions comes from quantum noise and from thermal noise of mirror coating and suspensions. Seismic noise dominates below 10Hz and is not represented.

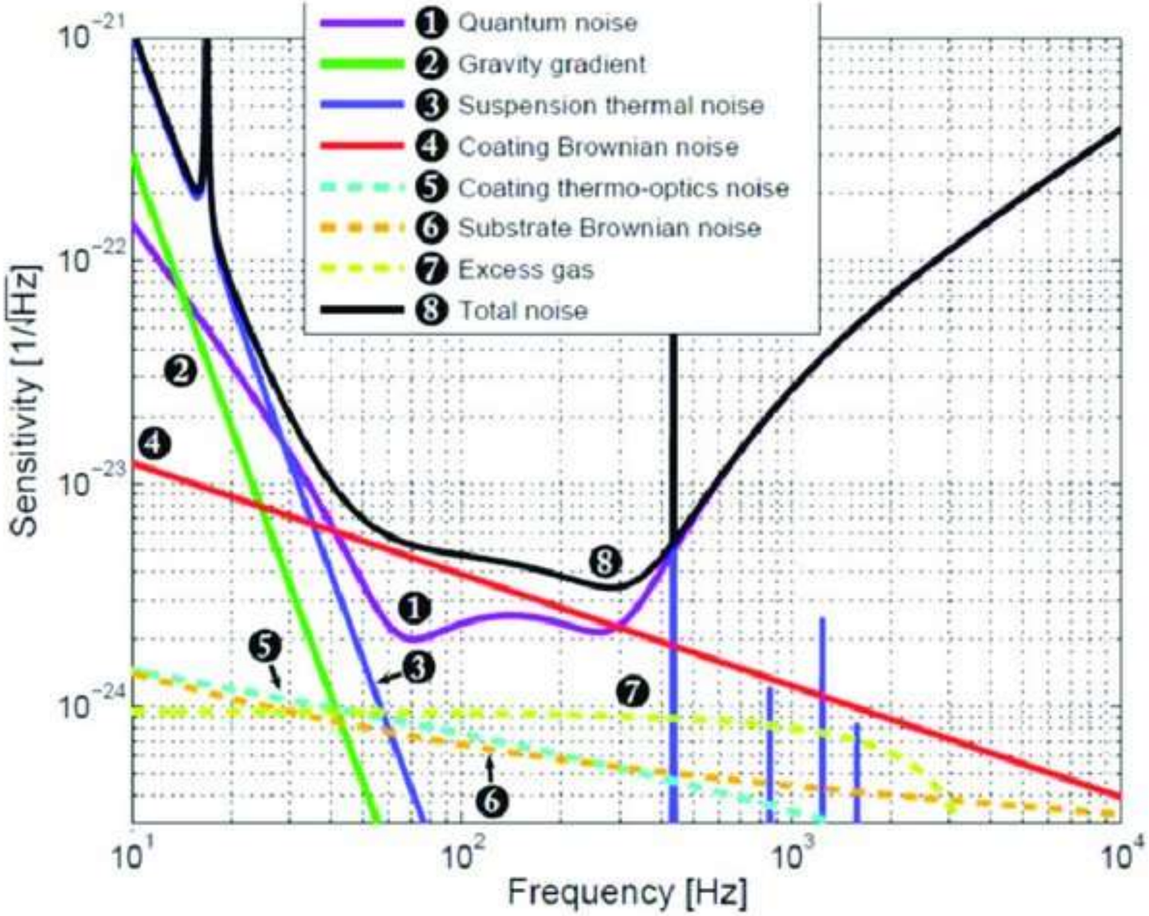

New laser produces an output power of 180 W and an amplitude steady to a billionth. The mirror and suspension are of the same material leading to a much better reduction of thermal disturbances. Furthermore with another mirror the output signal can be superimposed with itself (“signal recycling”). This technique has been tested first at GEO600 and has been shown to enable a further improvement of the detector sensitivity.

An initial measurement of the particle’s position imparts an unknown momentum to it via radiation pressure, which prevents one from predicting the outcome of a later position measurement (Heisenberg uncertainty principle (HUP); all meteorological parameters are monitored. Seismic noise does not appear in the picture but becomes the main limit below 10Hz. Noise analysis: such a strong signal could be produced by accidental fluctuations only once in 200,000 years.

Data analysis techniques used to detect gravitational-wave signals and infer the physics (source properties)

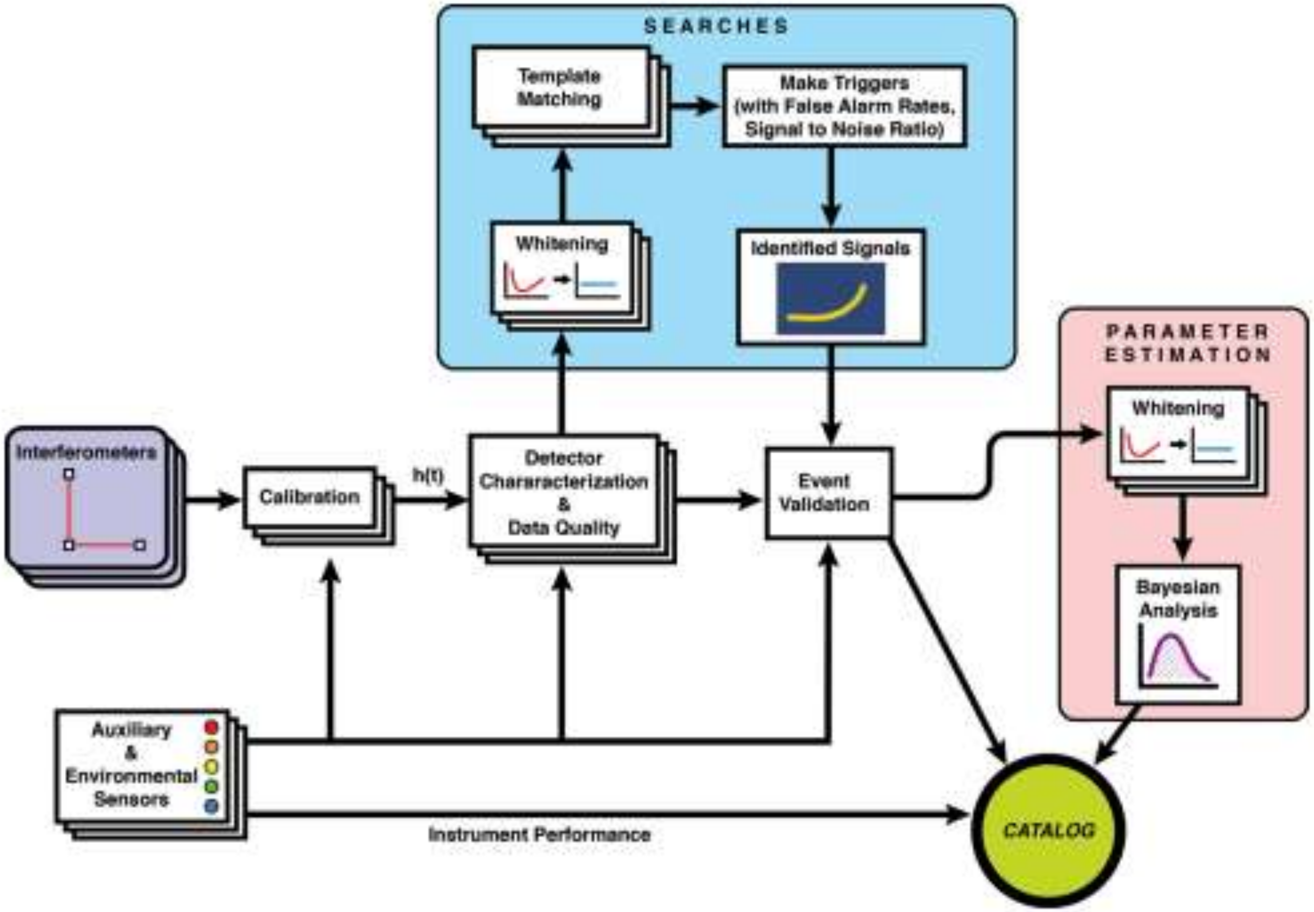

Correlations between the LIGO-Hanford and LIGO-Livingston detector data

A time lag of 7.3 ms is highlighted as a dotted vertical line.

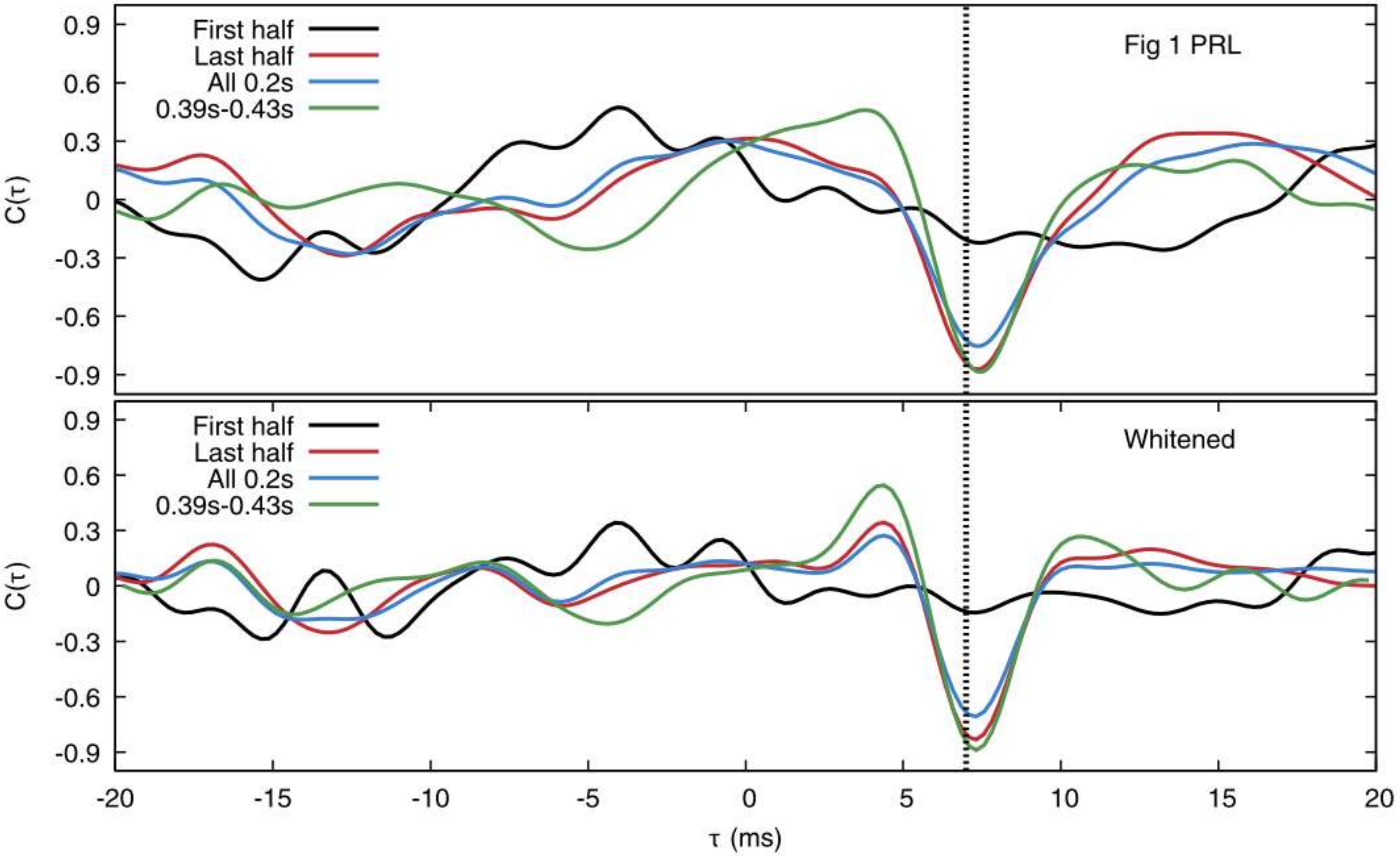

On November 3-5, 2021, CME hit the magnetosphere, sparking a **G3-class** geomagnetic storm

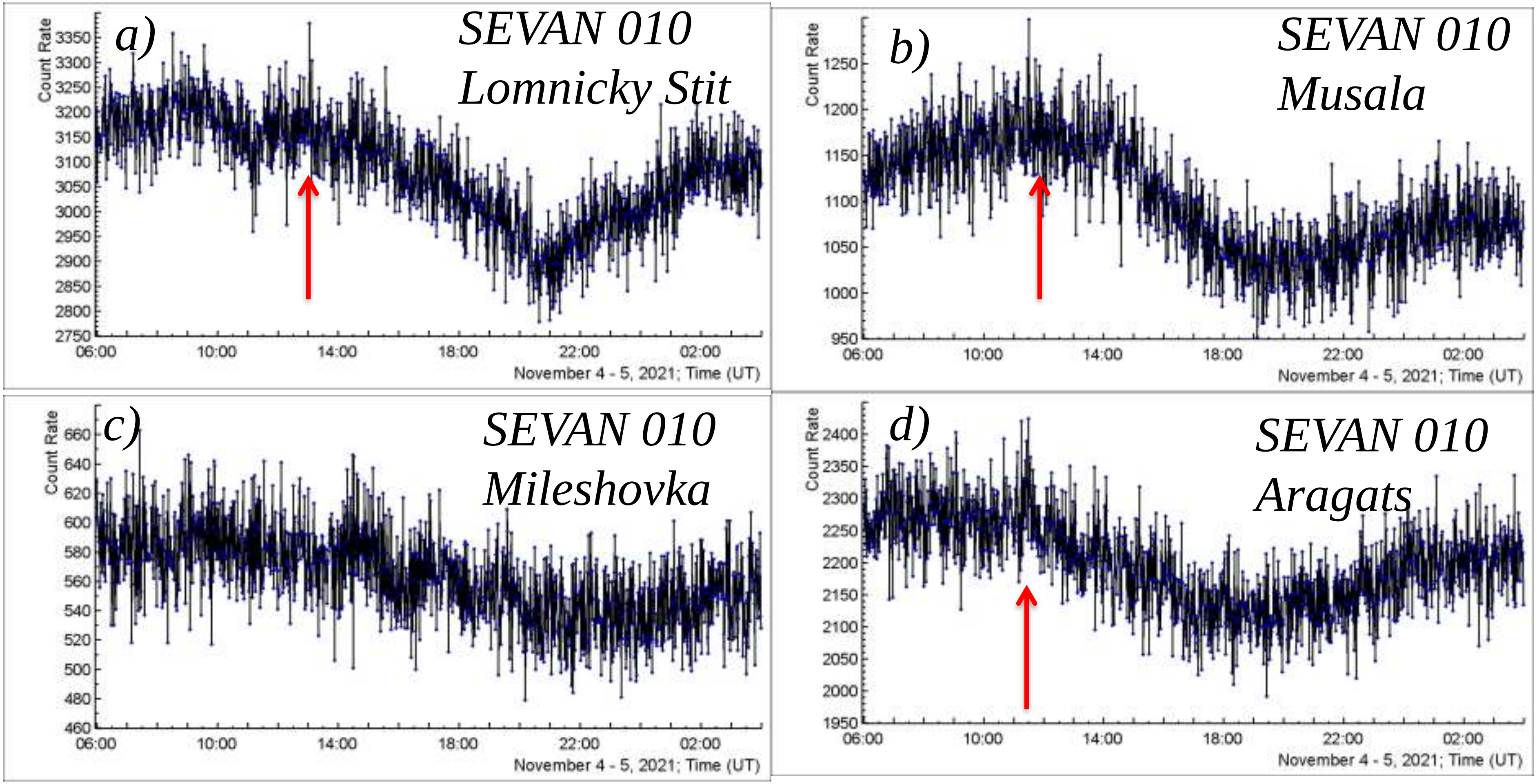

Near-surface electric field and Bx: delayed correlations ≈1 hour

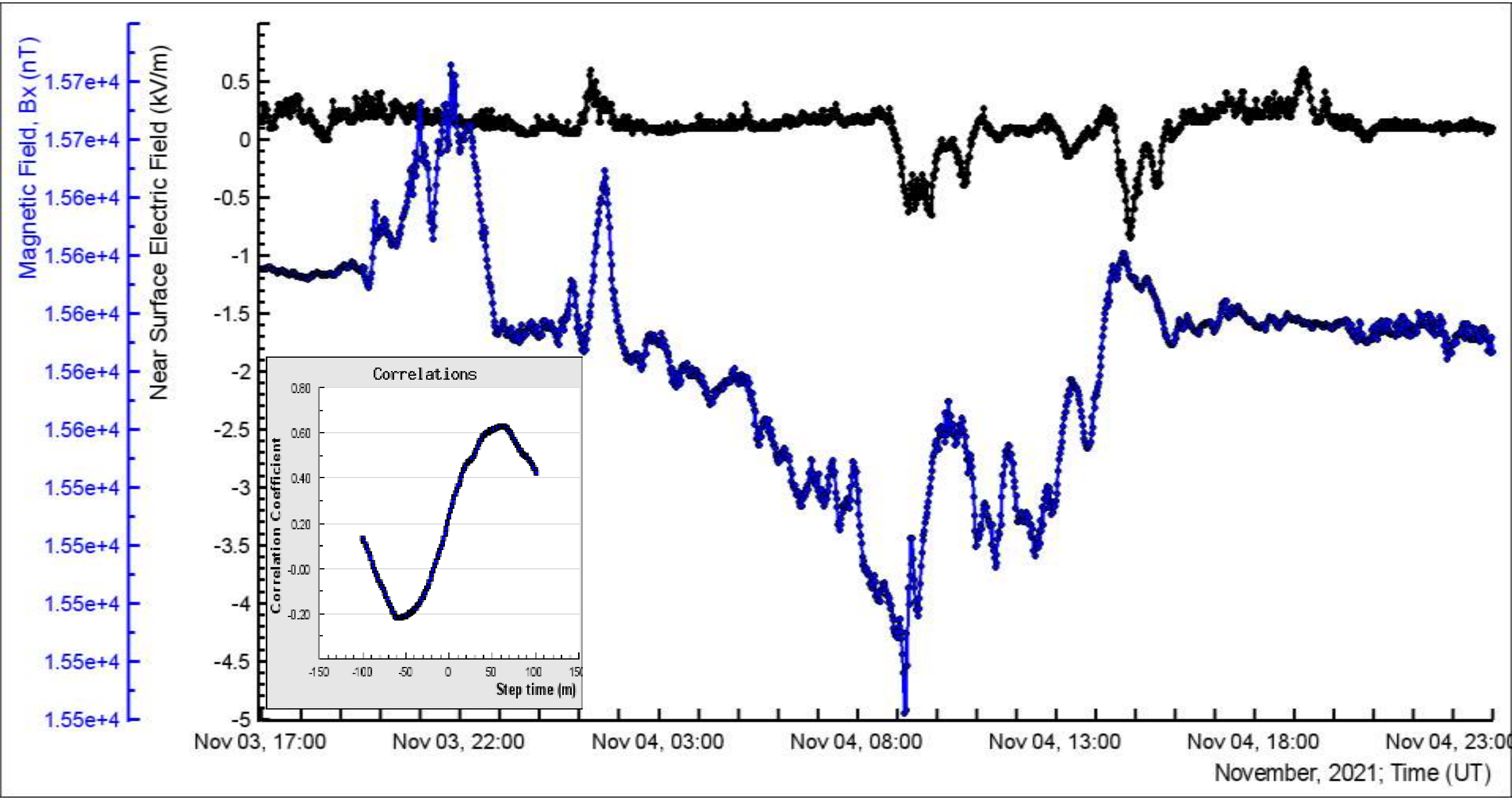

TEPA-2022, Prague , 2022

Multisensory detection of neutron star merger in NGC4993 galaxy

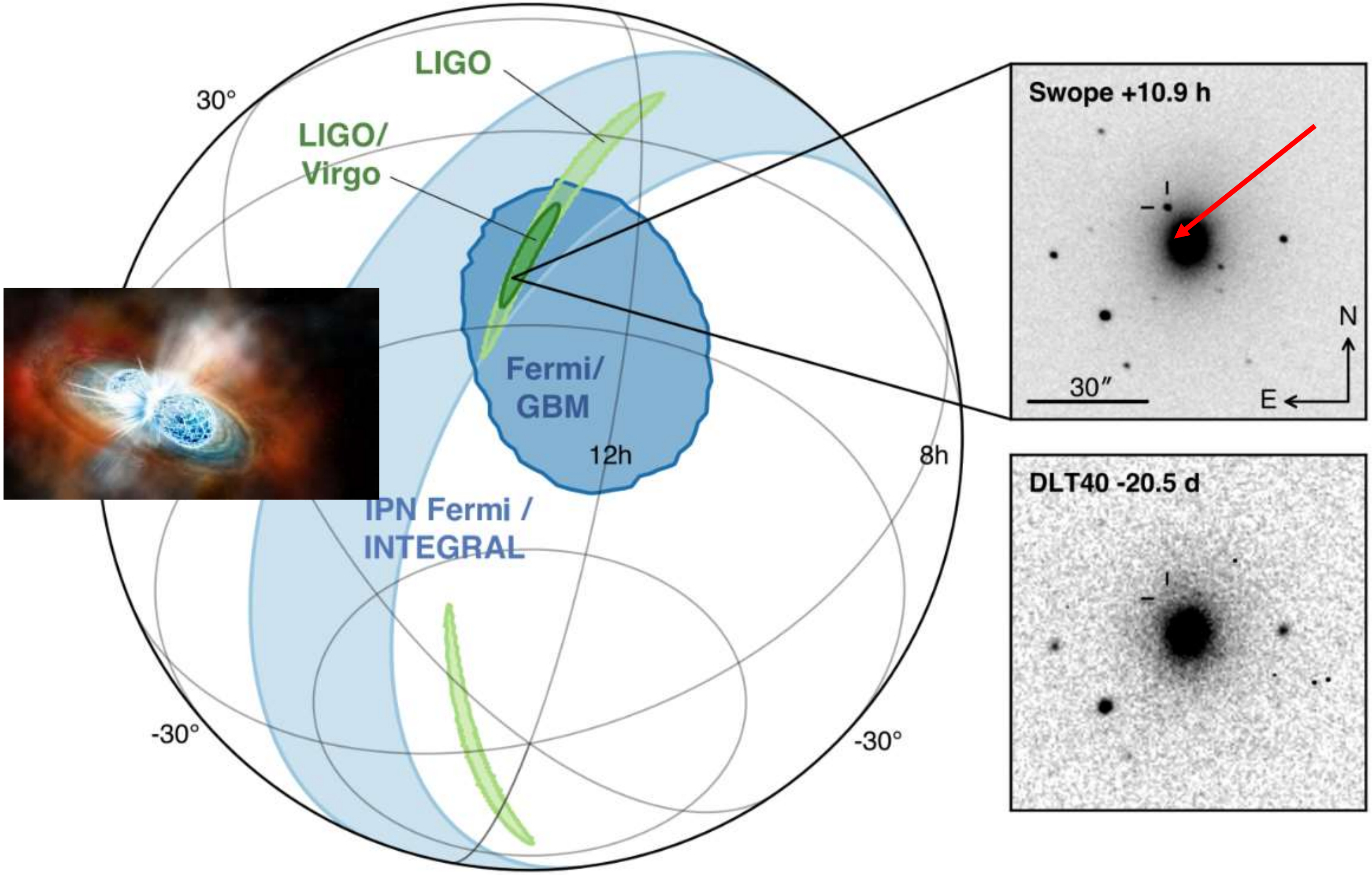

Localization of the gravitational wave (from the LIGO-Virgo 3-detector global network), gamma-ray (by the Fermi and INTEGRAL satellites) and optical (the Swope discovery image) signals from the transient event detected on the 17th of August, 2017

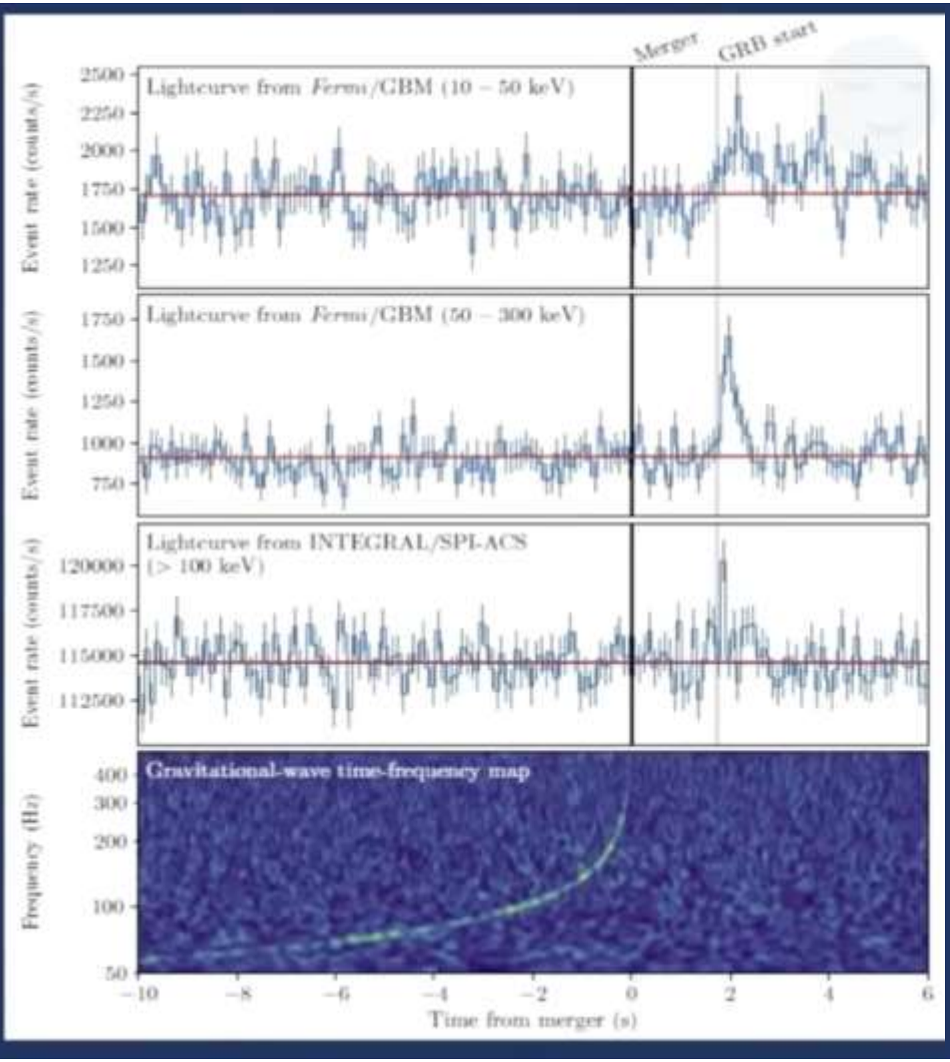

Слияния НЗ – «фабрики золота» во Вселенной

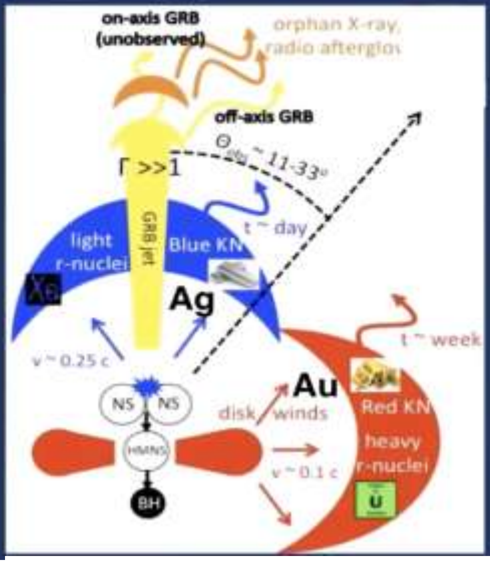

Gold production

$\sim 100 - 200 M_{\oplus}$

1000000000000000000000000000000

Lutovinov A.A., IKI

Образование элементов тяжелее железа

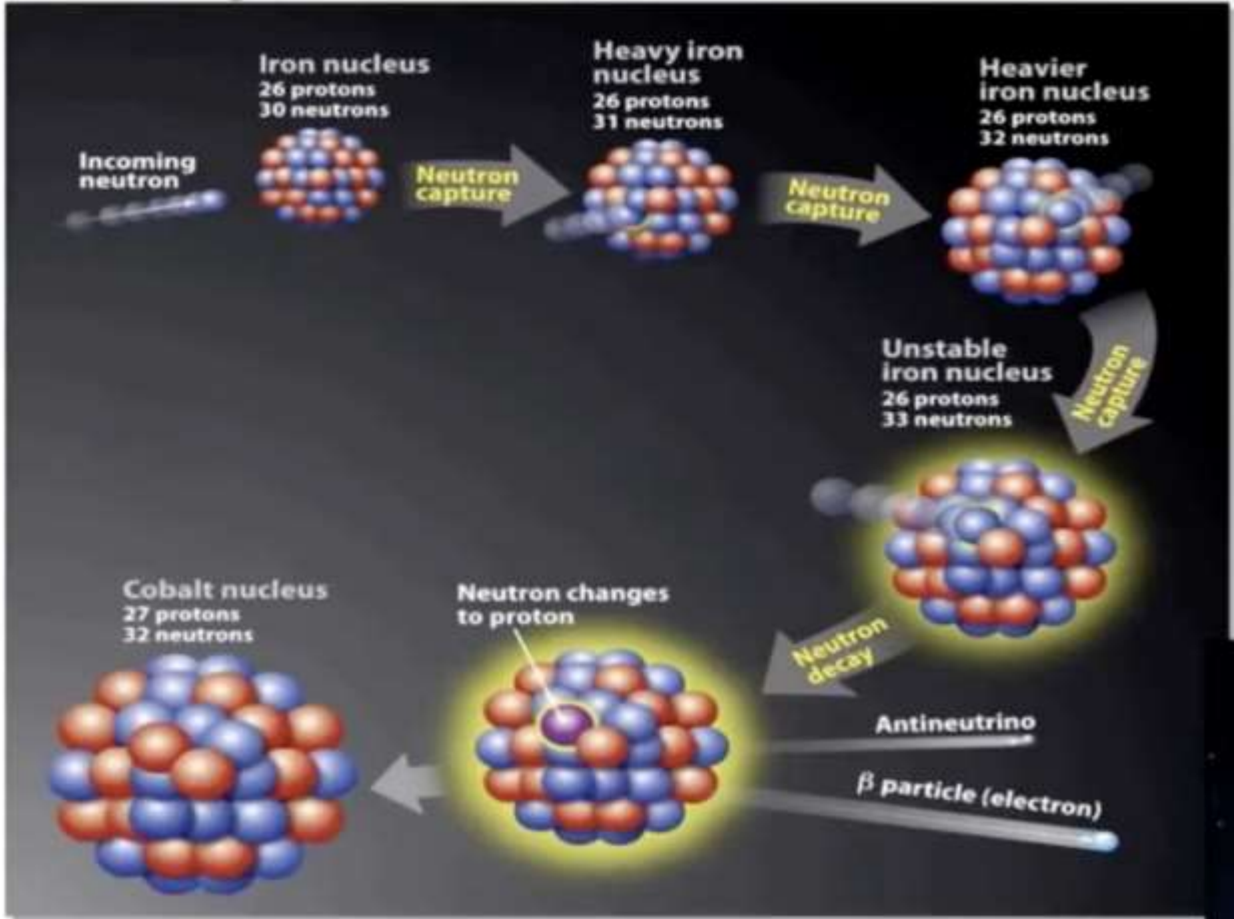

- атомы тяжелее железа не могут быть получены в ходе ядерного синтеза

- их образование происходит за счет захвата нейтронов

- необходимы условия, при которых концентрация нейтронов будет максимальной


Нейтронные звезды

Accretion discs of M87 and Sagittarius A* black holes made by Event Horizon Telescope (EHT) with 1.3 mm wavelength (25 micro-arc seconds accuracy)

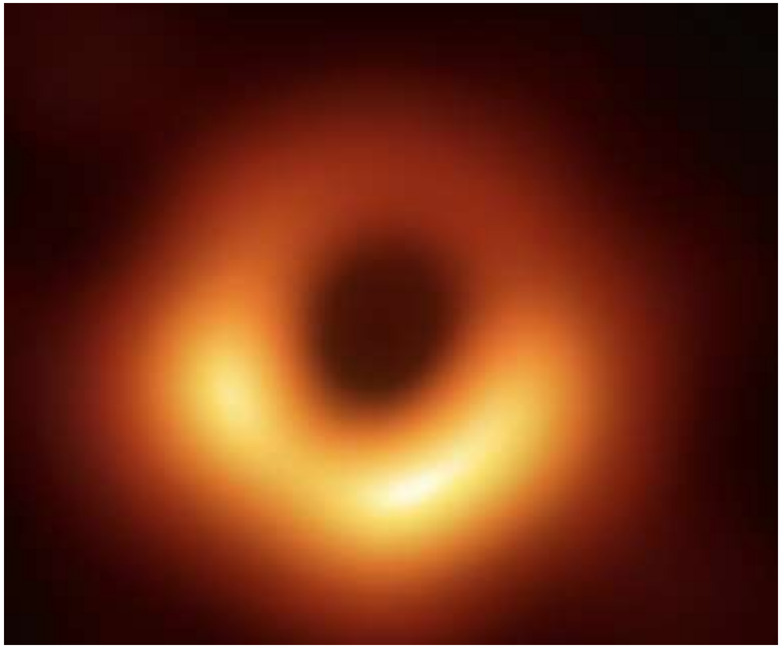

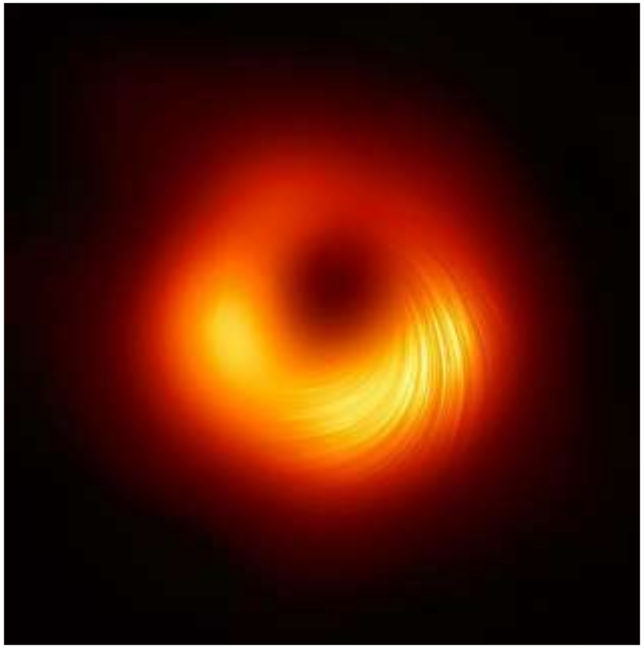

First direct visual evidence of the supermassive black hole in the center of the M87 galaxy and its shadow. While this may sound large, this ring is only about 40 micro-arc seconds across — equivalent to measuring the length of a credit card on the surface of the Moon. Although the telescopes making up the EHT are not physically connected, they are able to synchronize their recorded data with atomic clocks which precisely time their observations.

Although we cannot see the event horizon itself, because it cannot emit light, glowing gas orbiting around the black hole reveals a telltale signature: a dark central region (called a shadow) surrounded by a bright ring-like structure. The new view captures light bent by the powerful gravity of the black hole, which is four million times more massive than our Sun.

During a powerful solar blast on March 7, 2012 NASA's Fermi Gamma-ray Space Telescope detected the highest-energy light (4 GeV)ever associated with an eruption on the sun. The discovery heralds Fermi's new role as a solar observatory, a powerful new tool for understanding solar outbursts during the sun's maximum period of activity.

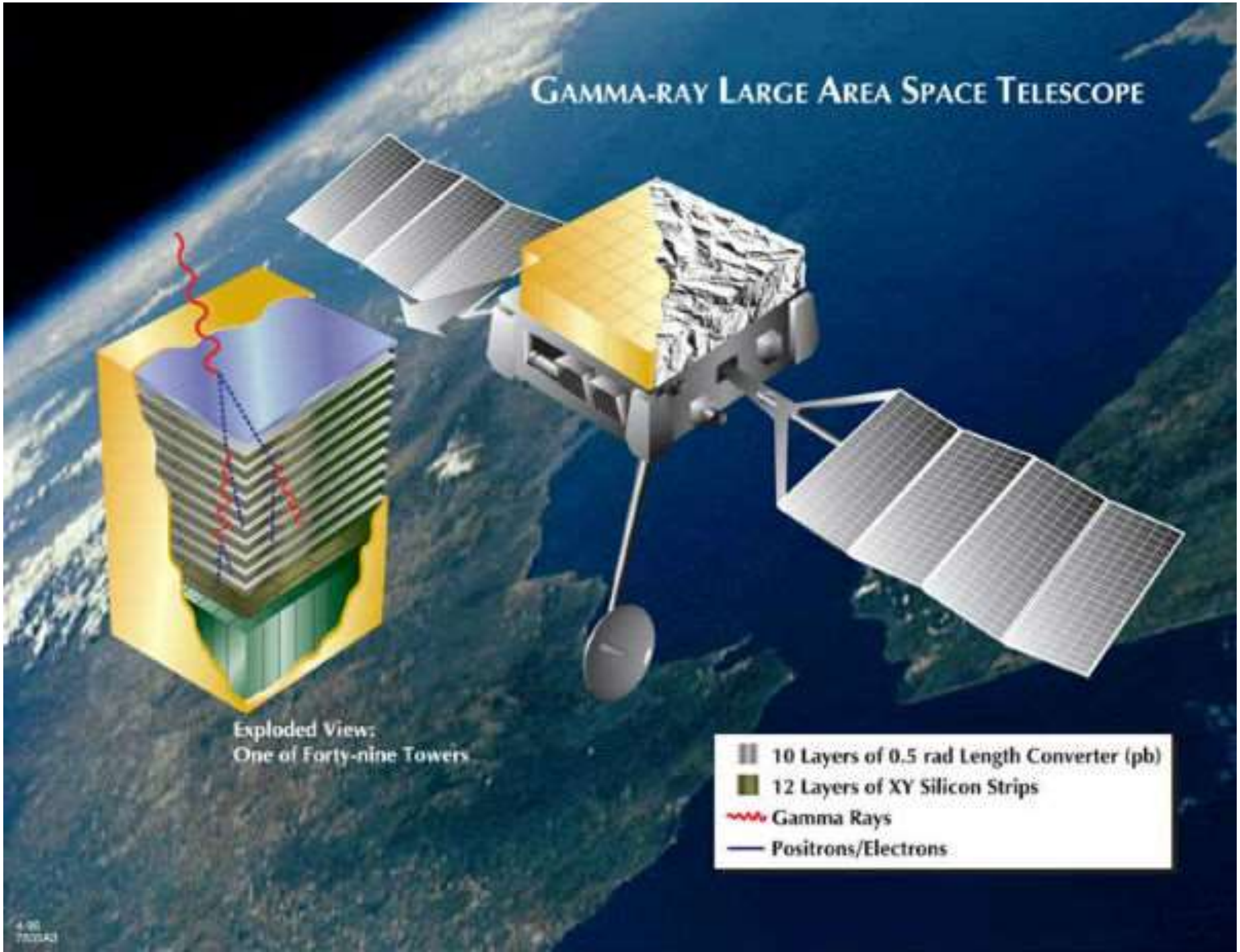

March 6, 2012

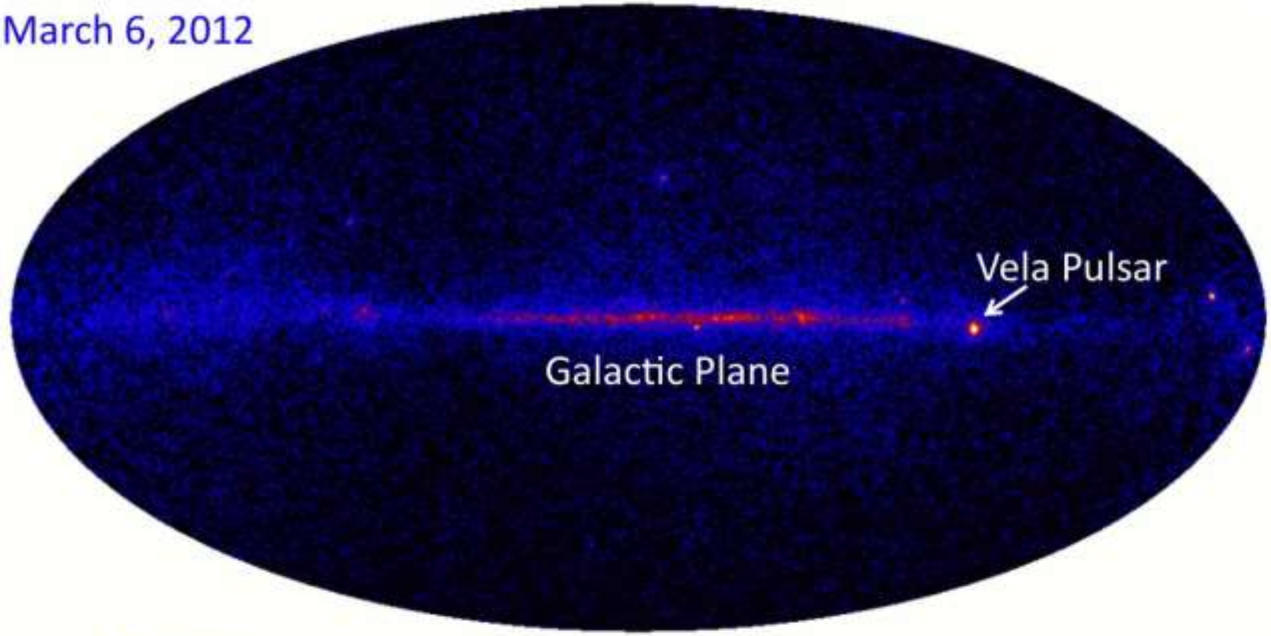

March 7, 2012

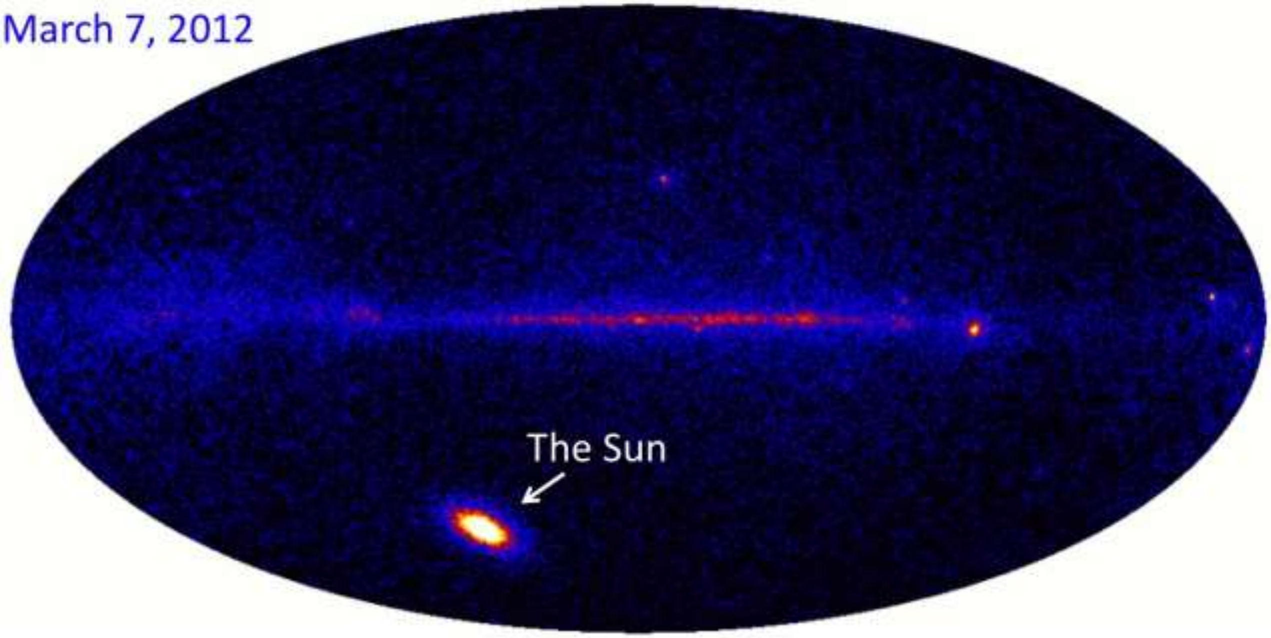

At the flare's peak, the Large Area Telescope (LAT) detected gamma rays with an energy of 4 GeV, setting a record for the highest-energy light ever detected during or just after a solar flare. The flux of high-energy gamma rays, beyond 100 MeV, was 1,000 times greater than the sun's steady output. The March 7 flare also is notable for the persistence of its gamma-ray emission.

Estimation of Solar accelerators maximal energy by detected secondary muons and gamma rays

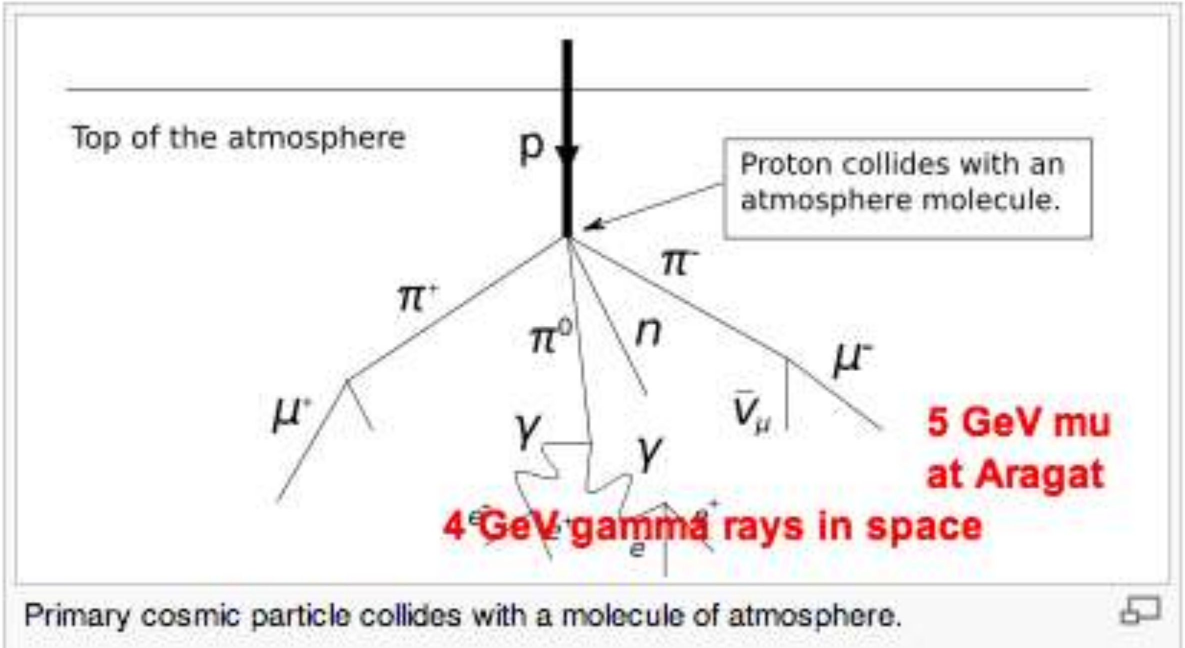

5 GeV mu at Aragat

4 GeV gamma rays in space

Primary cosmic particle collides with a molecule of atmosphere.

Proton energy is distrusted approximately equally between pi-mesons;
Decayed muon energy cannot exceed parent pion energy;
Pi_0 energy is distributed equally between 2 gamma rays.
Therefore, from FERMI 4 GeV gamma rays we arrive at minimal ener
protons interaction in the corona to be – 24 GeV; from Aragats muon

Discovery of the Highest energy Solar accelerators (> 20 GV): AMMM Detection of GLE 20 January 2005

Aragats Multidirectional Muon Monitor (AMMM)